RESTING-STATE FUNCTIONAL AND EFFECTIVE CONNECTIVITY CHANGES IN CEREBELLO-BASAL GANGLIA INTERCONNECTING NETWORK IN PARKINSON'S DISEASE AND ITS PATHO-PHYSIOLOGICAL AND THERAPEUTIC IMPLICATIONS

Vineeth Radhakrishnan

Ph.D. THESIS

2024

SREE CHITRA TIRUNAL INSTITUTE FOR MEDICAL SCIENCES AND TECHNOLOGY, TRIVANDRUM

An Institution of National Importance established by an Act of the Indian Parliament
(Act No.52 of 1980)

Dept. of Science and Technology, Govt. of India
www.sctimst.ac.in

RESTING-STATE FUNCTIONAL AND EFFECTIVE CONNECTIVITY CHANGES IN CEREBELLO-BASAL GANGLIA INTERCONNECTING NETWORK IN PARKINSON'S DISEASE AND ITS PATHOPHYSIOLOGICAL AND THERAPEUTIC IMPLICATIONS

A THESIS SUBMITTED BY

Vineeth Radhakrishnan

TO

SREE CHITRA TIRUNAL INSTITUTE FOR MEDICAL SCIENCES AND TECHNOLOGY, TRIVANDRUM.

IN PARTIAL FULFILMENT OF THE REQUIREMENTS

FOR THE AWARD OF

DOCTOR OF PHILOSOPHY

2024

श्री चित्रा तिरुनाल आयुर्विज्ञान और प्रौद्योगिकी संस्थान, त्रिवेन्द्रम
तिरुवनन्तपुरम - ६९५०११, केरल, इंडिया
SREE CHITRA TIRUNAL INSTITUTE FOR MEDICAL SCIENCES AND TECHNOLOGY, TRIVANDRUM
Thiruvananthapuram - 695 011, Kerala, India
(An Institute of National Importance under Govt. of India)
Grams : Chitramet, Phone : +91-471-2443152, Fax : +91-471-2550728 / 2446433, E-mail : sct@sctimst.ac.in, Website : www.sctimst.ac.in

DECLARATION BY THE STUDENT

CERTIFICATE

I, Vineeth Radhakrishnan, hereby certify that I had personally carried out the work depicted in the thesis titled, "Resting-state functional and effective connectivity changes in cerebello-basal ganglia interconnecting network in Parkinson's Disease and its pathophysiological and therapeutic implications", except where due acknowledgment has been made in the text. No part of this thesis has been submitted for the award of any other degree or diploma before this date.

Thiruvananthapuram
Date : 24/10/2024

Vineeth Radhakrishnan
2018/PhD/07

श्री चित्रा तिरुनाल आयुर्विज्ञान और प्रौद्योगिकी संस्थान, त्रिवेन्द्रम
तिरुवनन्तपुरम - ६९५०११, केरल, इंडिया
SREE CHITRA TIRUNAL INSTITUTE FOR MEDICAL SCIENCES AND TECHNOLOGY, TRIVANDRUM
Thiruvananthapuram - 695 011, Kerala, India
(An Institute of National Importance under Govt. of India)
Grams : Chitramet, Phone : +91-471-2443152, Fax : +91-471-2550728 / 2446433, E-mail : sct@sctimst.ac.in, Website : www.sctimst.ac.in

This is to certify that Vineeth Radhakrishnan, Comprehensive Care Center for Movement Disorders, Department of Neurology, of this institute, has fulfilled the requirements prescribed for the Ph.D. degree of the Sree Chitra Tirunal Institute for Medical Sciences and Technology, Trivandrum.

The thesis entitled, "Resting-state functional and effective connectivity changes in cerebello-basal ganglia interconnecting network in Parkinson's Disease and its pathophysiological and therapeutic implications" was carried out under our direct supervision. No part of the thesis was submitted for the award of any degree or diploma before this date.

*Clearance was obtained from the Institutional Ethics Committee of SCTIMST for carrying out the study.

Dr. Asha Kishore
Research Guide
(2018-2021)

Dr. Syam K*
Research Guide
(2021-2024)

*Following the superannuation of Dr. Asha Kishore in 2021, the guideship was transferred to Dr. Syam K. Dr. Asha Kishore continued to supervise the research related activities in the capacity of a member of the Doctoral Advisory Committee.

श्री चित्रा तिरुनाल आयुर्विज्ञान और प्रौद्योगिकी संस्थान, त्रिवेन्द्रम
तिरुवनन्तपुरम - ६९५०११, केरल, इंडिया
SREE CHITRA TIRUNAL INSTITUTE FOR MEDICAL SCIENCES AND TECHNOLOGY, TRIVANDRUM
Thiruvananthapuram - 695 011, Kerala, India
(An Institute of National Importance under Govt. of India)
Grams : Chitramet, Phone : +91-471-2443152, Fax : +91-471-2550728 / 2446433, E-mail : sct@sctimst.ac.in, Website : www.sctimst.ac.in

Prof. C. Kesavadas

Professor Senior Grade and Head,

Department of Radiology, SCTIMST, Trivandrum

This is to certify that Vineeth Radhakrishnan, Comprehensive Care Center for Movement Disorders, Department of Neurology, of this institute, has fulfilled the requirements prescribed for the Ph.D. degree of the Sree Chitra Tirunal Institute for Medical Sciences and Technology, Trivandrum.

The MRI patient data acquisition and image analysis work under the thesis entitled, "Resting-state functional and effective connectivity changes in cerebello-basal ganglia interconnecting network in Parkinson's Disease and its pathophysiological and therapeutic implications" was carried out under my direct supervision. No part of the thesis was submitted for the award of any degree or diploma before this date.

*Clearance was obtained from the Institutional Ethics Committee of SCTIMST for carrying out the study.

Thiruvananthapuram
Date: 24\10\2024

Prof. C. Kesavadas
(Research Co-guide)

श्री चित्रा तिरुनाल आयुर्विज्ञान और प्रौद्योगिकी संस्थान, त्रिवेन्द्रम
तिरुवनन्तपुरम - ६९५०११, केरल, इंडिया
SREE CHITRA TIRUNAL INSTITUTE FOR MEDICAL SCIENCES AND TECHNOLOGY, TRIVANDRUM
Thiruvananthapuram - 695 011, Kerala, India
(An Institute of National Importance under Govt. of India)
Grams : Chitramet, Phone : +91-471-2443152, Fax : +91-471-2550728 / 2446433, E-mail : sct@sctimst.ac.in, Website : www.sctimst.ac.in

The thesis entitled

Resting-state functional and effective connectivity changes in cerebello-basal ganglia interconnecting network in Parkinson's Disease and its pathophysiological and therapeutic implications.

Submitted by

Vineeth Radhakrishnan

for the degree of

Doctor of Philosophy

of

SREE CHITRA TIRUNAL INSTITUTE FOR MEDICAL SCIENCES AND TECHNOLOGY, TRIVANDRUM

is evaluated and approved by

(Name & Signature of the Guide)

डॉ श्याम कृष्णन नायर/Dr. Syam Krishnan Nair
Reg. No : 28740, TCMC
प्रोफेसर, न्यूरोलॉजी विभाग/Professor, Department of Neurology
प्रभारी/In-Charge
व्यापक संचलन अनियमितता देखभाल केंद्र (सीसीसीएमडी)
Comprehensive Care Center for Movement Disorders(CCCMD)-
श्री चित्रा तिरुनाल आयुर्विज्ञान और प्रौद्योगिकी संस्थान
Sree Chitra Tirunal Institute for Medical Sciences&Technology
त्रिवेन्द्रम/Trivandrum

(Name & Signature of thesis examiner)

Dr ROSE DAWN BHARATH
KMC 53292
Professor
Department of Neuroimaging & Interventional Radiology
NIMHANS, Bengaluru-560 029

ACKNOWLEDGEMENTS

It is with immense gratitude that I acknowledge the support and contributions of many individuals and institutions who have made this thesis journey possible. Firstly, I am deeply indebted to the Sree Chitra Tirunal Institute for Medical Sciences and Technology and its leadership. For the excellent facilities and infrastructure that enabled my research, I extend my sincere gratitude to the Director, Sree Chitra Tirunal Institute for Medical Sciences and Technology. I extend my gratitude towards the Dean, Associate Dean, Registrar, and the entire academic division and directors' office for their unwavering assistance throughout my academic journey.

My deepest appreciation goes to my esteemed mentors, Prof. Asha Kishore and Prof. Syam K, for their invaluable guidance, encouragement, and support. Their insightful feedback, timely advice, and mentorship were instrumental in shaping my research and helped me navigate the challenges during my PhD. I am also grateful to my co-guides and DAC members, Dr. Cecile Gallea, Prof. C. Kesavadas, and Prof. Bejoy Thomas for their unparalleled technical support in acquiring and analyzing patient data. Their expertise and collaboration greatly contributed to the success of my research. Their support and suggestions significantly improved the quality of my research. I would also like to thank, the teaching faculty of my coursework, for providing me with a strong foundation in my field.

I acknowledge the generous financial support I received, from the International Parkinson and Movement Disorder Society (MDS) for the travel grant that enabled me to attend the MDS Congress 2023 in Denmark. Also, I thank the International Brain Research Organization (IBRO), for the grant that allowed me to participate in the IBRO World Congress of Neuroscience in Granada, Spain, 2023. I would like to thank the Movement Disorders Society of India (MDSI) for the travel grant to attend the MDSICON conference at Trivandrum, India, in 2020.

My heartfelt gratitude goes to the staff of the Comprehensive Care Center for Movement Disorders, Department of Neurology, SCTIMST. I thank Mr. Gangadhara Sarma, Mrs. Glenda Mary, Mrs. Anju Vijilal, Mr. Praveen James, my seniors, and other fellow graduate students for their continuous support throughout my years of study and for collaborating on various projects alongside me. Additionally, I am grateful to Mr. Mahesh, Mr. Alex Jose, Mrs. Githakumari, and Mrs Sheebakumari, Department of Imaging Sciences and Interventional Radiology, for their assistance with MRI data acquisition and learning the basics of MRI.

I would like to thank my parents and my wife for their unwavering love, support, and encouragement. I am indebted to God almighty for his blessings and guidance throughout my life. This thesis would not have been possible without the invaluable support and contributions of these individuals and institutions. I am truly grateful to each one of them.

TABLE OF CONTENTS

LIST OF FIGURES

LIST OF TABLES

LIST OF ABBREVIATIONS

AAL3	:	Automated Anatomical Labeling Atlas 3
ACC	:	Anterior Cingulate Cortex
ACE	:	Addenbrooke's Cognitive Examination
ACE-M	:	Addenbrooke's Cognitive Examination-Malayalam
ART	:	Artifact Detection Tools
BET	:	Brain Extraction Tool
BMS	:	Bayesian Model Selection
BOLD	:	Blood Oxygen Level Dependent
CAT12	:	Computational Anatomy Toolbox
CB-BG	:	Cerebellum-Basal Ganglia
CDR	:	Clinical Dementia Rating scale
CM	:	Central Median
CSD	:	Constrained Spherical Deconvolution
CST	:	Corticospinal Tract
CTC	:	Cerebello Thalamo Cortical
CTS	:	Cerebello-Thalamo-Striatal
DBS	:	Deep Brain Stimulation
DCM	:	Dynamic Causal Modelling
dMRI	:	diffusion-weighted Magnetic Resonance Imaging
DN	:	Dentate Nucleus
DTI	:	Diffusion Tensor Imaging
DWI	:	Diffusion-Weighted Imaging
EEG	:	Electroencephalogram
EPI	:	Echo Planar Imaging
FA	:	Fractional Anisotropy
FBA	:	Fixel Based Analysis
FC	:	Fiber Cross-section
FD	:	Fiber Density
FDC	:	Fiber Density Cross-section
FDR	:	False Discovery Rate
FDT	:	FMRIB's Diffusion Toolbox
FFX	:	Fixel Effects

fMRI	:	functional Magnetic Resonance Imaging
FOD	:	Fiber Orientation Distribution
FSL	:	FMRIB Software Library
GABA	:	Gamma-aminobutyric acid
GLM	:	General Linear Model
GPe	:	Globus Pallidus externus
GPi	:	Globus Pallidus internus
HCP	:	Human Connectome Project
L-Dopa	:	Levodopa
LEDD	:	Levodopa Equivalent Daily Dosage
LID	:	Levodopa Induced Dyskinesia
M1	:	Primary Motor Cortex
MD	:	Mean Diffusivity
MEG	:	Magnetoencephalography
MMSE	:	Mini-Mental State Examination
MNI	:	Montreal Neurological Institute
mPFC	:	medial Prefrontal Cortex
MP-PCA	:	Marchenko-Pastur Principal Component Analysis
MPRAGE	:	Magnetization-Prepared Rapid Gradient-Echo
MPTP	:	1-methyl-4-phenyl-1,2,3,6-tetrahydropyridine
MRI	:	Magnetic Resonance Imaging
MSA	:	Multiple System Atrophy
NDED	:	Number of Diffusion Encoding Directions
PD	:	Parkinson’s Disease
PET	:	Positron Emission Tomography
PN	:	Pontine Nuclei
PPN	:	Pedunculo Pontine Nucleus
PSP	:	Progressive Supranuclear Palsy
PwPD	:	Patients with Parkinson's Disease
RAVLT	:	Rey Auditory Verbal Learning Test
ROI	:	Region of Interest
rsfMRI	:	resting state functional Magnetic Resonance Imaging
SN	:	Substantia Nigra
SNpc	:	Substantia Nigra pars compacta
SNr	:	Substantia Nigra pars reticulata

SNR	:	Signal-to-Noise Ratio
SPC	:	Subthalamo-ponto-cerebellar
spDCM	:	spectral Dynamic Causal Modelling
SPM12	:	Statistical Parametric Mapping toolbox
STC	:	Striato-Thalamo-Cortical
STN	:	Subthalamic nucleus
TE	:	Echo Time
TIV	:	Total Intracranial Volume
TR	:	Repetition Time
UKPDSBB	:	United Kingdom Parkinson's Disease Society Brain Bank
UPDRS	:	Unified Parkinson's Disease Rating Scale
VA/VL	:	Ventral Anterior/Ventral Lateral
Vim	:	Ventral intermediary nucleus
VOI	:	Volume of Interest
VTA	:	Ventral Tegmental Area

SYNOPSIS

The basal ganglia and cerebellum are important sub-cortical structures involved in voluntary movements. In the classical view, these were considered to be part of independent loops connected to the cerebral cortex, namely the striato-thalamo-cortical (STC) and cerebello-thalamo-cortical (CTC) loops. Recent research in non-human primates has demonstrated the presence of disynaptic projections between the cerebellum and basal ganglia without involving the cerebral cortex,[1] suggesting direct communication. These recently identified pathways could play a significant role in motor control and the pathophysiology of movement disorders such as Parkinson's Disease (PD) and Dystonia.

The study by Bostan. et al. on non-human primates made use of retrograde transneuronal transport using the rabies virus to reveal the disynaptic projections from the subthalamic nucleus (STN) to the cerebellar cortical regions of C7b and Crus IIp.[2] Similarly, injections targeting the putamen labeled the neurons in the dentate nucleus and minor projections to the fastigial and interposed nuclei.[3] These tracks display a topographical organization with motor, cognitive, and affective regions of each node connected congruently, suggesting a structured network. The projections from the associative and limbic territories of the STN to CrusIIp indicate that the role of the network is associated with non-motor functions, including cognition and emotion.

The disynaptic connections between the two networks could potentially play a role in motor and non-motor aspects in the pathophysiology of movement disorders such as PD and dystonia. Indeed, STN is influenced by striatal and pallidal efferents

from the indirect pathway. The dysregulation of the dopaminergic system at the striatal region following the degeneration of nigro striatal dopaminergic pathway in PD patients could interfere with STN activity and its influence on the cerebellum. A better understanding of network dysfunction in PD could contribute to the development of new therapeutics and enlarge our understanding of the existing ones such as Deep Brain Stimulation (DBS) and Dopamine Replacement Therapy (DRT). In addition, this understanding could widen our knowledge about functional brain circuits associated with healthy human movement.

PD is a heterogenous neurological disorder characterized by the degeneration of dopamine neurons in Substantia nigra pars compacta.[4] The resulting loss of nigro-striatal dopaminergic activity disrupts motor control and leads to motor symptoms such as akinesia/bradykinesia, rest tremor, and rigidity. Even though PD has been classically defined as a basal ganglia disorder, recent studies have adopted a network approach to the study of its pathophysiology. For instance, tremor which is a cardinal symptom of PD, has been associated with alterations in cerebellar activity.[5] Dopamine replacement therapy can alleviate the symptoms of tremor in PD, but its complete physiological basis remains unclear. The occurrence of tremor in PD has been explained using models such as the "dimmer-switch" model where both the BG and cerebellar circuits are involved in the pathophysiology of PD tremor[5]. When the dopamine levels are low, transient tremor-related activity arises in the BG circuit, which acts as a switch turning the tremor symptoms on and off like a switch. The CTC circuit acts like a modulator turning the amplitude of the induced tremor higher and lower. Voxel-based morphometric (VBM) studies have demonstrated reduced cerebellar volume in PD patients.[6] The ventral intermediary nucleus of the thalamus

which receives projections from the cerebellar input, is an effective target to treat tremors in patients undergoing DBS.[7] Also, STN-DBS and Vim-DBS reduce the hyperactivity of the cerebellum in PD patients.[8,9]

The complex interplay between the cerebellum and basal ganglia regions highlights the need for a system-level approach to the study of the pathophysiology of PD. With this background, this study hypothesizes that "Connectivity between basal ganglia and cerebellum can be demonstrated by rs-functional MRI and Diffusion Weighted Imaging (DWI) in healthy volunteers and is altered differentially in patients with PD in its early stage where it could be compensatory and late stage contributing to the pathophysiology; levodopa could accordingly influence the functional and effective connectivity".

To test the hypothesis, the following objectives were considered;

a. To compare different Diffusion-Weighted Imaging (DWI) acquisition schemes for establishing non-dominant crossing fibers using multi-shell DWI data from the Human Connectome Project (HCP)
b. To establish cerebellum-basal ganglia (CB-BG) structural connectivity in healthy subjects during resting state and to study the effect of age on properties of CB-BG tracts.
c. To examine functional, and effective connectivity between CB-BG reciprocal networks in early and late-stage Parkinson's patients, with and without levodopa.

The study of CB-BG tracts in healthy human subjects remains an ongoing effort. Studying these tracts on a large subject group of healthy controls with a larger

age range will disentangle the effect of “natural neurodegeneration” with aging from “disease neurodegeneration” related to PD. Additionally, the role of these tracts in PD pathophysiology is yet to be explored. The functional interplay between these tracts as a function of disease duration could play an important role in the evolution of PD as well as the therapeutic option adopted. Indeed, recent work suggests the role of the cerebellar reserve to compensate for dysfunction related to neurodegeneration.[10] To address these knowledge gaps, DWI and fMRI were used to perform tractography, and functional connectivity analysis respectively.

The efficient tracking of these crossed pathways relies on the quality of the diffusion-weighted images and the DWI acquisition schemes. Technical factors such as the number of diffusion encoding directions (NDED), gradient strength (b-value), voxel size, and data modeling techniques are significant in delineating the crossing fibers in the CB-BG network. The trade-off between image quality, SNR, scan time, and computing requirement has to be assessed for different combinations of settings for diffusion imaging to select the parameters appropriate for the application.

After the structural connections between the regions in the network were established, we studied their functional connectivity. The structural integrity of connectivity between the regions is a pre-requirement of functional connectivity, but miscommunication between brain regions or abnormal functional connectivity can be observed for structurally intact connections. These measures help to understand the role of different nodes in the network that could be associated with different symptoms, disease severity, and disease duration. The combined study of structural, functional, and effective connectivity helps us to gain valuable insights into the role

of the network in health and disease, leading to improved treatment options for PD and other movement disorders.

The thesis is divided into 7 chapters;

Chapter 1 introduces the research problem and identifies the knowledge gap. I also explain how the hypothesis was developed and objectives were defined based on the identified research problem, and emphasize the novelty of my approach. I also explain (i) the role of basal ganglia in human movement via the striato-thalamo-cortical (STC) circuit, and (ii) how the cerebello-thalamo-cortical circuit (CTC) communicates with it at the cortical level. I then present how the identified di-synaptic subcortical network and the reciprocal loop observed in macaque monkeys could contribute to explaining PD pathophysiology with the progressive evolution of dopaminergic neurodegeneration. Beforehand, we need to delineate these tracts in healthy subjects and to understand their changes with age-associated neurodegeneration. I also discuss in the first chapter, an overview of the different techniques used in my project to study these tracts non-invasively in humans (tractography, and functional and effective connectivity).

In Chapter 2, I review the main findings of the literature that paved the way for my thesis, focusing on the work previously done in the field. This includes the animal studies reporting the presence of the CB-BG interconnecting network. I also discuss previous attempts at establishing these tracts in human subjects using tractography along with their limitations on data acquisition techniques, sample size, and analysis techniques. Other non-invasive in-vivo modalities such as Transcranial Magnetic Stimulation that investigate the role of a CB-BG interconnecting network in movement disorders are also discussed, emphasizing the knowledge gap arising

from the lack of research that successfully establishes the functional role of different nodes in the CB-BG network. In particular, I discuss the role of the age-related change in the microstructure of these tracts, which I studied in this project, and their role in the progressive loss of memory and learning abilities during "natural neurodegeneration". The novel aspect here is elucidating the effect of "natural neurodegeneration" in the CB-BG network in healthy subjects. Also, the importance of investigating the directed influence of one node in the network on the other in health and disease stages is explained.

In Chapter 3, I elaborate on the study subject recruitment and data acquisition for three separate experiments. The data used for the first experiment arises from the Human Connectome Project (HCP). The combination of acquisition parameters studied in each trial of tractography is explained. The tractography of the lateral projections of the Cortico Spinal Tract (CST) was studied as they contain major crossing fibers from the Superior Longitudinal Fasciculus (SLF). In the second experiment, the healthy subject recruitment along with the inclusion and exclusion criteria are discussed. The diffusion MRI data acquisition parameters and Constrained Spherical Deconvolution (CSD) steps in Mrtrix3 software are explained in detail. The steps to develop the ROI mask for the data analysis are explained in detail. The details on the regression and correlation analysis to study the relation between the tract parameters, age, and cognitive scores are explained as well. In the third experiment, the subject recruitment and the condition for data acquisition in the medication ON and OFF states of PD are explained. The details of T1 and fMRI data acquisition in patients and considerations to improve the data accuracy and quality are discussed. The steps in functional and effective connectivity analysis using the CONN and SPM

toolbox are detailed along with the steps for ROI selection. The statistical steps to compare the data for the patients and control group at different conditions depending on disease duration and medication state are discussed for functional connectivity analysis. In effective connectivity analysis steps such as model specification and Bayesian Model Selection are explained in detail.

Chapter 4 presents the results of all three experiments. In the first experiment, the figures comparing the images of the tractography results for the lateral projections of the Cortico Spinal Tract at different combinations of the acquisition parameters are compared. The density of fiber bundle and false positive tracts for different combinations is visually compared to select the best combination for establishing CB-BG tracts. In the second experiment, the ascending tracts from the dentate nucleus to the putamen and descending tracts from STN to the cerebellar cortex for the CB-BG network are drawn. As a control tract, the well-established, CTC tract is also drawn in tractography. The tract parameter of fiber density (FD) is shown to have a negative linear relationship with age for the CB-BG tract. Also, the correlation between the cognitive assessment score for registration and learning shows a positive correlation with FD for the ascending tracts while the descending tracts along with the cerebellum frontal tracts via medio dorsal nuclei and Ventral Tegmental Area (VTA) correlated with the memory recall scores in Addenbrooke's Cognitive Examination (ACE). In the third experiment, the functional connectivity analysis revealed different changes in the connectivity within the network for different group comparisons. Effective connectivity analysis results show the winning model for the communication between the left cerebellum and right basal ganglia.

Chapter 5 provides a discussion of the results of the three experiments. The tractography results for the CST demonstrate how a small b-value of 1000s/mm^2 was able to delineate the lateral projections of CST. In the comparison for NDED, 64 directions were found to be ideal for the application. Also, the voxel size of 1.5mm was selected comparing the trade-off between the computational demands and the benefit of delineating the tract features. Based on these results, a DWI acquisition scheme with a b-value of 1000 s/mm^2, NDED=64, and a voxel size of 1.5mm was selected. Also, the Constrained Spherical Deconvolution model was selected for analyzing the data instead of the diffusion tensor imaging model. In the second experiment, the specific CB-BG and cerebello-cortical pathways and their concordance with the thalamic nuclei route are discussed in detail. The age-related morphometric changes in the CB-BG connections support similar observations in other regions such as corpus callosum. The psychometric and behavioral correlations within the CB-BG tract microstructure, discussed in detail along with the cerebello-frontal tracts imply the significant role played by the tracts in memory and learning. In the third experiment, the functional connectivity between the left cerebellum and right putamen was found to be higher in the PD patients during OFF compared to the healthy subjects, which supports the hyperactivity observed in the cerebellum in other studies.[11] The change in connectivity during OFF as a function of disease duration suggested the need for studying the effect of levodopa on disease duration as well. The functional connectivity changes in the early stages were observed primarily in the Cerebello-thalamo-striatal (CTS) pathway while the subthalamo-ponto-cerebellar (SPC) pathway was affected in the later stages of the disease. The effect of a single dose of levodopa was found to be different with disease duration. In the early stage of

the disease, the levodopa acted on the CTS pathway by normalizing the increased functional connectivity but during the later stages, the action also involved restoration of the reduced connectivity in the SPC pathway. Further inferences were drawn based on the directional information obtained during effective connectivity analysis in association with the FC results. In the ascending tracts, the model with the connection from dentate to the putamen and in the descending tracts, the model with connections from the STN to C7b was found to have higher posterior probability. Thus the role of CB-BG subcortical network in health and disease was studied in the resting state.

Chapter 6 concludes and summarises the findings from the entire study. The study, standardized the tractography protocol to establish the non-dominant fibers using the cortico-spinal tract. It established the tractography of CST lateral projections with crossing fibers using minimal gradient strength and acquisition time. A b-value=1000s/mm2, NDED=64, and vox size =1.5mm were selected for the CB-BG tractography. This study confirms the existence and trajectories of subcortical connections between the CB and BG in a large group of human subjects, as reported in non-human primates. The study observed for the first time, that FD in reciprocal CB-BG tracts was negatively correlated with age and positively correlated with specific cognitive psychometric scores associated with memory and learning. This study provides the first evidence for the functional role of the cerebellum basal ganglia direct subcortical network in the pathophysiology of PD. It is the first study to examine the effective connectivity changes in the cerebello-thlamo-striatal and subthalamo-ponto-cerebellar pathways in PD. The ascending CTS pathway was affected primarily in the early stages suggesting a compensatory role of the cerebellum in the early stages of PD and the descending SPC pathways were affected

only during the later stages suggesting a more pathological role. The directional information regarding the ascending tract during early PD stages provides evidence for the compensatory effect of the cerebellum in PD.

Chapter 7 lists the citation under the title bibliography. The thesis includes other relevant sections such as acknowledgment, table of contents, list of figures, declarations, and publications.

CHAPTER 1 INTRODUCTION

1.1 Movement Disorders

Movement disorders are a class of neurological disorders that affect the person's ability to control their movements. These are a widely studied classes of neurological disorders, particularly Parkinson's disease (PD), in which the response to treatment and progression of biochemical changes in the brain can be monitored and evaluated more effectively. Although a considerable amount of research has been conducted in this field, further insights into the neural basis of these diseases could help the development of better and personalized interventions.

Movement disorders are classified into several groups based on the nature of motor symptoms. Based on phenomenology movement disorders are classified into hyperkinetic and hypokinetic disorders.(Fahn, 2011) The common hypokinetic movement disorders (otherwise called "Parkinsonism") include Parkinson's Disease (PD), Progressive Supranuclear Palsy (PSP), and Multiple System Atrophy (MSA). Hyperkinetic movement disorders include those that cause abnormal movements such as dystonia, chorea, tremor, tics and myoclonus. Several genetic, degenerative and acquired conditions can cause them. Research on the changing view of movement disorder pathophysiology has led to a better understanding of these conditions and their management(Wichmann, 2018). Neurophysiologically these conditions are associated with the changes in firing rates and /or patterns in the basal ganglia, thalamus, and motor cortex. Later, the focus shifted towards the study of

synchronization of low-frequency oscillations in different nodes of the motor network in these diseases. In Parkinson's disease, regions remote from the basal ganglia such as the Pedunculopontine Nucleus (PPN) and the cerebellum also exhibit pathophysiological changes.(French and Muthusamy, 2018; Poewe et al., 2017) A better understanding of the pathophysiology can lead to more effective pharmacologic and surgical therapies with fewer side effects.

1.2 Role of BG and Cerebellum in Human Movement

The basal ganglia and the cerebellum are the regions primarily associated with human movement. From an evolutionary perspective, the basal ganglia and cerebellum form largely the evolved structures, of the motor network in the brain. Movement disorders mainly arise from the dysfunction of these structures and the circuitry associated with them. Functionally, the basal ganglia is attributed to action selection and action planning,(Fermin et al., 2016; Mink, 2018) while the cerebellum performs the fine adjustment to motor movements and error correction based on feedback from peripheral input signals. Basal ganglia and the cerebellum interact at the cortical level via the Striato-Thalamo-Cortical (STC) and Cerebello-Thalamo-Cortical (CTC) network loops respectively. Since the STC and CTC networks project to distinct thalamic nuclei and were thought to communicate only at the cortical level, they were considered to be independent networks. Many studies proposed that the STC and CTC networks have a closed-loop architecture and identified them to perform complementary functions in the motor network.(Peters et al., 2016; Rădulescu et al., 2017; Sha et al., 2020) However

recent studies based on viral retrograde transneuronal transport have shown that the basal ganglia and the cerebellum communicate bidirectionally at the sub-cortical level.(Bostan and Strick, 2018) These findings led to a dramatic shift in the perspective of cerebellum basal-ganglia interactions, which led to several investigations to determine if and how these two structures interact in health and disease.

1.2.1 Role of Basal Ganglia

The segregated re-entrant loop of the cortico-striato-thalamo-cortical loop is primarily involved in action selection and planning.(Brittain et al., 2014; Kropotov and Etlinger, 1999; Mink, 2018; Schroll and Hamker, 2013) This network contains multiple parallel loops for handling the functions associated with motor, oculomotor, prefrontal, and limbic modules. A dysfunction within the motor circuit leads to movement disorders. The putamen and caudate nuclei of the striatum serve as the input to the basal ganglia. The input reaching the striatum is processed via the ‘direct’ and ‘indirect’ pathways, consisting of the cholinergic and GABAergic interneurons. Globus Pallidus internal (GPi) segment, along with Substantia Nigra pars reticulate (SNr), forms the output structures which project to the thalamus and then to the cortex. The direct and indirect pathways have opposing influences on overall motor control. The direct pathway tends to increase cortical activity while the indirect pathway inhibits it. Dopamine plays an essential role in this circuit by differentially regulating the direct and indirect pathways. Dopamine acts on D1 receptors on the Direct pathway and D2 receptors on the Indirect pathway. The balance

between these pathways enables movement. Any imbalance in the action of dopamine can affect the synchrony between the circuits and cause movement disorders. A relatively recent addition to this model of information flow in the basal ganglia is the hyper-direct pathway, which enables direct connection from the cortical areas to the subthalamic nucleus (STN), bypassing other input and processing nuclei of the basal ganglia. The fact that the signal flow bypasses the intermediate nuclei in the direct and indirect pathways enables quick modification or control over ongoing movement through the hyperdirect pathway.

1.2.2 Role of Cerebellum

The cerebellum primarily performs the function of fine control of movement by performing movement error correction based on proprioceptive signal feedback from the periphery.(Manto et al., 2012) The communication between the cerebellum and the cortical areas primarily occurs via the CTC network. The cerebellum receives peripheral input through various afferent tracts and the output is conveyed to the cortical regions via the deep cerebellar nuclei and ventral intermediary (Vim) nuclei in the thalamus. Purkinje cells process the input from the climbing fibers, stellate cells, and basket cells by forming extensive dendritic arbors extending throughout the molecular layer. The Purkinje cell axons project to the deep cerebellar nuclei and into the Vim, hence controlling the motor movements and compensating for the adjustments required based on the peripheral feedback signals. The projection from the

deep cerebellar nuclei to the Vim in the CTC network is specifically distinct from the basal ganglia projection to the VA/VL nuclei in the STC network.

1.3 Recently- identified connections interconnectingBasal ganglia and Cerebellum interconnecting network

Conventionally, the basal ganglia and the cerebellum were identified to communicate only at the cortical level via STC and CTC networks. However, recent studies in non-human primates using retrograde transneuronal transport by rabies virus have shown extensive disynaptic projections between the regions.(Bostan and Strick, 2018) Using rabies virus injection, STN was shown to have dense disynaptic projections to the cerebellar cortical areas such as C7b and CrusIIp. Also, injection to putamen labeled neurons mainly in the dentate nucleus and few in the fastigial and interposed nuclei of the cerebellum. One interesting finding was that the topographical organization was preserved in the projections between these regions, which implies the interconnecting network is involved not only in the motor but also in non-motor associations such as cognition, affect, and behavior. This is evident from the interdependency of the regions in functions that were once considered confined to one area. Specific behavioral tasks such as reward-based reinforcement learning and coding of reward prediction errors were considered restricted to activity in basal ganglia regions. However recent animal models and human studies have shown that the cerebellum is also involved in these processes.(Carta et al., 2019) This has caused a shift in the analysis towards a network perspective of the subcortical structures of the cerebellum and basal

ganglia. Synaptic modification or abnormal activity in one of the nodes in the network has a network-wide effect along the basal ganglia, cerebellum, and cerebral cortex. These structures cooperate to maintain synchrony and enable normal functional behavior.

Even though the regions have been hypothesized to interact at the subcortical level and maintain functional balance in the behavior, the exact functional relevance or the dynamics of the pathway is not understood. Studies have shown third-order neurons projecting to the dentate nucleus of the cerebellum after injection of the virus at GPe.(Hoover and Strick, 1999) These studies have strengthened the speculation that the cerebellar output is biased towards the indirect pathway in basal ganglia rather than the direct one. The thalamus primarily acts as a gateway for all the sensory input. In rodents the cerebellum projects to a region in the thalamus called the central lateral nucleus.(Ichinohe et al., 2000) The intralaminar nuclei are also sites for projecting tracts from the cerebellum onto the striatum. In humans, the thalamic regions holding the projections from the cerebellum to the striatum and its functional relevance are yet to be understood.

In macaque monkeys, the STN projects to the cerebellar cortex via the pontine nucleus and pedunculopontine tegmental nucleus.(Bostan and Strick, 2018) STN being an output nucleus of the basal ganglia, a reduction in STN activity can reduce the activity of cerebellar Purkinje cells leading to increased activity in deep cerebellar nuclei. Computational models on the CB-BG-Cerebral cortex have shown that hyperactivity in STN can propagate to the Cerebral

cortex and contribute to tics, a type of involuntary movement disorders.(Caligiore, Mannella, et al., 2017) The cerebellum-basal ganglia-cerebral cortex interconnecting network is active in the motor and the limbic networks. Learning of any kind is gradually implemented at the topographical level in these circuits. The CB-BG interconnecting network regions are also part of other networks such as the executive control network, limbic network, etc. The executive control network, which consists of regions such as the caudate, lateral cerebellum (Crus I and II), and dorsal lateral prefrontal cortex, is involved in working memory, executive functions, and verbal fluency. Abnormal activity in the executive control network causes cognitive dysfunction and is observed in conditions such as Alzheimer's Disease, anxiety, Friedrich ataxia, and Spinocerebellar Ataxia type 6.(Etkin and Wager, 2007; Globas et al., 2003) Similarly, the limbic network, with regions including striatum/cerebellum (Cerebellum VI and crus I)/Dorsal anterior cingulate cortex, is involved in processing interoceptive autonomic and emotional information. Such limbic regions of the CB-BG interconnecting network are affected by non-motor symptoms such as anxiety, depression, eating disorders, etc. The CB-BG interconnecting network is a topographically organized and functionally distinct network that operates over movement, cognition, and affect. Any abnormality in a network node can percolate to other network regions.

Changes in the CB-BG network can have critical role in the development of motor symptoms in PD. The progressive role of dopaminergic neurons in the

substantia nigra, could disrupt the balance in the CB-BG network. The hyperactivity observed in cerebellum could be mediated by tracts in the CB-BG network. As the disease progresses, the motor and cognitive symptoms worsen in PD. The evolution of pathological signalling between CB and BG could be mediated by the direct subcortical tracts in the CB-BG network. Understanding the PD associated pathophysiological changes in the networ could help identify target nodes for therapeutics, such as TMS cerebellar target for dyskinesia treatment, it could lead to identification of safer target for DBS surgeries etc.

1.4 Neuroimaging techniques available to study brain networks

The different techniques to explore brain connectivity have enabled an understanding of the pathophysiology of several neurodegenerative diseases.(McMackin et al., 2019; Sala and Perani, 2019) Changes in brain networks have been identified as a biomarker for detecting movement disorders such as Parkinson's disease and Dystonia.(Holtbernd and Eidelberg, 2012) They have vastly enabled the study of the integrity of functional brain networks non-invasively.

1.4.1 Diffusion-Weighted MRI

Diffusion Weighted Imaging (DWI) helps to study how the water molecules move around in the brain via the white matter tracts. Thus, they help to assess the integrity of white matter tracts in normal and pathological conditions. Data acquisition is performed using the diffusion MRI sequence, which introduces large gradient fields in addition to the three MRI gradients. The algorithm fits

a diffusion tensor model into every voxel of the image, and the tracts are drawn connecting one voxel to the other. Several metrics, such as Fractional Anisotropy (FA), Mean Diffusivity (MD), etc., are used to study the integrity of white matter tracts. Tracts from different regions of interest are combined into a connectome to explore the network perspective.

However recent studies have shown that 90% of the white matter voxels consist of two or more crossing fibers which means that fitting a single direction into a voxel using the diffusion tensor model is an inadequate representation of the complexity within a voxel.(Jeurissen et al., 2013) Thus, in combination with appropriate data modeling techniques, advanced diffusion encoding schemes such as q-ball imaging and high angular resolution schemes are used to delineate crossing fibers in tractography techniques. It is of paramount importance to study the effect of different field strengths and the number of gradient directions in establishing non-dominant tracts, which will be covered as one of the objectives of the thesis. Tractography methods offer insights into the structural integrity of the connections between distinct brain regions, but they do not provide information about the functional interactions between these areas. The functional information of the network is studied primarily via functional MRI (fMRI), Magneto Encephalography (MEG), or Positron Emission Tomography (PET) scans..

1.4.2 Functional MRI

Functional MRI measures the changes in the level of Blood Oxygen Level Dependent (BOLD) signal, which reflects changes occurring due to varying

levels of Oxygenated and Deoxygenated blood.(Raichle, 1998) Several volumes acquired over time help identify the changes in brain activity during that short time. It identifies the regions of the brain whose neural activities are correlated. The fMRI has excellent spatial resolution compared to techniques such as EEG but a poor temporal resolution. Different changes occur in the brain's functional activity associated with motor and non-motor manifestations of a neurological disease. In the case of PD, functional network changes specific to symptoms such as bradykinesia and tremor have also been identified using fMRI.(Concurrent decoding of distinct neurophysiological fingerprints of tremor and bradykinesia in Parkinson’s disease - PubMed, n.d.; Filippi et al., 2019) They also help to study the neural activity changes associated with the intervention.

1.4.3 Magnetoencephalography (MEG)

MEG uses magnetic sensors to detect the changes in the magnetic field associated with electrical activity in the brain. MEG is a non-invasive technique with significant spatial and temporal resolution.(Singh, 2014) It uses a large number of sensors (~300) and uses advanced source reconstruction algorithms. Connectivity measures such as time domain beamforming, imaginary coherence, phase lag index, synchronization likelihood, and envelope correlation metrics have been employed to study brain functionality.

1.4.4 Positron Emission Tomography

Positron Emission Tomography (PET) is one of the nuclear imaging techniques, which measures physiological function by monitoring, metabolic changes, neurotransmitter levels, blood flow, or radiolabeled drugs. During PET scans, a tracer labeled with oxygen-15, fluorine-18, carbon-11, etc is administered intravenously. The tracers upon decay emit positrons, which emit two gamma rays upon collision with an electron. These gamma rays are captured by gamma detectors and a three-dimensional image is reconstructed. For neurological applications, ^{15}O is used to measure changes in blood flow which correlates with changes in brain activity. In PD, PET scans have been used to study the activity of regions such as the cerebellum.(Ma et al., 2007; Network biomarkers for the diagnosis and treatment of movement disorders - ClinicalKey, n.d.) In this thesis, DWI and fMRI are used to study the structural, functional, and effective connectivity changes in CB-BG subcortical networks.

1.5 Overview of the pathophysiology of Parkinson's Disease

Parkinson's Disease (PD) is a heterogenous and diffuse neurodegenerative disorder; its cardinal motor manifestations emerges primarily from the dopaminergic neuron degeneration in Substantia Nigra pars compacta (SNpc).(Wichmann, 2018) PD exhibits motor symptoms such as akinesia/bradykinesia, resting tremors, and rigidity. The reduction of dopaminergic transmission in the nigro-striatal pathway underlies the motor symptoms in PD. Deficiency of dopamine affects the processing of

sensorimotor input from the cortex happening in the basal ganglia, and the final motor output.

Several models of basal ganglia circuit dysfunction in the pathophysiology of PD have been studied. 1-methyl-4-phenyl-1,2,3,6-tetrahydropyridine (MPTP) has been used to study PD models in animals.(Wichmann and DeLong, 2003) It causes permanent loss of dopamine neurons in the substantia nigra, thus leading to Parkinsonian symptoms. The dopaminergic neuronal loss leads to global changes in neural activity, reduces neuronal firing in GPe, and increases firing in STN and SNr in primates.

In Parkinsonian state, the neural activity of BG neurons and the surrounding areas tend to fall in synchrony and fire in a correlated fashion. An interesting feature of the pathophysiology involves burst discharge from GPi and SNr regions of BG.(Wichmann and Soares, 2006) This activity in the GPi and SNr nuclei is correlated with tremors. Explaining tremor physiology has always been challenging because tremor correlates with both the activity in the M1 and the cerebellar input-receiving region of the thalamus.(Parihar et al., 2015) The tremor is reduced with dopaminergic medications, but its mechanism is not yet fully understood.Both basal ganglia and cerebellar circuits are believed to participate in the genesis of Parkinsonian tremor. The other cardinal symptoms of PD- rigidity and bradykinesia- correlate more with nigrostriatal dopaminergic dysfunction and the resultant changes in the basal ganglia circuits. This explains why tremor, which involves non-dopaminergic cerebellar mechanisms too, remains refractory to dopaminergic medications

in many patients while rigidity and bradykinesia are generally amenable to them. Pathophysiological changes related to gait problems in PD have been associated with cholinergic and non-cholinergic neuronal loss in other areas like the PPN also and hence these are also sometimes refractory to dopaminergic medications.(Jf, 2009)

1.6 Role of the recently identified CB-BG network in the pathophysiology of PD

Even though PD has been identified as a classical basal ganglia disorder, recent neuroimaging studies have shown that the cerebellum is also involved in the pathophysiology of PD. Voxel-based morphometry studies have shown a reduction in the volume of the cerebellum in Patients with Parkinson's Disease (PwPD).(Benninger et al., 2009) Vim has been identified as an effective site for Deep Brain Stimulation (DBS) surgeries for treating tremors in PD.(Kumar et al., 1999) Vim is a region for Cerebellar input in the thalamus rather than basal ganglia input, which reinforces the findings that the cerebellum could be a source of abnormal signals contributing to resting tremors in PD. Cerebellar hyperactivation is associated with later stages of PD. STN-DBS and Vim-DBS have been shown to ameliorate hypermetabolism in the cerebellum.(Yu et al., 2007) (Hilker et al., 2004)

1.7 Hypothesis

With this background, the study hypothesizes that "Connectivity between basal ganglia and cerebellum can be demonstrated by rs-functional MRI and

Diffusion Weighted Imaging (DWI) in healthy volunteers and is altered differentially in patients with PD in its early stage where it could be compensatory and late stage contributing to the pathophysiology; levodopa could accordingly influence the functional and effective connectivity".

To validate the hypothesis, the following objectives were considered;

a. To compare different Diffusion-Weighted Imaging (DWI) acquisition schemes for establishing non-dominant crossing fibers using multi-shell DWI data from the Human Connectome Project (HCP)
b. To establish cerebellum-basal ganglia (CB-BG) structural connectivity in healthy subjects during resting state and to study the effect of age on properties of CB-BG tracts.
c. To examine functional, and effective connectivity between CB-BG reciprocal networks in early and late-stage Parkinson's patients, with and without levodopa.

1.8 The rationale for the study

Studies by Bostan et.al have established the CB-BG tracts in non-human primates, but their presence in human subjects needs further investigation. Further validation of current research on this topic is necessary on a larger dataset. Also, the role of the tracts in PD and its effects on the early and late stages of the disease remains unexplored. The question of whether the recently identified network has any role in therapeutic effects, such as the effects of levodopa, remains unanswered. Studying the structural, functional, and

effective connectivity of different nodes in the CB-BG network is necessary to address these questions.

The choice of diffusion encoding scheme for tractography is primarily driven by application. Hence, it is necessary to compare the effect of diffusion imaging parameters such as the number of diffusion encoding directions (NDED), gradient strengths (b-value), voxel size, and data modeling techniques on the tractography results. At lower field strengths, higher b-value acquisitions have been shown to have lower SNR, but at higher field strengths, a higher b-value acquisition provides better contrast and fewer artifacts. To compare the DWI acquisition schemes, the open-source dataset of MGH-USC Human Connectome Project Data is used, as it consists of multi-shell data with b-values 1000, 3000, 5000, and 10000 along with directions of 64, 64, 128, and 256 respectively. This step helps to select the correct DWI acquisition sequence, ensuring that the trade-off between acquisition time and reconstructed tract quality is addressed.

Structural connectivity doesn't necessarily ensure the connected nodes are functionally active. Hence, functional connectivity analysis is performed to study how the correlation in the activity of different nodes of the cerebellum-basal ganglia network is statistically dependent. The functional role of different subregions of the CB-BG network is poorly understood. Once the underlying mechanism of the circuit is explored in the healthy and disease state of PD, it helps in identifying newer therapeutic targets and the basis for new insights into a clinical intervention.

CHAPTER 2 LITERATURE REVIEW

Studies using retrograde and anterograde viral transport in non-human primates revealed a topographically mapped projection between basal ganglia and cerebellum indicating the regions are involved in more than just motor processing but also cognitive and emotional functions.(Bostan and Strick, 2018) DBS surgeries target STN to improve PD symptoms. It is hypothesized that suppressing aberrant activity in STN reduces abnormal and hyper-synchronised oscillations in the BG circuits, leading to decreased PD symptoms. DBS of STN is also very effective for the tremor of PD, for which cerebellar circuits also play a major role in addition to BG circuits. Further experimental studies are needed to characterize the role of different nodes in this motor BG network and their interaction with cerebellum. Also, several studies have validated the need for a system-level approach to studying the CB-BG network.(Caligiore, Pezzulo, et al., 2017)

The discussion of CB-BG connectivity starts with anterograde and retrograde viral transport studies on rats, which demonstrated disynaptic projections from the cerebellum to the laterodorsal striatum via the Central Lateral Nucleus.(Ichinohe et al., 2000) Similarly, a transneuronal virus study on macaque monkeys identified disynaptic projections from the dentate nucleus (DN) to the striatum, the input stage of basal ganglia. (Hoshi et al., 2005) The connection from basal ganglia to cerebellum was established later via viral injection to the cerebellar cortex and tracing the disynaptic projections back to the subthalamic nucleus (STN).(Bostan et al., 2010)

2.1 Structural connectivity studies on the CB-BG interconnecting network in healthy subjects

An attempt to establish the structural connectivity of the interconnecting network between CB-BG in humans was performed using Diffusion Tensor Imaging (DTI) on twelve subjects.(Pelzer et al., 2013) The study utilized a standardized segmentation protocol to obtain distinguished anatomical reliability and inter-observer stability. The study used the FDT toolbox in FSL software to perform probabilistic diffusion tractography. The results showed the tracts from the dentato-thalamo-striato-pallidal projections and the subthalamic-cerebellar connections. One of the major drawbacks of this study was that the problem of crossing fibers was not addressed in the analysis procedure. To distinguish crossing fibers, further studies with a wider age range along with a larger sample size is required.

Another study investigated CB-BG connectivity using Diffusion-Weighted Imaging and tractography capable of delineating crossing fibers, namely Constrained Spherical Deconvolution.(Milardi et al., 2016) The study performed probabilistic tractography on selected ROI in the basal ganglia and cerebellum in both the ipsilateral and contralateral fashion. The study used the number of streamlines between targets as a metric for establishing connectivity. The study confirmed streamlines from the dentate nucleus to the contralateral thalamus. However, the study also established streamlines connecting the dentate nucleus to the ipsilateral thalamus, which was not present in animal transneuronal viral transport study. The study showed

streamlines connecting the STN to the ipsilateral cerebellar cortex running through the ventral-basilar regions of the pons. Such a connection for the above laterality of streamlines was not found in the viral transport study in animals. The study claimed to have found an ipsilateral link from the dentate nucleus of the cerebellum to the Substantia Nigra (SN). Also, the authors claimed to be the first to establish extensive ipsilateral connections from the dentate nucleus to the Globus Pallidus. Even though they successfully showed these tracks, the study suffered from a low sample size and looked only into the young age group of 25-32 yrs with a mean age of 29 yrs. The CB-BG network using Diffusion-Weighted Imaging is yet to be studied on a larger sample size of subjects. The alteration of the structural integrity of the network with age is yet to be explored.

2.2 Functional connectivity studies on the CB-BG interconnecting network in healthy subjects

Neuroimaging studies conducted on healthy subjects showed coactivations in the cerebellum and basal ganglia regions during various tasks. During event-related fMRI during the study of temporal difference learning which is a model for Pavlovian Conditioning, the studies found that regions of the cerebellum and basal ganglia are correlated with the temporal difference prediction error metric, suggesting that cerebellum and basal ganglia function together during appetitive condition with a pleasant reward.(O'Doherty et al., 2003) Similar studies on higher-order aversive conditioning demonstrated coactivations between the regions of the cerebellum and basal ganglia.(Seymour et al., 2004)

A PET imaging study on movement vigor showed an increase in the regional cerebral blood flow in both the regions of the cerebellum and basal ganglia.(Turner et al., 2003) During adaptation tasks involving visuomotor rotation, using a joystick while inside an fMRI, the sensorimotor adaptation is associated with increased activity in the cerebellar and basal ganglia regions.(Seidler et al., 2006) During sequence learning tasks, in the early stages, the STN and cerebellar regions are co-activated.(Lehéricy et al., 2005) Even though similar coactivation studies have been reported, the exact functional connectivity within the regions of the CB-BG network, reported in non-human primates, remains unexplored.

2.3 Structural changes in the CB-BG network regions in PD

Atrophic changes associated with PD in individual regions within the CB-BG network have been documented. Nigral and putaminal structural changes have been recorded in PD patients and their structural integrity was demonstrated to play a crucial role in the improvement of motor symptoms as a response to levodopa treatment.(Schröter et al., 2022) Also, deformation-based morphometric studies show an accelerated decrease in the volume of putamen in PD patients as the disease progresses.(Pieperhoff et al., 2022) Morphological changes associated with STN in mild-to-moderate PD patients show a reduction in volume and Fractional Anisotropy (FA) values.(Patriat et al., 2020) Similar changes in morphometry have been observed in the cerebellum in PD patients. Iron accumulation was observed in the dentate nuclei in tremor-dominant PD patients positively correlating with tremor

severity.(Acosta-Cabronero et al., 2017; Guan et al., 2017; He et al., 2017) Atrophic changes in the cerebellum have a significant effect on the network connectivity in PD.(O'Callaghan et al., 2016) Even in pedunculopontine nuclei, mitochondrial abnormalities cause type-specific neuronal loss and changes to cell morphology in PD.(Henrich et al., 2020) Even though structural changes have been observed in individual regions of the CB-BG interconnecting network, the changes to the white matter bundle connecting these regions haven't been studied.

2.4 Functional connectivity changes in the CB-BG network in PD

Earlier studies show that the functional connectivity between the striatum and the rest of the brain is reduced in PD patients compared to controls which indicates a disruption of the striatal network with PD which leads to loss of motor control and coordination.(Baggio et al., 2019) Also, the posterior putamen has been shown to have a reduced functional connectivity with regions including brainstem and cerebellum which shows a change in connectivity between these regions in PD patients.(Hacker et al., 2012) In PD patients with tremor, the putamen was found to be transiently activated and the CTC network activity correlated with the tremor amplitude, pointing towards a pathological interaction between the basal ganglia and the CTC network in PD.(Helmich et al., 2021) But the question about the exact mechanism of interaction remains unanswered. Similar to the putamen involvement in tremor, increased dentato-cerebellar connectivity and lower dentato-prefrontal connectivity were observed in PD.(Ma et al., 2015)

Similarly functional connectivity between pons and regions associated with affective processing and motor functions such as the striatum, brainstem, thalamus, and cerebellum has been reported.(Huot, 2015) All the findings imply a change in connectivity in all the regions involved in the recently identified direct subcortical CB-BG network in non-human primates, but the exact pathway facilitating these changes in human subjects needs further exploration.

2.5 Research Gap and Novelty in the research

There is an absence of research in humans that specifically investigates the structural connections from the cerebellum to basal ganglia and vice versa discovered in non-human primates. The age-associated degeneration of white matter tracts in the CB-BG interconnecting direct subcortical network remains largely unexplored. Understanding how these microstructural changes happen with age will help explain the neurological processes that underlie motor impairment in Parkinson's disease (PD). Functional connectivity changes within this network haven’t been explored in the present literature. Exploring how functional connectivity changes manifest in PD can offer crucial insights into the disease progression and its effect on motor and non-motor symptoms. Additionally, the effective connectivity within the CB-BG network in PD hasn’t been investigated. Understanding the directional influences and information flow within this network can shed light on the neural mechanisms underlying motor or non-motor impairments in PD. Moreover, the impact of medication on functional connectivity within this network remains under

explored. Investigating how pharmacological interventions influence network connectivity can provide valuable information on the mechanisms through which dopamine replacement ameliorates motor symptoms in PD.

The novelty of this study lies in its comprehensive approach to establishing both the structural and functional connectivity within the CB-BG network. By examining age-related degeneration in white matter bundles, exploring changes in functional and effective connectivity across different stages of PD, and investigating the effects of medication on network dynamics, this study aims to address critical gaps in the current literature, thereby increasing our understanding of the PD's pathophysiological underpinnings.

CHAPTER 3 MATERIALS AND METHODS

In this chapter, the experiment design and techniques to test the hypothesis that "Connectivity between basal ganglia and cerebellum (structural, functional and effective connectivity) can be demonstrated by rs-fMRI and DTI in healthy volunteers and is altered in patients with PD differentially in its early and late stages; the drug levodopa can influence the functional and effective connectivity", is discussed. To test the hypothesis, three objectives were formulated and the experiments mentioned below were conducted,

1. Comparison of DWI acquisition schemes for Tractography
2. Establishing structural connectivity of the CB-BG network
3. Functional and effectivity connectivity changes in the CB-BG network in PD patients compared to healthy controls

In the first experiment, a comparison of DWI acquisition schemes for establishing non-dominant crossing fibers using multi-shell DTI data from the Human Connectome Project (HCP) was performed. The lateral projections of the Corticospinal Tract (CST) were selected as the non-dominant fiber bundle of interest. This specific tract was selected because the lateral projections are rare to be observed using tensor-based fiber tracking but are well known to be present. A study by Lee et.al demonstrated the effect of crossing fibers in determining the lateral projections of CST due to crossing fibers from superior longitudinal fasciculus by comparing the results from tensor-based fiber tracking in healthy subjects and patients with the congenital bilateral

perisylvian syndrome.(Lee et al., 2015) The CB-BG interconnecting tract being studied has similar characteristics as they travel from one hemisphere to the contralateral end during which the possibility of encountering crossing fibers is higher. Thus different combinations of parameters of b-value, NDED, and voxel size were studied. Here CSD was used for tractography as it was able to delineate tracts with crossing fibers better compared to tensor-based fiber tracking. In the second experiment, tractography of the CB-BG tract was performed in healthy subjects to establish the tracts as seen in non-human primates. Also, age-associated changes in this WM bundle were studied. Also, an attempt was made to study the role of these tracts in memory and learning. In the third experiment, the functional, and effective connectivity between the CB-BG reciprocal network was studied for healthy subjects and PwPD in early and late-stage, with and without levodopa. The materials and methods, results, and discussion sections are explained in detail for the three experiments conducted.

3.1 Comparison of DWI acquisition schemes for Tractography

3.1.1 Data Acquisition

The Diffusion-Weighted Imaging (DWI) data for the study was obtained from the MGH-USC Human Connectome Project (HCP) dataset. The study is designed as shown in **Figure 1**. The data was acquired from healthy adults in the age range of 20-59 using the customized Siemens 3T Connectome Scanner, which is a modified 3T Skyra system(Setsompop et al., 2013) (MAGNETOM

Skyra Siemens Healthcare) with a 64-channel, tight-fitting brain array coil(B et al., 2013).

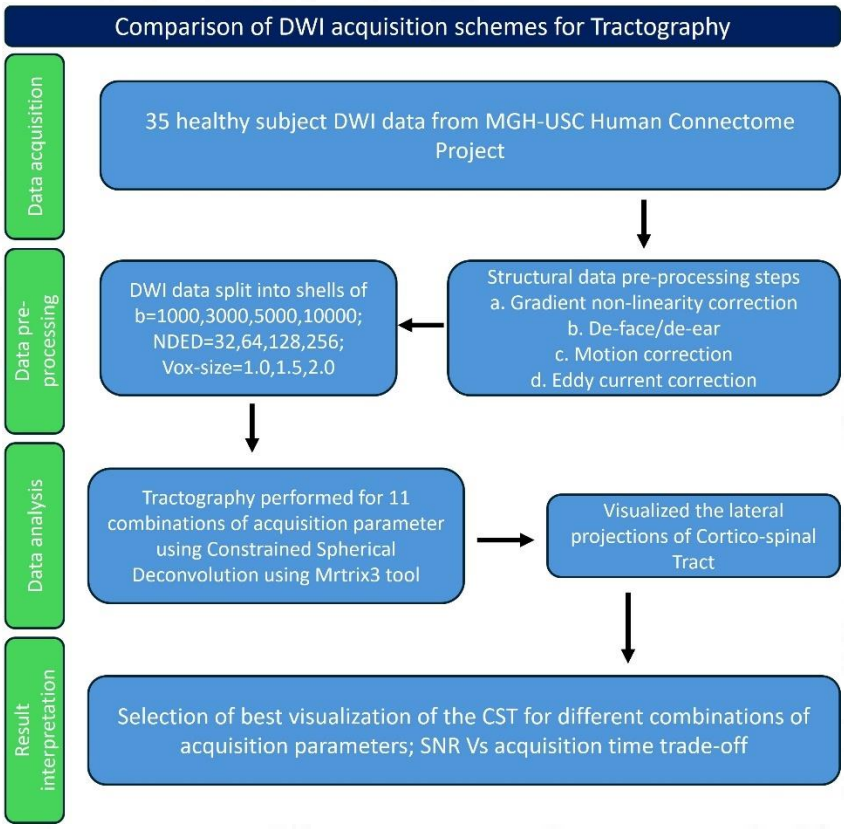

Figure 1: Study design for comparison of DWI acquisition schemes for tractography.

The MGH Young Adult HCP dataset consists of an MPRAGE scan, high-resolution T2 scan, and diffusion scan with 4 different b-values (s/mm2) (1000, 3000, 5000, 10000) as in **Figure *2***. Diffusion scans have been acquired in oblique axial slices with mono-polar gradients. The diffusion scans comprised of 5 runs with b-values, directions, and acquisition times as follows; (1000: 64 directions: 11:44 min; 3000: 64 directions: 11:44 min; 5000: 128 directions, 21:55 min; 10000: 128 directions: 21:55 min; 10000: 128

directions: 21:55 min). The diffusion scans were acquired using a spin-echo EPI sequence with 1.5mm isotropic voxels (TR/TE=8800/57 ms, FOV=210x210, image matrix=140x140, 96 slices, slice thickness=1.5mm). One non-diffusion weighted (b=0) image was collected every 14 volume acquisitions, making the total number of volumes to be 552. Structural scan acquired using a 3-D MPRAGE sequence T1w images consists of 1mm isotropic voxels with TR and TE of 2530 ms and 1.15 ms respectively and acquisition time of 6:02 min. The T2w image consists of 0.7mm isotropic voxels with TR and TE of 3200 ms and 561 ms respectively and an acquisition time of 6:48 min.

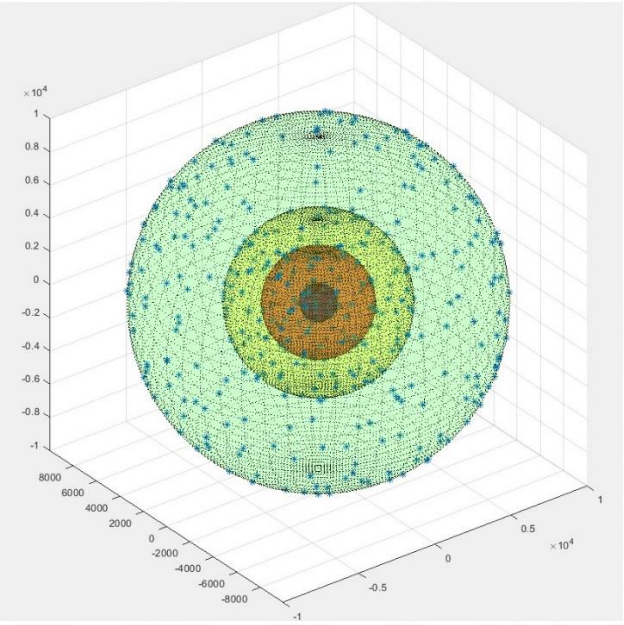

Figure 2: Representation of multishell data. Figure showing the multi-shell data with each point representing the direction of the gradient vector and concentric spheres representing the different b-valued shells.

3.1.2 Preprocessing

The minimally pre-processed data from the HCP dataset was used for tractography analysis. The minimal pre-processing pipeline for the structural scans consists of gradient non-linearity correction based on spherical harmonic coefficients(Jovicich et al., 2006; Mf et al., 2013) followed by de-face and de-ear. The diffusion scans underwent gradient non-linearity correction, motion correction, and eddy current correction.(Andersson and Sotiropoulos, 2016)

3.1.3 Multishell data extraction

To study the effect of different acquisition parameters namely b-value, NDED, and voxel size on delineating the non-dominant crossing fibers in the cerebellum and basal ganglia interconnecting network, the HCP multi-shell data was split into multiple combinations of different parameters and analyzed separately. The tractography was done using the Mrtrix3 toolbox(Tournier et al., 2019) and functions in the FSL toolkit. To study the effect of the b-value in delineating the crossing fibers, the different shells were split using the *dwiextract* function in mrtrix3 as shown in **Figure 3**. To study the effect of the NDED, multiple subsets of the total directions were extracted for shells of b=1000 (32,64 directions) and b=10000 (128,256). To ensure that the spherical distribution of encoding gradient angles is uniform, the gradient vector file is sorted using the *dirorder* command in mrtrix3(Tournier et al., 2019). The *dirorder* command reorders the set of directions and ensures near-uniformity upon truncation at a certain number of directions. **Figure 4**, shows the distribution of the gradient vector with 64 and 128 directions before and after

ordering them using the *dirorder* function. While trying to improve the SNR by adjusting the voxel size, it has been shown that tractography results are significantly affected by the partial volume effects, and reducing the voxel dimensions has been shown to reduce the partial volume effects in cross-callosal connections between the bi-hemispheric visual cortices(Analysis of partial volume effects in diffusion-tensor MRI - Alexander - 2001 - Magnetic Resonance in Medicine - Wiley Online Library, n.d.; Functional organization of human occipital-callosal fiber tracts | PNAS, n.d.; Kim et al., 2006). Thus, to study, the effect of spatial resolution, the raw image with the voxel size of $1.5mm^3$ (resolution of 1.5x1.5x1.5) was rescaled into three different datasets by using the *mrgrid* function in mrtrix3 using the cubic interpolation. The three datasets consisted of voxel sizes of $1.0mm^3$ (resolution of 1.0x1.0x1.0), $5.625mm^3$ (resolution of 1.5x1.5x2.5), and $8.0mm^3$ (resolution of 2.0x2.0x2.0). The diffusion data were fitted with Fibre Orientation Distribution (FOD) using the option of 'iFOD2' in the '*tckgen*' function of mrtrix3 which performs fiber tractography.

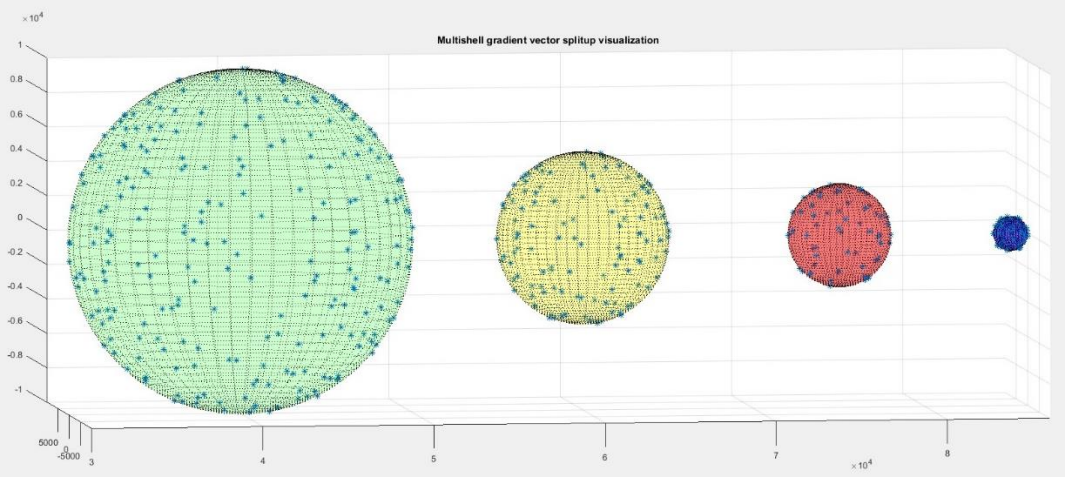

Figure 3: Visualization of multishell gradient vector split-up. Figure showing the different shells and the distribution of gradient vectors on them after splitting them using the dwiextract function from mrtrix3.

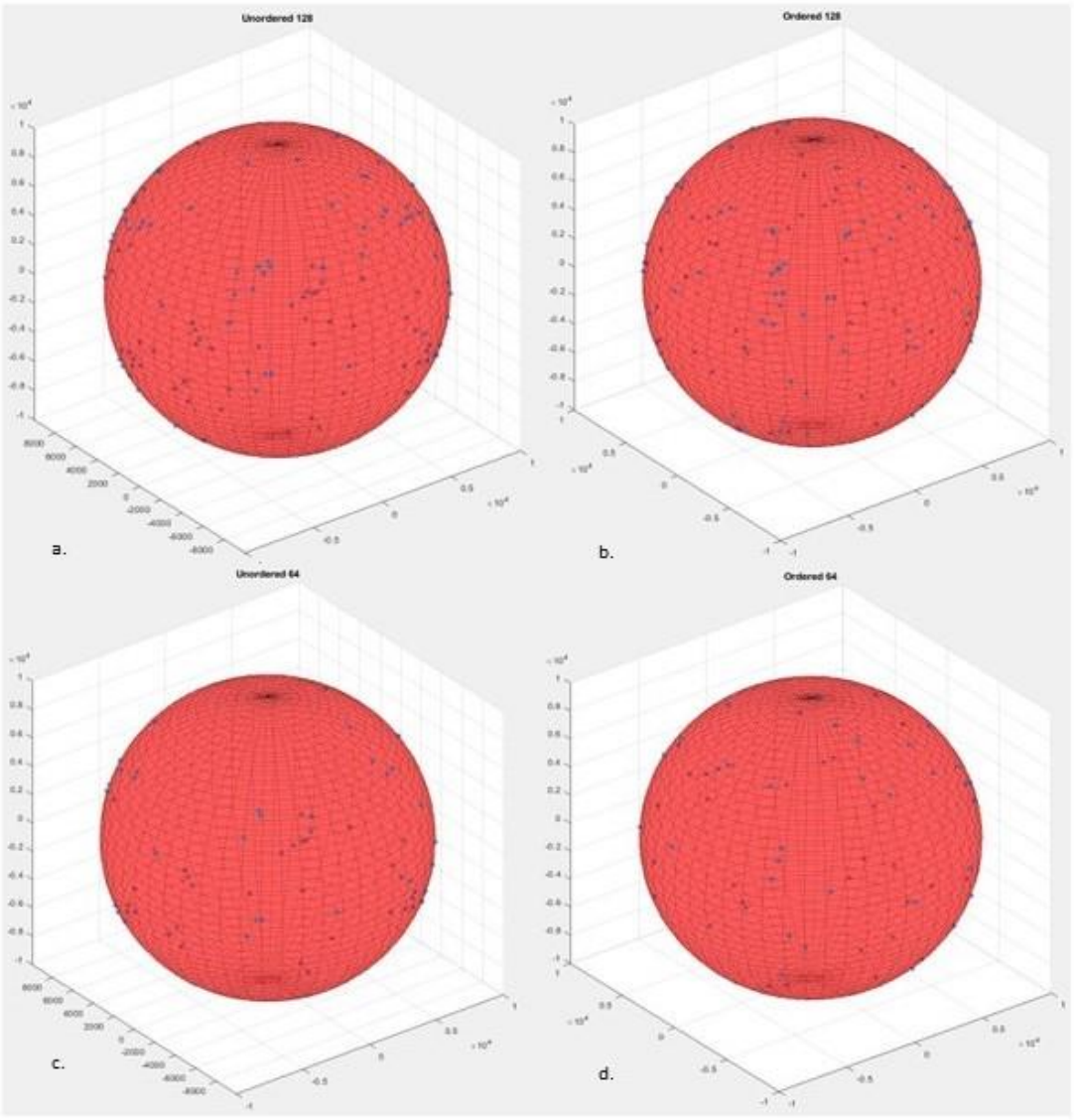

Figure 4: Distribution of ordered and unordered gradient vectors. Figure showing the distribution of 128 and 64-direction unordered vs ordered gradient vectors extracted from b=10000 value shell data with 256 directions.

3.1.4 Tractography

The Mrtrix3 toolbox was used to perform the tractography analysis (Tournier et al., 2019) along with a few other functions in the FSL toolkit. First, the Brain Extraction Tool (BET) was used to remove the non-brain tissue(Smith, 2002;

Smith et al., 2004). The *dwi2response* function with the "dhollander" algorithm was used to estimate the response function from the brain-extracted pre-processed data(Tournier et al., 2004). Following this, *dwi2fod* function was used to estimate fiber orientation distribution (FOD) based on Constrained Spherical Deconvolution (CSD). The fiber tracking was performed using the *tckgen* function with the "iFOD2" option which performs improved 2nd order integration over fiber orientation distribution. This option enhances anatomical plausibility by facilitating more accurate fiber reconstruction in heavily curved regions(Tournier et al., n.d.). During the tracking process, the probability of a particular direction is set to be proportional to the amplitude of the FOD along that direction. The following additional *tckgen* settings were used: max angle between successive steps=22.5º, max length= 250 mm, min length=10 mm, cut off FA value=0.4, FOD is raised to a power of 1, and the maximum number of fibres=10000. The tractography results for the combinations of acquisition parameters in **Error! Reference source not found.**, were visually compared to study the effect of NDED, b-value, and voxel size.

Table 1: Table showing the different combinations of acquisition parameters compared during each trial to study their effects on the tractography results.

S. No	NDED	b-value	Voxel size
1	64	1000	1.5x1.5x2.5
2	64	3000	1.5x1.5x2.5
3	64	5000	1.5x1.5x2.5
4	64	10000	1.5x1.5x2.5
5	32	1000	1.5x1.5x2.5
6	64	1000	1.5x1.5x2.5
7	128	10000	1.5x1.5x2.5
8	256	10000	1.5x1.5x2.5
9	64	1000	2.0x2.0x2.0

10	64	1000	1.5x1.5x1.5
11	64	1000	1.0x1.0x1.0

3.2 Establishing structural connectivity of the CB-BG network

3.2.1 Subject recruitment and clinical data acquisition

Sixty-four healthy volunteers aged between 30 and 80 years, with a mean age of 55.69 ± 9.96 years, were recruited over 3 years from the Sree Chitra Tirunal Institute for Medical Sciences and Technology in India. Recruitment was done through notifications at the hospital campus. The study was designed as shown in **Figure 5**. These volunteers had no history of neurological or psychiatric conditions and had more than 6 years of formal education. MRI scans were examined by a radiologist to ensure no structural asymptomatic lesions were present. Among the 64 participants, 20 individuals with a Clinical Dementia Rating (CDR) score of 0, with a mean age of 56.8 ± 8.7 years and an age range of 41–66 years, underwent neuropsychological tests. The tests included the vernacular (Malayalam) adaptation of Addenbrooke's Cognitive Examination battery (ACE-M) and the Rey Auditory Verbal Learning Test (RAVLT). The assessment focused on learning and retention through various domains of the ACE neuropsychological analysis, such as ACE-M-Reg-24 for registration and learning, ACE-M-Recall for recall, and the overall ACE-M score. Additionally, retention scores included delayed recall and total scores from the RAVLT.

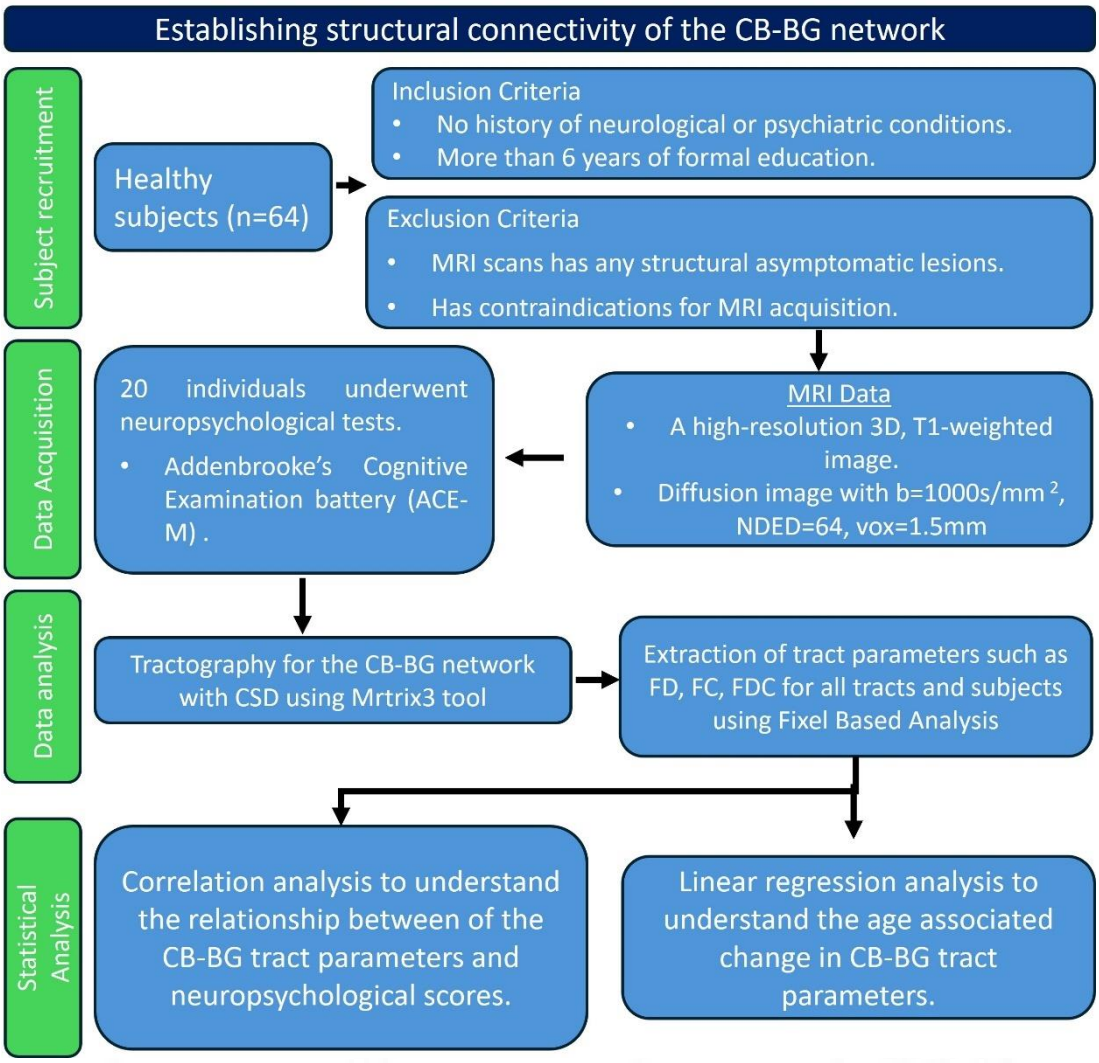

Figure 5: Figure showing the study design for establishing the structural connections in CB-BG network.

3.2.2 MRI data acquisition

The structural and diffusion MRI data were obtained using a 3-tesla scanner (GE MEDICAL SYSTEMS, Discovery MR750w, Chicago, Illinois, United States) equipped with a 32-channel, phased-array head coil designed for parallel imaging. For structural imaging, a high-resolution 3D, T1-weighted, fast spoiled, gradient-echo sequence was utilized with the following parameters: TR = 7.924 ms, TE = 2.984 ms, Flip angle = 12, matrix = 256 ×

256, and 172 sections of 1 mm each. On the other hand, diffusion-weighted MRI (dMRI) was conducted using a single-shot echo-planar spin-echo sequence with 64 directions, TR = 9,000 ms, TE = 99.8 ms, matrix = 256 × 256, b = 0 and 1,000 s/mm^2, and 57 slices of 2 mm thickness for each subject.

3.2.3 Tractography

The tractography analysis was conducted using the Mrtrix3 toolbox and functions within the FSL toolkit, as illustrated in **Figure 6**. Initial preprocessing steps involved denoising through the Marchenko-Pastur Principal Component Analysis (MP-PCA), followed by the removal of Gibbs ringing and correction for Eddy currents. Non-brain tissues were eliminated using the Brain Extraction Tool (BET). The estimation of the response function from the brain was achieved through the dwi2response function using the "dhollander" algorithm. Subsequently, the determination of the fiber orientation distribution (FOD) was based on eighth-order CSD using the dwi2fod function. Fiber tracking for each subject was performed using the tckgen function with the "iFOD2" option, which enhances anatomical plausibility by improving fiber reconstruction accuracy in highly curved regions. Direction probability during tracking was set proportionally to the FOD amplitude. Specific tckgen settings were applied, including constraints on angle (22.5°), length (min=10mm, max=250mm), FA(0.4), and fiber count (1 million) to minimize false positives. Manual segmentation of Regions of Interest (ROIs) by two independent observers was conducted, with the final ROI defined by the intersection of the two ROIs with overlap exceeding 80%.

To extract tract parameters, a fixel mask for the tracts was generated using the tck2fixel function and applied to FD, FC, FDC, and logFC fixel images in a common template space after transforming the individual subjects to template space.

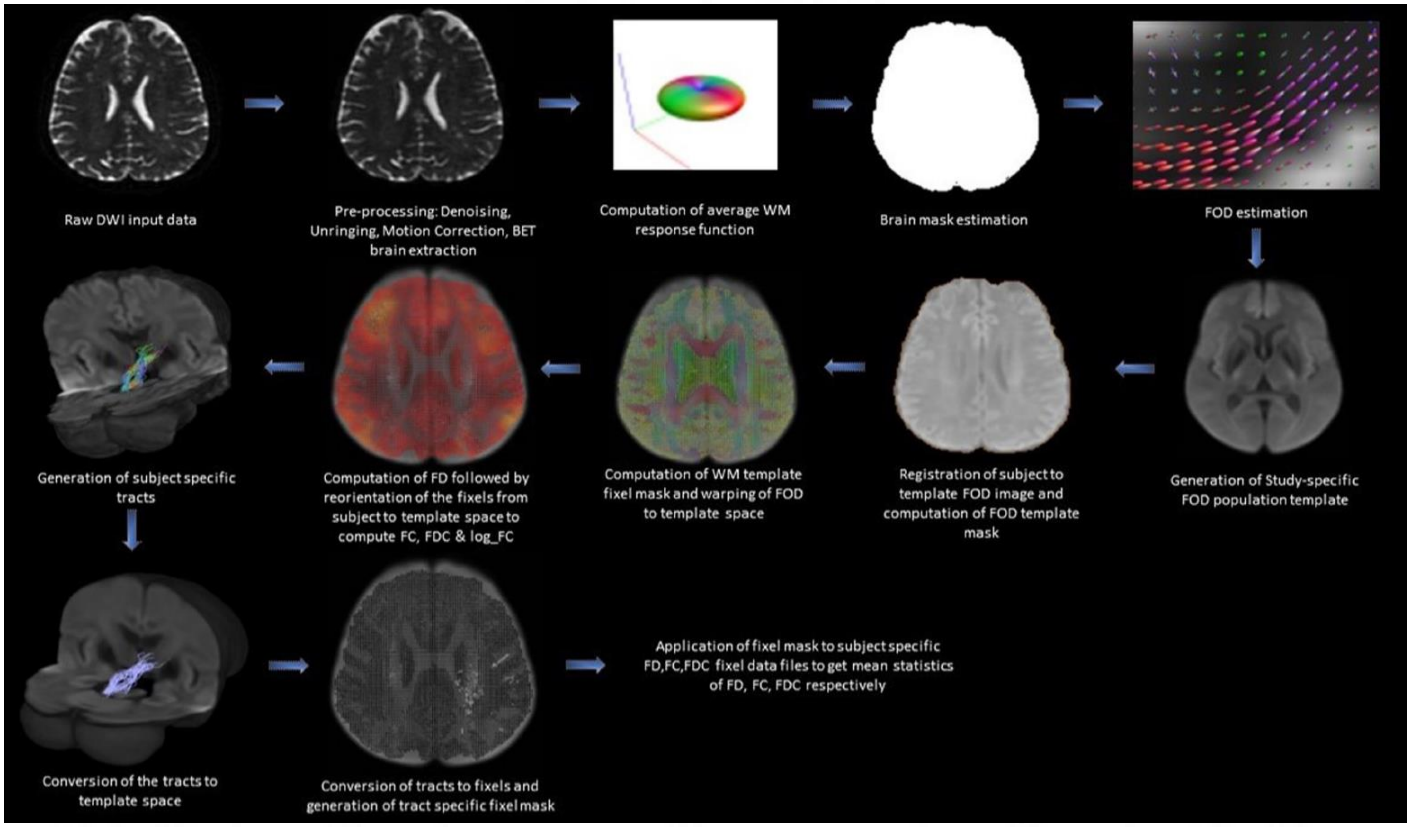

Figure 6: Steps in Fixel-Based Analysis using CSD. Figure showing the steps involved in the creation of tract-specific Fixel-Based Analysis (FBA) metrics. Reprinted from Vineeth et al. (2023, 10.3389/fnagi.2023.1019239).

3.2.4 Definition of regions of interest

Regions of Interest (ROIs) were obtained using the automated anatomical labeling atlas 3 (AAL3),(Rolls et al., 2020) containing the motor (region indexes: 1–2, 15–16, 61–62, 73–74) and prefrontal cortices (region indexes 19–20, 151–156). Subsequently, the masks were transformed from MNI to

individual native space using the inverse transform. In cases where the inverse transform lacked spatial precision for deep and small nuclei, a manual segmentation approach was adopted. Two independent observers delineated the ROIs using FSLeyes(McCarthy, 2019) on T1w MRI images (Thalamus and Putamen) and FOD images (STN and Dentate Nucleus). To address inter-observer variability, voxels overlapping between the observers were selected for analysis. The analysis involved calculating (i) the volume of the intersection of the ROIs by multiplying the binary mask of the ROI from both observers using fslmaths and fslstats; (ii) determining the total volume of their combination by adding them using fslmaths and fslstats. The ratio between the volume of intersection and the combined volume of ROIs was then computed. The ROIs drawn by the two observers with an overlap exceeding 80%, only were used in the analysis.

The segmentation of the thalamus was conducted on the T1-weighted image of each participant in the coronal plane (**Figure 7**A). The stria terminalis defines the anterior boundary, while the internal capsule forms the lateral and ventromedial boundaries. The dorsolateral boundary was established by the genu and the caudate nucleus. Corrections were made in the sagittal and axial planes to refine the segmentation process.

The segmentation of the putamen was carried out on the T1-weighted image of each individual in the axial plane (**Figure 7**B). The external capsule defined the lateral border, while the anterior limb of the internal capsule marked the ventromedial boundary, and the posteromedial boundary was delineated by the

posterior limb. Corrections were made to the mask in the sagittal and coronal planes to ensure accuracy in the segmentation process.

The segmentation of the subthalamic nucleus (STN) was performed on the Fiber Orientation Distribution (FOD) image derived from the diffusion-weighted image. Its location was determined in relation to the red nucleus, identifiable as a hypointense area in the brain stem on the axial slice (**Figure 7**C). The STN was delineated 3 mm anterolaterally from the red nucleus, situated beneath the thalamus.

The dentate nucleus (DN) was delineated on the FOD image derived from the diffusion-weighted image of each subject (**Figure 7**D). It was characterized by the hypointense semi-circular region within the cerebellum, oriented with the opening directed towards the midline. The ventral tegmental area (VTA) was delineated on the axial slice of the FOD image derived from the diffusion image, following the methodology described by Ballard et al.(Ballard et al., 2011) and illustrated in Figure **Figure 7**E.

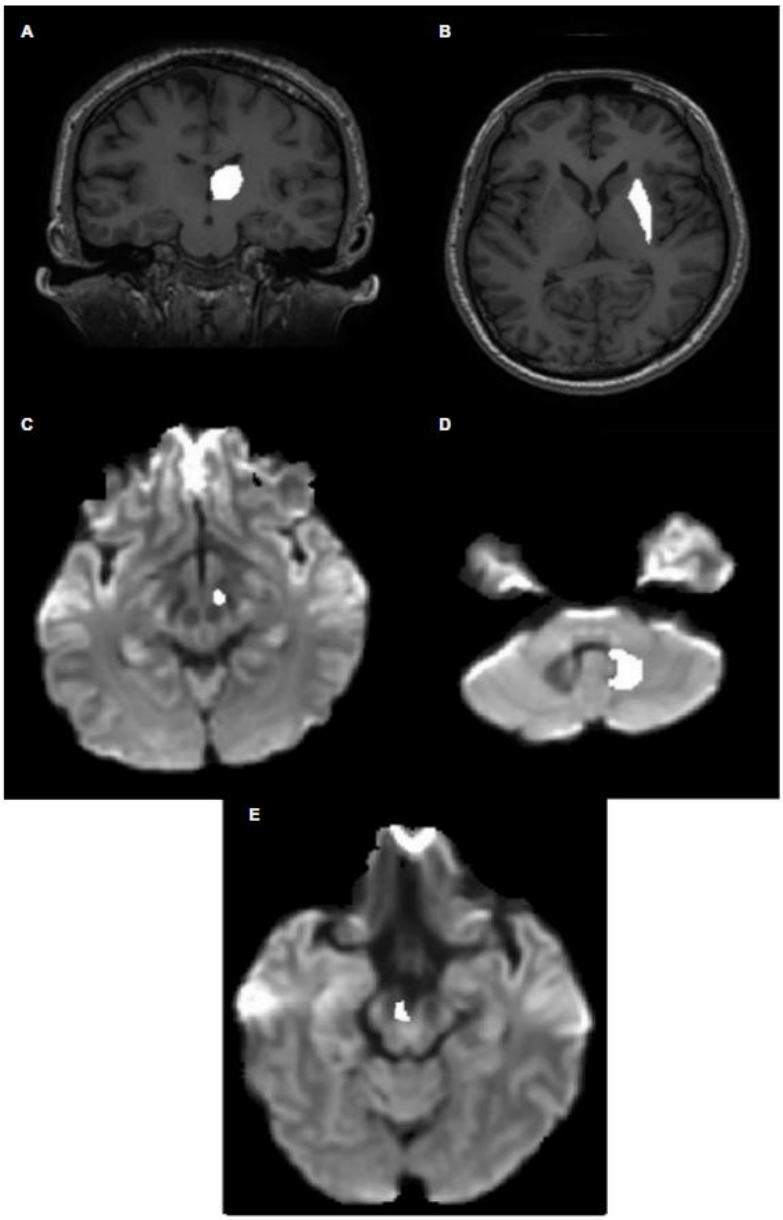

Figure 7: Manual segmentation of Regions of Interest. Figure showing the definition of Regions of Interest (ROIs) within the individual native space. (A) Overlay of Thalamic ROI mask on the T1 image. (B) Overlay of Putamen ROI mask on the T1 image. (C) Overlay of STN ROI on the Fiber Orientation Distribution (FOD) image. (D) Identification of hypointense regions surrounding the DN in the cerebellum on the FOD image. (E) Overlay of VTA ROI on the FOD image. CB refers to the cerebellum; DN denotes the dentate nucleus; STN represents the subthalamic nucleus; VTA signifies the ventral tegmental area. Reprinted from Vineeth et al. (2023, 10.3389/fnagi.2023.1019239).

3.2.5 Total Intracranial Volume (TIV) calculation

The total intracranial volume (TIV) was determined by processing the T1-weighted images through the Computational Anatomy Toolbox (CAT12) within the SPM12 software running in MATLAB (R2019a: The MathWorks, Inc., Natick, MA, United States). TIV was calculated by adding the volumes of WM, GM, and CSF obtained by the segmentation of the T1-weighted images into specific components.

3.2.6 Tract reconstruction

In the reconstruction of the ascending tracts detailed below, the thalamus was used as an inclusion mask to establish a reliable trajectory based on the anatomical features observed in human and non-human primates.(Bostan et al., 2010; Bostan and Strick, 2018; Hoshi et al., 2005) To identify contralateral tracts, exclusion masks consisting of the opposite cerebellar hemisphere and an interhemispheric mask consisting of the corpus callosum were used.

3.2.6.1 Ascending Cerebello-thalamocortical Tracts

The Cerebello-thalamocortical (CTC) tracts projecting to known cortical motor areas with documented trajectories(Yamada et al., 2010) were studied as controls. The cerebellar dentate nucleus was used as the seed region, with contralateral cortical motor areas serving as target regions (inclusion mask = contralateral thalamus).

3.2.6.2 Ascending Cerebello-thalamo-striatal (CTS) Tract

To study the ascending, cerebello-thalamo-striatal tract, the dentate nucleus was identified as the seed region, and the contralateral putamen was designated as the target region (inclusion mask = contralateral thalamus).

3.2.6.3 Descending Subthalamo-ponto-cerebellar (SPC) Tract involving crus II and VIIb

To study the descending, subthalamo-ponto-cerebellar tract, the subthalamic nucleus (STN) was defined as the seed region, with the contralateral Crus II and VIIb as the target regions.

3.2.6.4 Cerebello-prefrontal Tracts via VTA and Thalamus

To study the cerebello-prefrontal tracts, tractography was performed on tracts originating from the dentate nucleus and extending to the contralateral prefrontal cortex (ACC/mPFC) with either the VTA(Carta et al., 2019) or thalamus as the inclusion regions.

3.2.7 Statistical analysis

After confirming the normal distribution of data, the impact of age on the morphological characteristics of cerebellar tracts was studied using a linear regression model. The correlation between the average parameters of Fiber Density (FD), Fiber Cross-section (FC), and Fiber Density and Cross-section (FDC) across fixels within each tract (cerebello-thalamo-striatal and STN-Crus7b;), with age as the focal covariate was studied. The analysis included sex, education, and total intracranial volume (TIV) of the participants as nuisance regressors. The analysis was conducted using the statistics and machine learning toolbox within MATLAB (R2019a: The MathWorks, Inc.,

Natick, Massachusetts, United States). Bonferroni correction was used to adjust for multiple comparisons at a statistical significance level of $p < 0.05$. Furthermore, to explore the relationship between neuropsychological scores derived from ACE-M/RAVLT and FBA tract parameters, Pearson's correlation analysis was performed, controlling for age, sex, and education variables. Similar to the previous analysis, Bonferroni correction was used to adjust for multiple comparisons a statistical significance level of $p < 0.05$.

3.3 Functional and effectivity connectivity changes in the CB-BG network in patients compared to controls

3.3.1 Subject recruitment and clinical data acquisition

Thirty-six PD patients (mean age = 53.2±9.61 years, men 19) diagnosed with PD based on the United Kingdom Parkinson's Disease Society Brain Bank (UKPDSBB) Clinical Diagnostics Criteria were recruited by experienced movement disorder specialist from the Movement Disorders Clinic of the hospital. The study is designed as shown in Figure 8. Patients were categorized based on the duration of the disease as Early (disease duration <5 years) or Late PD (disease duration >5 years). Thirty-one age-matched, healthy volunteers (HV) with no history of neurological or psychiatric illness were recruited as controls via call notification exhibited on the hospital premises. Inclusion criteria for all the subjects included; age between 30 and 70 years, formal education >10 years, vision and hearing adequate for the completion of the examination. Inclusion criteria for the patients included stable PD medications for the previous 3 months and a Mini-Mental State Examination

(MMSE) score of 24 or greater. Exclusion criteria included, severe cognitive deficits, tremor-dominant PD, or severe LID, unable to cooperate with ON-state MRI, patients with severe systemic diseases, or psychiatric or other neurological illnesses. Participants with contraindications for undergoing an MRI were also excluded from the study. All patients were required to visit the Movement Disorders Clinic without taking their morning dose of medications and their clinical assessment was performed by the movement disorder specialist using the Unified Parkinsons Disease Rating Scale III (UPDRS III) in the medication OFF state. The patients were given L-Dopa/Carbidopa (100/25mg) and their UPDRS-III scores were recorded every 15 minutes to obtain the UPDRS score in their best-ON state. The study was approved by the Institutional Ethics Committee and all the subjects provided written consent as per the declaration of Helsinki.

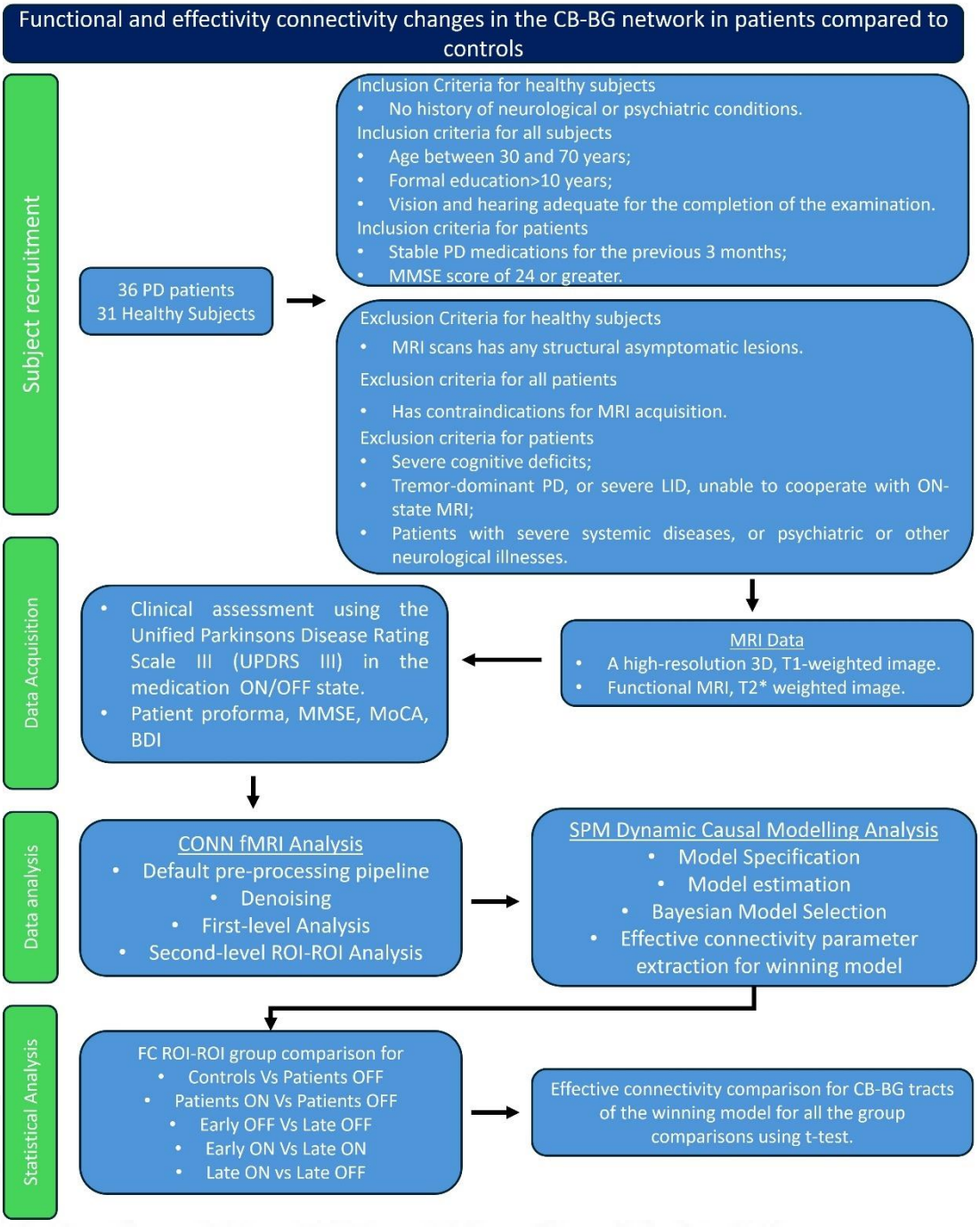

Figure 8: Functional and effectivity connectivity changes in the CB-BG network.

3.3.2 MRI data acquisition

All patients and controls underwent an MRI. Structural and functional MRI data were acquired with a 3-tesla scanner (GE MEDICAL SYSTEMS,

Discovery MR750w) using a 32-channel, phased array head coil designed for parallel imaging. Blood Oxygen Level Dependent (BOLD) signal was acquired using the single-shot echo-planar images (TR=2500 ms, TE=30 ms, Flip angle=80, 64x64 matrix, 43 contiguous 3.20-mm-thick axial slices, 150 volumes, acquisition time= 6.25 min) in the resting condition. Participants were instructed not to consume any tea/coffee or any other stimulant, for a minimum of 6 hours before the scan. All the participants were instructed to lie down awake, in a supine position inside the scanner with their eyes closed during the entire duration of the scan. A high-resolution 3D T1-weighted fast spoiled gradient echo sequence (TR=7.924 ms, TE=2.984 ms, Flip angle=12, matrix=256x256, 172 sections of 1mm each) was also acquired for each participant.

For the patient group, the OFF-state fMRI was acquired during their worst-off state in the morning after a 12-hour withdrawal of the drug. The patients were asked to stop dopamine agonists 48 hours before their scheduled MRI scans. The ON state fMRI was acquired in the best-ON state. Any patient developing head tremor or neck dyskinesia while in the scanner, resulting in a motion parameter greater than 1.5mm measured, was excluded from the study.

3.3.3 Pre-processing and functional connectivity analysis

Statistical Parametric Mapping version 12 (SPM12) and CONN functional connectivity toolbox version 21.a RRID: SCR_009550)(Whitfield-Gabrieli and Nieto-Castanon, 2012) were used for the analysis of resting-state fMRI data to infer functional connectivity changes. The default pre-processing

pipeline in the CONN toolbox was used for volume-based analysis (in Montreal Neurological Institute (MNI) space). Each subject's functional volumes were realigned to the first volume and unwarped to estimate and remove movement-by-susceptibility-induced variance in the fMRI time series.(Andersson et al., 2001) The images were slice-time corrected and all the structural images were segmented into GM, WM, and CSF for co-registration with the functional images, and normalization to MNI space. A Gaussian kernel (FWHM = 5 mm) was used to smooth the images. Outlier volumes with high motion were detected using the ART-based scrubbing method (ART parameters, 2mm subject motion threshold, and a global signal threshold set at z=9). Six realignment parameters and the first five principal components from the white matter and CSF along with the outlier volumes from the scrubbing procedure were added as the nuisance variables and regressed out of the signal.(Behzadi et al., 2007) The data were linearly detrended and band-pass filtered (0.008 to 0.09 Hz).(Weissenbacher et al., 2009)

3.3.4 Effective connectivity analysis setup

To model the intrinsic dynamics of the circuit in the resting state, effective connectivity, which subtends the information on regional correlations from functional connectivity to the causal influence of one region on the other, among the coupled neuronal populations, was studied using spectral DCM (spDCM). Once the plausible models are specified, spDCM, estimates the model parameters and hemodynamic variables which quantifies the effective

connectivity between the regions.(A DCM for resting state fMRI - PubMed, n.d.) Model specification was performed by extracting the time series data from the spherical volume of interests (Dentate nucleus, Thalamus (Central Lateral Nucleus), Putamen, STN, Pontine Nucleus, Cerebellum C7b) and model space was defined based on the hypothesized equally plausible connections between the regions. The time series were extracted from the Volume of Interests (VOIs) as the principal eigenvariate of spheres centered on peak voxel in the region. The connections between the ROIs in each plausible model were based on results from previous neuroanatomical studies on the network and the results from the functional connectivity. General Linear Model (GLM) with a discrete cosine basis set consisting of characteristic frequencies of resting-state dynamics, 0.0078-0.1Hz, along with movement regressors from the realignment step and signal from CSF as a confound were used to model the resting-state. The model parameters were estimated and Bayesian Model Selection (BMS) was used to identify the most likely model. The directional intrinsic connectivity value between the regions at the resting state was compared between the groups for the winning model using statistical tests.

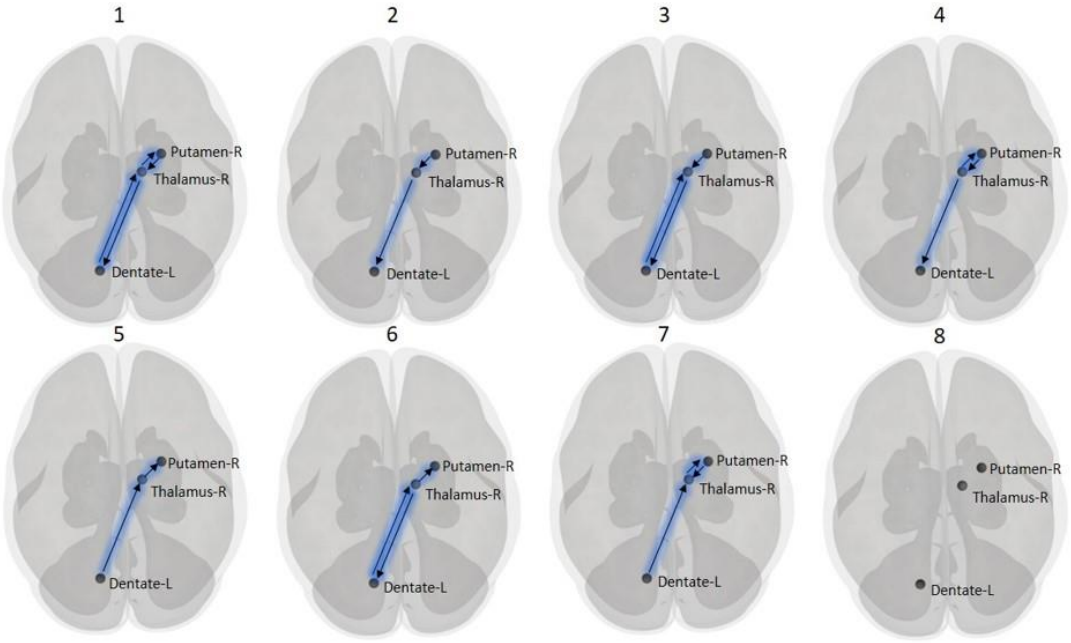

Figure 9: DCM models for ascending tract. Figure showing the reduced models compared using DCM to test the hypothesis on connections in the CTS pathway in health and disease groups.

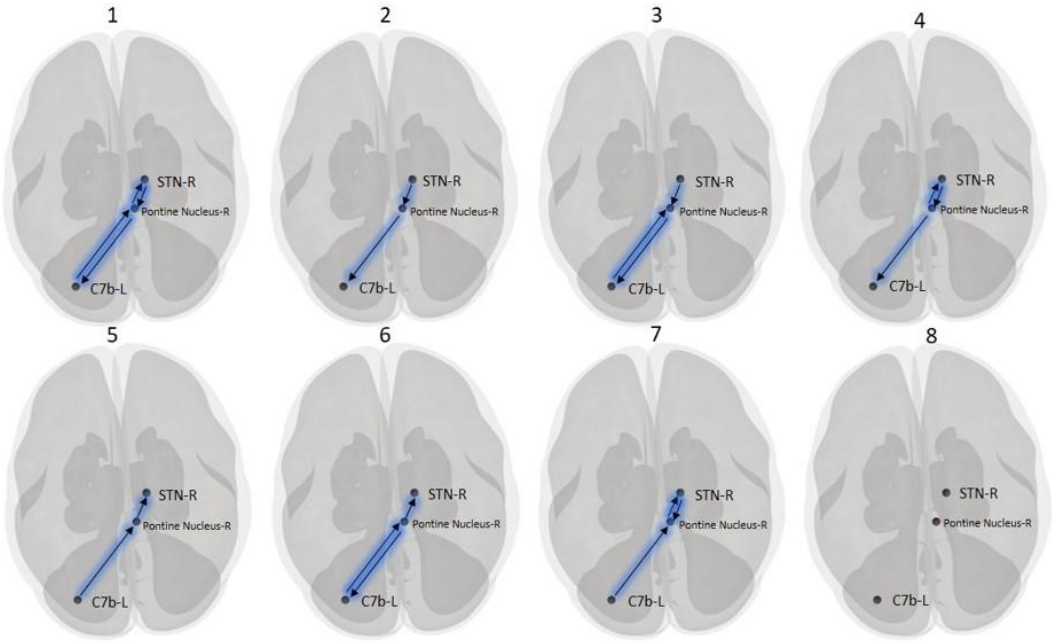

Figure 10: DCM models for descending tracts. Figure showing the reduced models compared using DCM to test the hypothesis on connections in the SPC pathway in health and disease groups.

3.3.5 Statistical analysis

The two-sample t-test was applied to estimate the difference between the patient and control group based on age and education. The gender difference between the groups was estimated using the chi-squared test. For fMRI data statistical analysis, the CONN toolbox was used to perform the ROI-to-ROI analysis using bilateral dentate nucleus, thalamus (central lateral nuclei), putamen, STN, Cerebellar cortex (C7b/Crus2) as ROIs from the automated anatomical labeling atlas 3(AAL3).(Rolls et al., 2020) The connectivity between the regions was compared in the control and PD in the medication-off-state referred to as “OFF” to study the effect of disease on the connectivity values, considering age and sex as covariates. To study the effect of a single

dose of levodopa, the patients in “OFF” and “ON” were compared considering age and sex as covariates. An attempt was made to split the patient group into “Early” and “Late” stages using an arbitrary cut-off of 5 years of disease duration to study the underlying physiological changes during disease progression in PD. ROI-ROI analysis was performed on the OFF stage of both Early and Late PD groups considering age, sex, Levodopa Equivalent Daily Dosage (LEDD), and the age at onset as covariates. The effect of levodopa (during best ON) in the Early and Late stages was also studied separately.

For DCM analysis, multiple models were compared for the groups of controls and patients (OFF and ON) for the CTS and SPC pathways as in **Figure 9** and **Figure 10**. Fixed Effects Bayesian Model Selection (BMS) was used to identify the best model that fits the data with minimum model complexity. The effective connectivity parameter from the best model was compared across the groups using a t-test for each connection to identify the significant difference between the groups.

CHAPTER 4 RESULTS

In this chapter, the results of three experiments are described below under separate sections. In the first experiment, the tractography results for the different combinations of the DWI acquisition schemes are compared. The results for the second experiment comprise tractography results for the ascending CTS and descending SPC tract together forming the CB-BG subcortical interconnecting network. The third section shows the ROI-ROI functional connectivity analysis results from the CONN toolbox and the effective connectivity changes in the network in PD compared to healthy controls.

4.1 Comparison of DWI acquisition schemes for Tractography

The lateral projections of the CST were delineated using even the lowest b-value setting of 1000s/mm^2 as in **Figure 11**A. As the b-value increases to 3000s/mm^2, the lateral projections are more detailed and provide further information about the complexity of the structure as in **Figure 11**B. But as we

go higher to 10000 s/mm^2, the information obtained visually from the tractography results plateaus as in **Figure 11**C and **Figure 11**D.

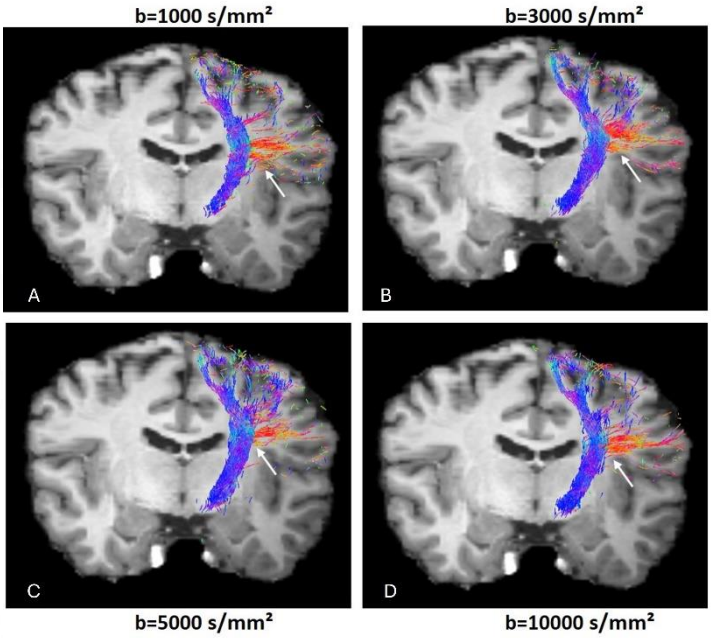

Figure 11: Tractography of CST for b-value comparison. Figure showing the comparison of the tractography of lateral projections of CST at different b values A) b=1000, B) b=3000, C) b=5000, D) b=10000

Comparing the NDED, at a constant lower b-value of 1000 s/mm^2, the details obtained for NDED=64 were larger compared to NDED=32 as in **Figure 12**A and **Figure 12**B. At a higher b-value of 10,000 s/mm^2, increasing the NDED value from 128 to 256 did not provide further information in the case of the lateral projections of CST as in **Figure 12**C and **Figure 12**D.

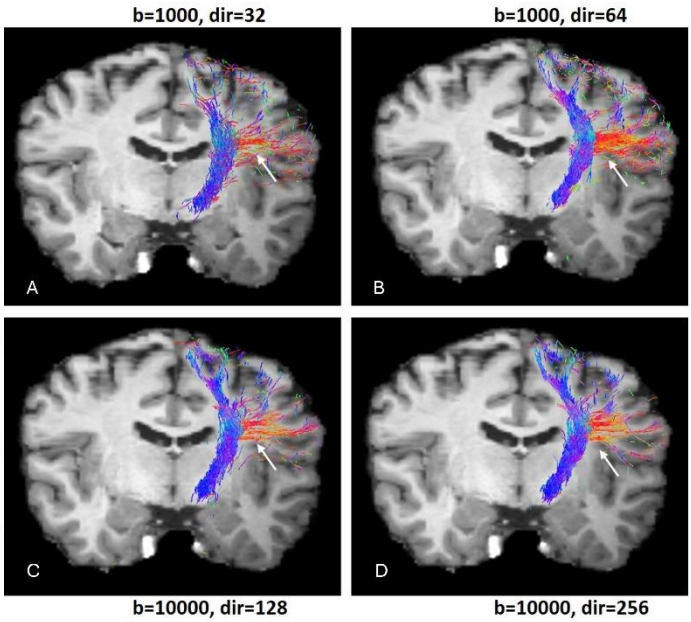

Figure 12: Tractography of CST for NDED comparison. Figure showing the comparison of the tractography of lateral projections of CST at different numbers of diffusion encoding directions A) NDED=32, B) NDED=64, C) NDED=128, D) NDED=256.

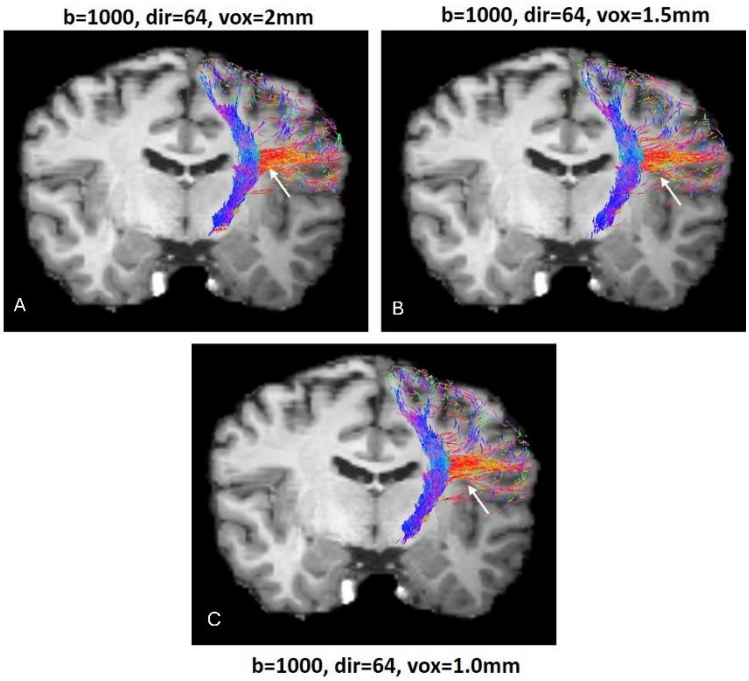

Figure 13: Tractography of CST for voxel size comparison. Figure showing the comparison of the tractography of lateral projections of CST at different voxel sizes A) vox=2.0x2.0x2.0, B) 1.5x1.5x1.5, C) vox=1.0x1.0x1.0

Upsampling the data from a voxel size of 2.0mm to 1.0mm did not increase much information regarding the lateral projections of CST as shown in **Figure 13**. **Figure 14**, shows the comparison of false positives in tractography results for combinations with higher b-values goes.

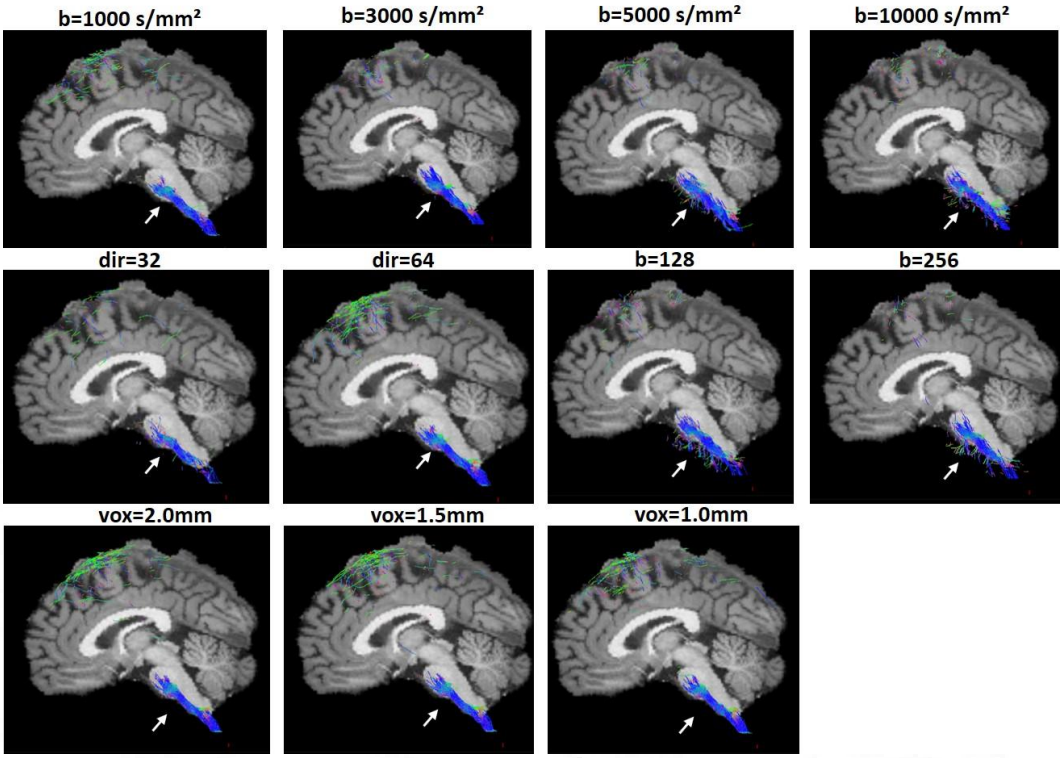

Figure 14: Tractography of CST for noise comparison. Figure showing the comparison of the tractography of the CST at the brainstem region. A-D shows the increase in noise at the brainstem as the b value increases. As the number of NDED increases from 32 to 64, the number of tracts increases as in E and F. G and H show the NDED value at 128 and 256 respectively, the details in the tract remain the same. I-K shows the changes in tracts as the voxel size decreases from 2.0 to 1.0. No increase in information or noise is observed visually.

4.2 Establishing structural connectivity of the CB-BG network

Error! Reference source not found. presents the demographic information and neuropsychological evaluations of the participants in the cognitive study.

4.2.1 Tractography of Cerebello-Basal Ganglia (CB-BG) Interconnecting Networks

The tractography analysis revealed the presence of bilateral and reciprocal pathways connecting the cerebellum (CB) and basal ganglia (BG). The

ascending pathway originating from the dentate nucleus to the contralateral thalamus traversed the superior cerebellar peduncles, decussated at the level of midbrain terminating in the Putamen as in **Figure 15** and **Figure 16**.

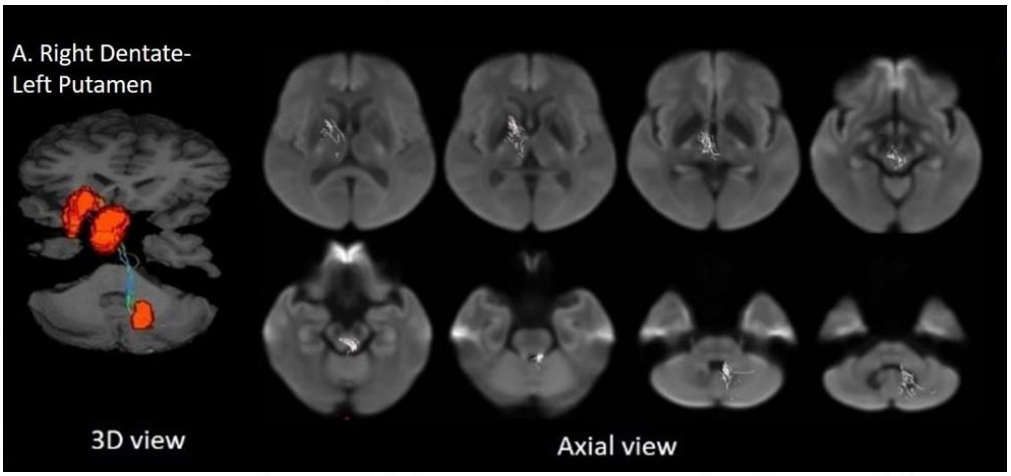

Figure 15: Tractography of CB-BG ascending pathway from right CB to left BG. The figure illustrates the ascending tracts connecting the cerebellum and basal ganglia, specifically depicting the pathways between the right Dentate Nucleus (DN) and the left Putamen, traversing the left Thalamus. Reprinted from Vineeth et al. (2023, 10.3389/fnagi.2023.1019239).

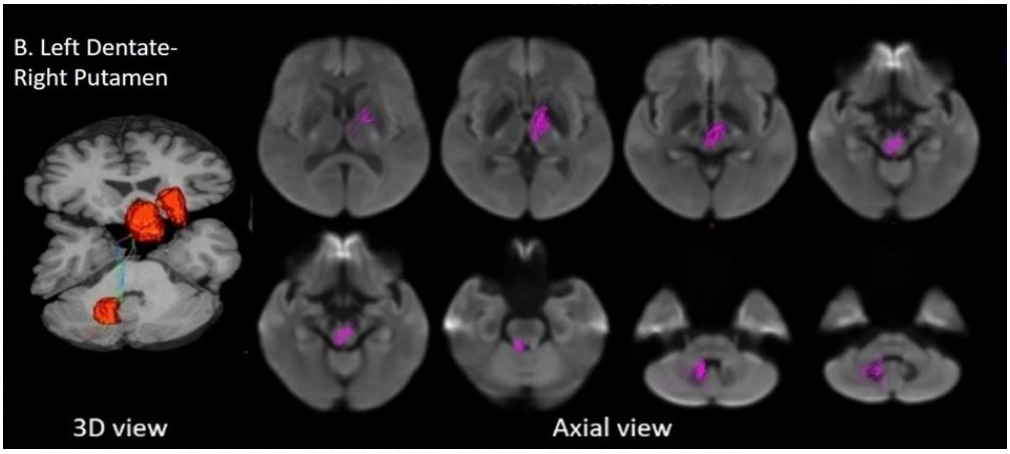

Figure 16: Tractography of CB-BG ascending pathway from left CB to right BG. The diagram displays the ascending tracts connecting the cerebellum and basal ganglia, specifically illustrating the pathways between the left Dentate Nucleus (DN) and the right Putamen,

traversing the right Thalamus. Reprinted from Vineeth et al. (2023, 10.3389/fnagi.2023.1019239).

Conversely, the descending pathway from the subthalamic nucleus (STN) to the contralateral cerebellar cortex, specifically C7b and Crus II, passed through the basilar part of the pons, underwent decussation in regions associated with the pontine nuclei, and traversed the middle cerebellar peduncle as in **Figure 17**, **Figure 18**, **Figure 19** and **Figure 20**.

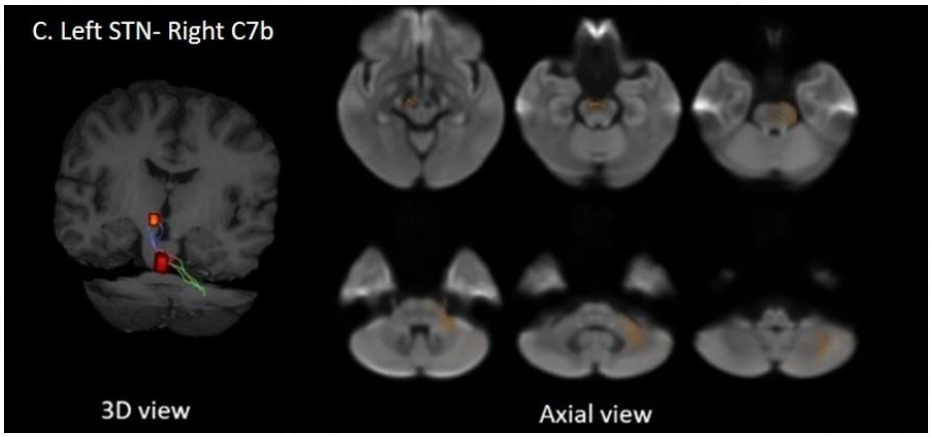

Figure 17: Tractography of CB-BG descending pathway from left BG to right CB (C7b). The figure depicts the descending tracts connecting the cerebellum and basal ganglia, specifically illustrating the pathways between the left Subthalamic Nucleus (STN) and the contralateral cerebellar cortex, C7b. Reprinted from Vineeth et al. (2023, 10.3389/fnagi.2023.1019239).

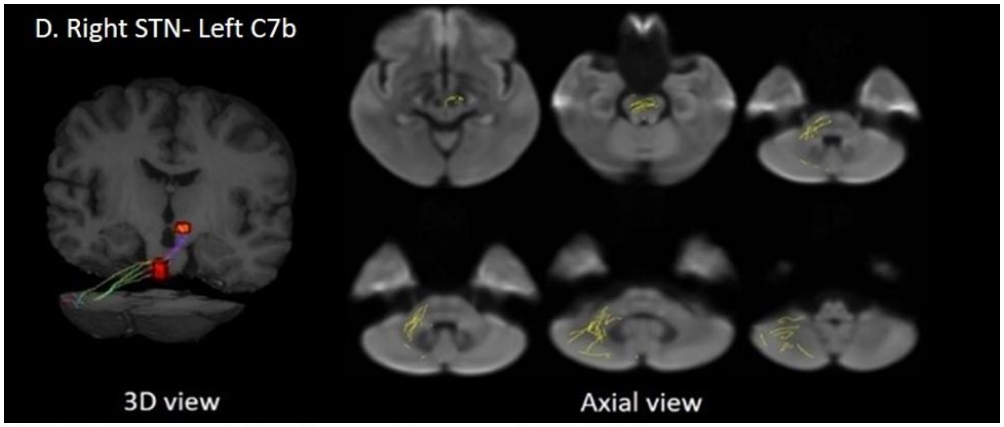

Figure 18: Tractography of CB-BG descending pathway from right BG to left CB (C7b). The diagram illustrates the descending tracts connecting the cerebellum and basal ganglia, specifically highlighting the pathways between the right Subthalamic Nucleus (STN) and the contralateral cerebellar cortex, C7b. Reprinted from Vineeth et al. (2023, 10.3389/fnagi.2023.1019239).

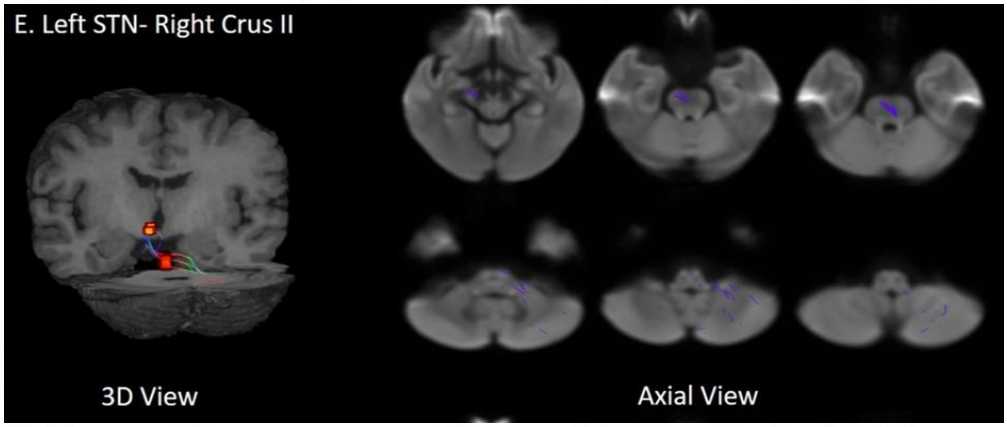

Figure 19: Tractography of CB-BG descending pathway from left BG to right CB (Crus II). The figure presents the descending tracts connecting the cerebellum and basal ganglia, specifically illustrating the pathways between the left Subthalamic Nucleus (STN) and the contralateral cerebellar cortex, Crus II. Reprinted from Vineeth et al. (2023, 10.3389/fnagi.2023.1019239).

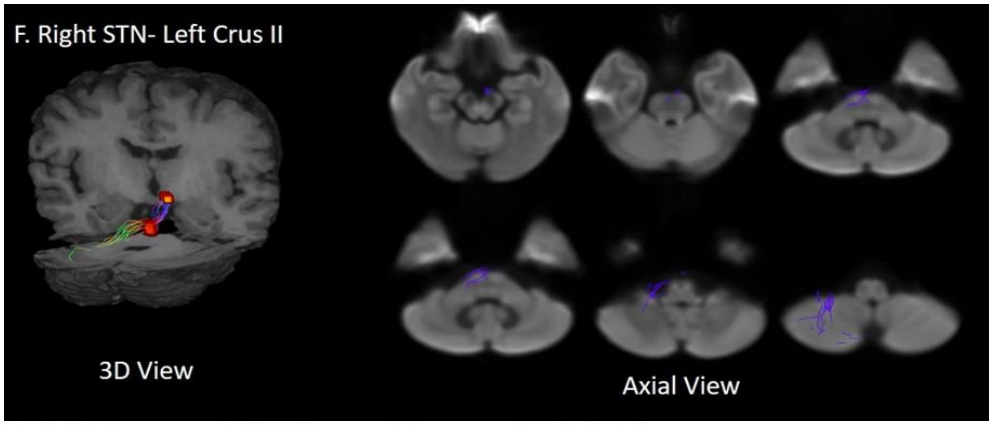

Figure 20: Tractography of CB-BG descending pathway from right BG to left CB (Crus II). The figure displays the descending tracts connecting the cerebellum and basal ganglia, specifically depicting the pathways between the right Subthalamic Nucleus (STN) and the contralateral cerebellar cortex, Crus II. Reprinted from Vineeth et al. (2023, 10.3389/fnagi.2023.1019239).

To analyze these specific tracts, individual fixel masks were created for the ascending and descending pathways in the study template space. These masks were generated by intersecting the individual's white matter Fiber Orientation Distribution (FOD) image, spatially normalized in the study template space, with the whole brain white matter Fiber Density (FD), Fiber Cross-section (FC), and Fiber Density and Cross-section (FDC) fixel data image to derive tract-specific metrics for each subject.

Table 2: Table displaying the demographic characteristics and neuropsychological assessments of the cognitive participant cohort.

Characteristic	Mean (*n=20*)	Std. Deviation
Age (yrs)	56.8	8.7
Sex (M/F)	11\09	
Education (yrs)	12.58	2.53
MMSE	29.1	0.95
ACE-M (Reg-24) *	21.86	1.58
ACE-M(Recall-10) *	7.52	1.53
ACE-M (Total)	92.9	3
ACE-Orientation	9.95	0.22
ACE-Attention	7.95	0.22
ACE-Memory	28.22	2.53
ACE-Verbal Fluency	13.6	0.66
ACE-Visuospatial	4.6	0.74
ACE-Language	27.85	0.65
RAVLT (Total)*	47.24	8.08
RAVLT Delayed Recall	9.62	2.85

4.2.2 Tractography analysis of Control Tracts

The reconstruction of Cerebello-thalamocortical (CTC) tracts was successfully performed as in **Figure 21**. The sensorimotor tracts exited from the dentate nucleus (DN) of the cerebellum (CB) via the superior cerebellar peduncle, decussated at the level of the midbrain, traversed the contralateral thalamus through the ventral intermediary nucleus (Vim), and extended to the contralateral primary motor and sensory cortices (**Figure 21**). In the associative pathway, the tracts exited the dentate nucleus of the CB through the superior cerebellar peduncle, passed through the contralateral thalamus via the mediodorsal nuclei, and reached the contralateral frontal cortex (anterior cingulate cortex/medial prefrontal cortex) as in **Figure 22**. Furthermore, tracts were reconstructed from the dentate nucleus to the contralateral frontal cortex

(anterior cingulate cortex/medial prefrontal cortex) via the ventral tegmental area (VTA) as in **Figure 23**.

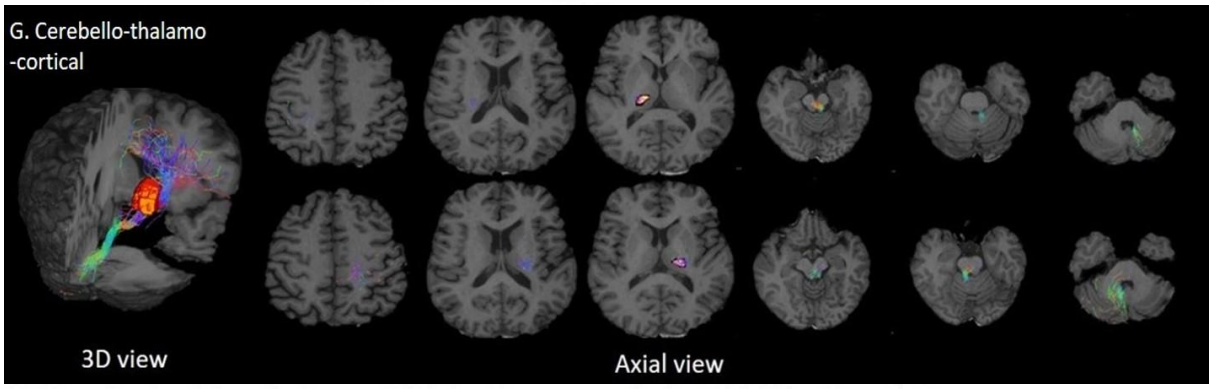

Figure 21: Tractography of the Cerebello-thalamo-cortical tract. The figure illustrates the cerebellar cortical tracts, specifically showcasing the pathways between the Dentate Nucleus (DN) and the sensorimotor cortex that pass through the ventral intermediary nucleus of the thalamus. The top and bottom rows present axial views of the right cerebellum-left thalamus/cortex and left cerebellum-right thalamus/cortex, respectively. Reprinted from Vineeth et al. (2023, 10.3389/fnagi.2023.1019239).

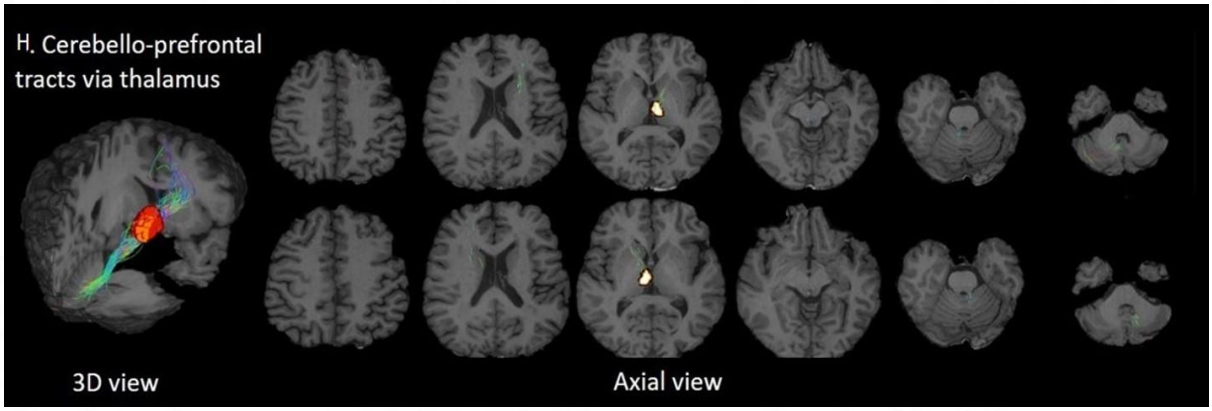

Figure 22: Tractography of the Cerebello-thalamo-prefrontal tract. The figure depicts the tracts connecting the Dentate Nucleus (DN) to the contralateral medial Prefrontal Cortex (mPFC)/Anterior Cingulate Cortex (ACC) through the medial dorsal nuclei of the thalamus. The top and bottom rows exhibit axial views of the left cerebellum-right thalamus/cortex and right cerebellum-left thalamus/cortex, respectively. Reprinted from Vineeth et al. (2023, 10.3389/fnagi.2023.1019239).

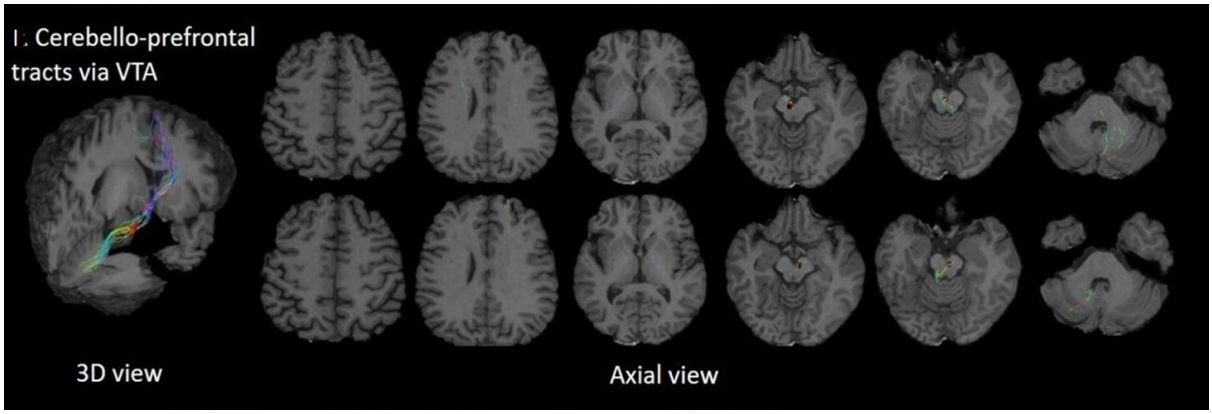

Figure 23: Tractography of the Cerebello-prefrontal tract via VTA. The figure illustrates the tracts originating from the Dentate Nucleus and extending to the contralateral medial Prefrontal Cortex (mPFC)/Anterior Cingulate Cortex (ACC) through the ventral tegmental area. Reprinted from Vineeth et al. (2023, 10.3389/fnagi.2023.1019239).

The reconstruction of the cerebellar tract used an inclusion mask containing the entire thalamus. Notably, the trajectories of these tracts through their thalamic relays aligned with established neuroanatomical findings: (i) the CB-BG tract passed through the central-medial nucleus; (ii) the CTC connecting sensorimotor regions traversed the Vim nucleus; (iii) the CTC linking prefrontal areas passed through the medial-dorsal nucleus. These thalamic relay pathways (**Figure 24**) corresponded with the existing understanding of these neural pathways.

The linear regression analysis revealed a significant negative linear correlation between Fiber Density (FD) and age for both the ascending and descending CB-BG tracts (**Figure 25**; **Error! Reference source not found.**). For all the tracts, mean Fiber Cross-section (FC) and logFC values remained unaffected by age. However, Fiber Density and Cross-section (FDC) values exhibited a negative correlation with age in the ascending tract from the right Dentate to

the left Putamen. Notably, the mean FDC values across fixels within all tracts displayed a significant positive linear relationship with Total Intracranial Volume (TIV) (**Error! Reference source not found.**). TIV also exhibited a significant positive linear association with the mean logFC parameter of the bilateral tract from the subthalamic nucleus (STN) to the cerebellar cortex. Moreover, TIV was notably higher in males compared to females, potentially indicating a gender-related impact. Multiple regression analysis of gray matter volume with age, considering education, TIV, and sex as covariates, did not reveal any significant relationships at a Family-Wise error-corrected p-value of 0.05.

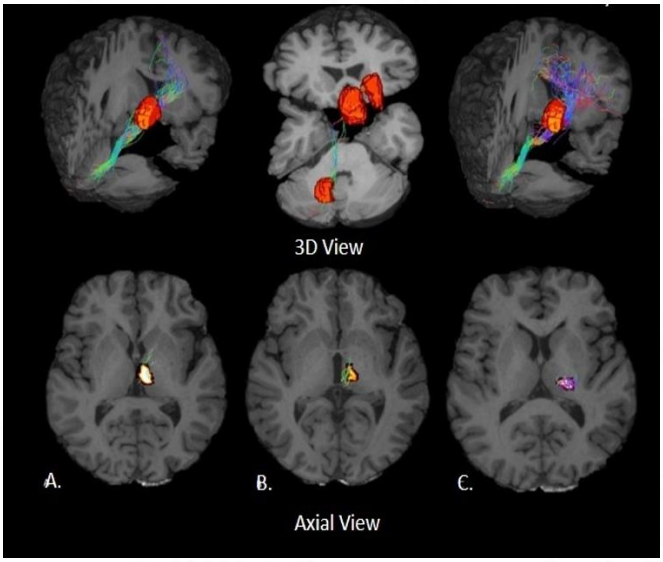

Figure 24: Anatomical concordance of cerebellar tracts with their thalamic relay. The figure displays the thalamic nuclei as distinct relays of the cerebellar tracts. Moving from left to right, it showcases the Medial Dorsal (MD) nuclei associated with cerebello-prefrontal tracts, the Central Median (CM) nuclei linked to cerebello-thalamo-striatal (CTS) tracts, and the Ventral Intermediary (VIM) nuclei involved in cerebello-thalamocortical (CTC) tracts. Reprinted from Vineeth et al. (2023, 10.3389/fnagi.2023.1019239).

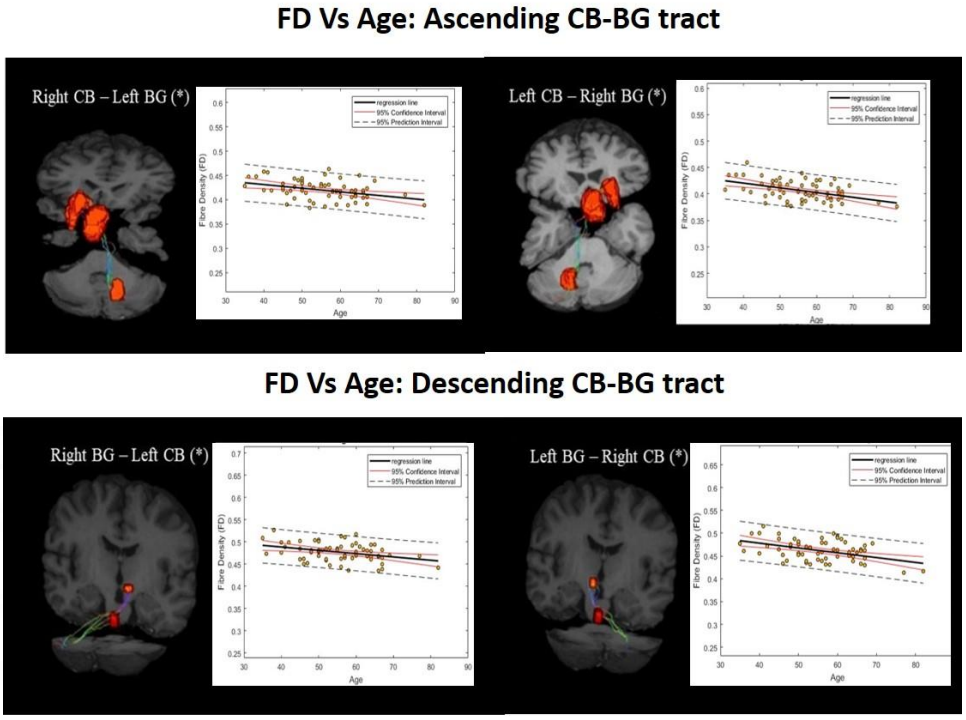

Figure 25: Linear regression between FD and Age. The scatterplots depict the average Fiber Density (FD) values of the respective cerebellum-basal ganglia (CB-BG) tracts considered in the study. The solid black lines indicate the regression line, while the red dashed lines signify the 95% confidence interval, and the black dashed lines represent the 95% prediction interval. The asterisk (*) denotes a significant linear relationship with age. Reprinted from Vineeth et al. (2023, 10.3389/fnagi.2023.1019239).

4.2.3 Neuropsychological analysis

4.2.3.1 Ascending Tracts

The Fiber Density (FD) within the cerebello-thalamo-striatal tracts exhibited positive correlations with the ACE-M (Reg-24) score, specifically from DN_L to Putamen_R (pcorrected = 0.0117) and from DN_R to Putamen_L (pcorrected = 0.0386 as shown in **Figure 26**A, **Figure 26**B). For the DN-mPFC tracts passing through thalamic or VTA relays, FD was positively correlated with the ACE-M (Recall-10) score (DN_L-VTA-ACC_R, pcorrected =

0.0070; DN_R-VTA-ACC_L, pcorrected = 0.0201; DN L-Thal-ACC_R, pcorrected = 0.0014; DN_R-Thal-ACC_L pcorrected = 0.0061), as in **Figure 26**C, **Figure 26**D, **Figure 27**E, **Figure 27**F. However, there were no significant correlations observed between FD in these tracts and the RAVLT, ACE-M (total), and ACE-M (Reg-24) scores. Regarding the Cerebello-thalamocortical (CTC) tracts, none of the tract parameters showed correlations with the neuropsychological parameters. Additionally, none of the other subdomains of ACE-M were found to be significant with any of the Fixel Based Analysis (FBA) metrics of the ascending tracts.

4.2.3.2 Descending Tracts

The Fixel Based Analysis (FBA) metrics were utilized to analyze the tracts from the Subthalamic Nucleus (STN) to the contralateral cerebellar cortex, on both STN-C7b and STN-CrusII tracts. The correlation analysis between the FBA metrics of the C7b tract and the neuropsychological scores of ACE-M and RAVLT did not reveal any significant relationships. However, the Fiber Density (FD) in the STN-R_CrusII_L tract showed a positive correlation with the ACE-M (Recall-10) score (pcorrected = 0.0431) as illustrated in **Figure 27**G, **Figure 27**H. Conversely, the ACE-M, ACE-M (Reg-24), ACE-M (total), RAVLT, and RAVLT Delayed Recall scores did not exhibit correlations with FD in this particular tract. Furthermore, none of the other subdomains of ACE-M demonstrated significance with any of the FBA metrics of the descending tracts.

Table 3: The table presents the estimated standardized regression coefficients for the metrics analyzed at the tract level, accompanied by their respective p-values.

FBA Metric	Tracts	Age		Sex		TIV		Education	
		β	p	β	p	β	p	β	p
FD	Dn_L--> Put_R	**-0.40994**	**0.00087457**	-0.03281	0.82751	-0.18287	0.2317	0.190501	0.10523
	Dn_R-->Put_L	**-0.49802**	**5.26E-05**	0.01276	0.93086	-0.1371	0.35745	0.097072	0.39419
	STN_R-->C7b_L	**-0.35857**	**0.00024516**	0.324362	0.59763	-0.23155	0.83761	0.184973	0.5422
	STN_L-->C7b_R	**-0.4552**	**0.0031548**	0.079334	0.053923	-0.03106	0.12995	0.070781	0.11418
FDC	Dn_L--> Put_R	-0.25413	0.0624673	-0.11796	0.40737	**0.502846**	**0.00083**	0.075748	0.4905
	Dn_R-->Put_L	**-0.29739**	**0.0054045**	-0.09823	0.45983	**0.563221**	**8.36E-05**	-0.01399	0.89133
	STN_R-->C7b_L	-0.10082	0.078241	0.124569	0.65756	**0.394158**	**0.00022**	0.114996	0.69805
	STN_L-->C7b_R	-0.22577	0.37206	-0.06085	0.38969	**0.542427**	**0.00865**	0.041124	0.30452
log_FC	Dn_L--> Put_R	-0.20606	0.1115	-0.11263	0.49373	-0.09478	0.56809	0.060059	0.6362
	Dn_R-->Put_L	-0.13495	0.29755	-0.1608	0.33275	-0.06666	0.68981	0.050139	0.69481
	STN_R-->C7b_L	0.128051	0.58676	-0.12466	0.26621	**0.507762**	**0.00575**	0.019757	0.74253
	STN_L-->C7b_R	0.067096	0.28536	-0.17672	0.4164	**0.455513**	**0.00163**	0.040131	0.86719

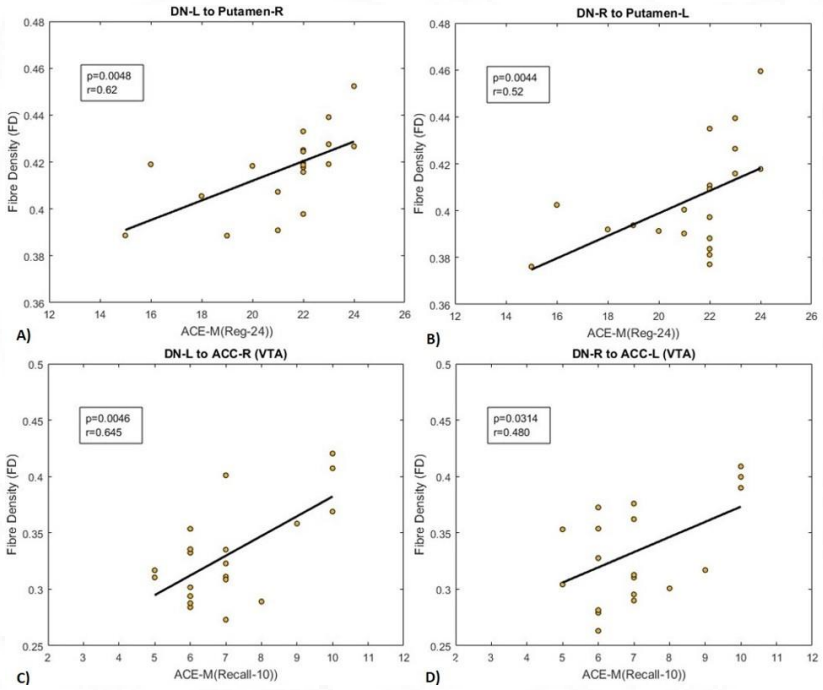

Figure 26: Correlation between FD (CTS and CB-prefrontal via VTA) and neuropsychological scores. The figure illustrates scatterplots depicting the relationship between Fiber Density (FD) and neuropsychological scores. In (A, B), the scatterplot represents ACE-M (Reg-24) plotted against FD for the tract from the dentate nucleus to the contralateral Putamen. In (C, D), the scatter plot displays ACE-M (Recall-10) plotted against

FD for the tract from the dentate nucleus to the prefrontal cortex via the Ventral Tegmental Area (VTA). Reprinted from Vineeth et al. (2023, 10.3389/fnagi.2023.1019239).

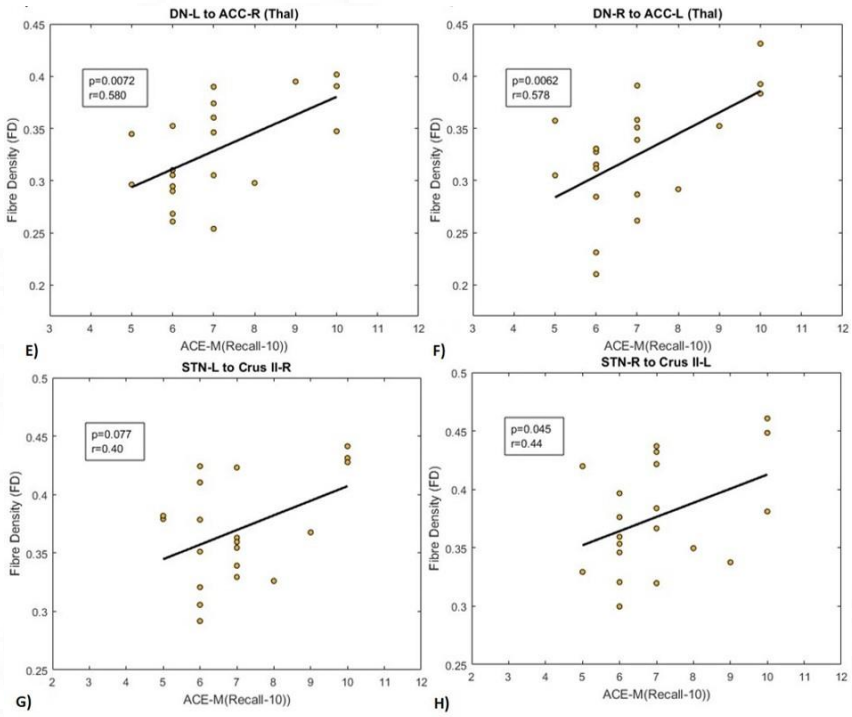

Figure 27: Correlation between FD (Cerebello-thalamo-prefrontal and SPC) and neuropsychological scores. The figure presents scatterplots illustrating the correlation between Fiber Density (FD) and neuropsychological scores. In (E, F), the scatter plot depicts ACE-M (Recall-10) plotted against FD for the tract from the dentate nucleus to the prefrontal cortex via the thalamus. In (G, H), the scatter plot shows ACE-M (Recall-10) plotted against FD for tracts extending from the Subthalamic Nucleus (STN) to the contralateral Crus II tract. Reprinted from Vineeth et al. (2023, 10.3389/fnagi.2023.1019239).

4.3 Functional and effectivity connectivity changes in the CB-BG network in patients compared to controls

Table 4: Table showing the demographics for the healthy volunteer and patient groups.

Characteristics	HV	PD
n	31	36
age (years)	51±8.55	53.2±9.61

Sex (M/F)	13/18	19/17
Education (years)	11.87±1.68	13.06±2.87
Body Mass Index	26.01±2.72	25.35±3.00

Table 5: Table showing the demographics, and mean clinical and psychological assessment scores for the Early and Late PD groups.

Characteristics	PD Early	PD Late	PD
n	16	20	36
age (years)	53.56±12.20	53.05±6.86	53.2±9.61
Sex (M/F)	8/8	11/9	19/17
Education (years)	13.38±3.18	12.8±2.56	13.06±2.87
BMI	25.35±3.24	25.35±2.79	25.35±3.00
Duration_of_Illness (Yrs)	2.82±1.26 (1-4.5)	8.40±2.79 (5-15)	6.11±4.02 (1-15)
LEDD	507.81±335.03	711.75±276.76	621.11±320.48
MoCA	26.81±1.67	26.47±1.96	26.62±1.84
MMSE	27.87±1.87	27.90±1.48	27.89±1.66
BDI	11.5±7.94	8.65±4.90	9.92±6.58
UPDRS-III in ON	10.447±8.45	14.55±11.68	12.72±10.57
UPDRS-III_in OFF	23.81±8.55	40.22±13.95	32.92±14.38

Table 6: Table showing the significant connections in ROI-ROI analysis of different groups comparisons.

Condition	Connection	T-value	FDR-corrected p-value
Controls > Patients_OFF	Den L-Put R	-3.92	0.0271
Patients_ON > Patients_OFF	Den L-Put R	-3.82	0.0351
Early_OFF>Late_OFF	STN R-C7b L	3.87	0.0246
Late_ON>Late_OFF	STN R-C7b L	3.86	0.0157
Early_ON>Early_OFF	Den L-Put R	-4.89	0.0052

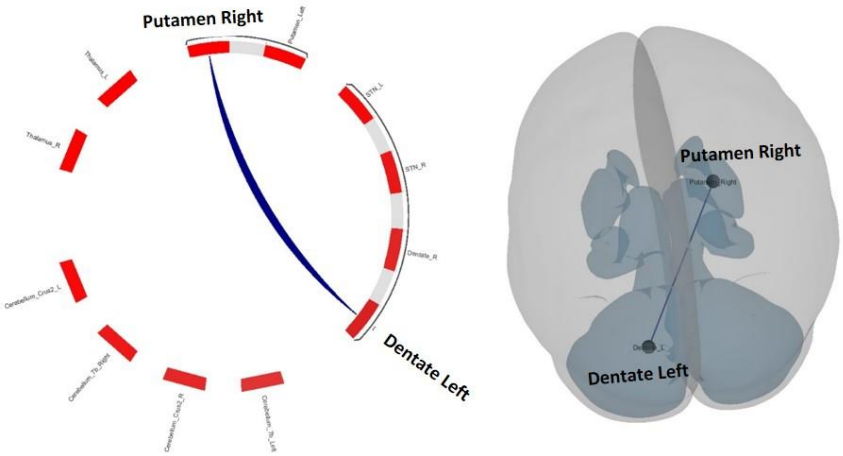

Figure 28: Functional connectivity changes in healthy controls vs. OFF. FC Figure showing the increased connectivity in the OFF compared to the healthy control group between the left dentate nucleus and the right putamen.

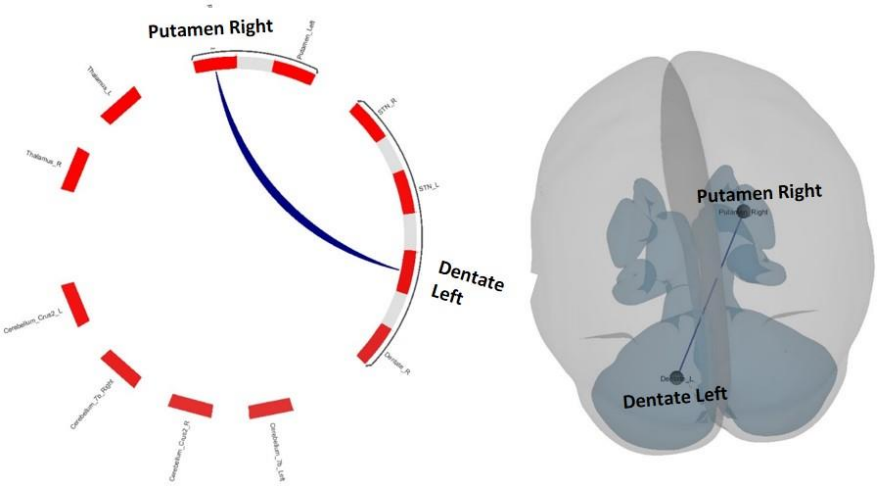

Figure 29: Functional connectivity changes in ON vs. OFF. Figure showing the increased connectivity in OFF compared to ON between the left dentate nucleus and the right putamen.

The results show that the functional connectivity between the left dentate nucleus and the right putamen is significantly higher in OFF compared to the healthy control group ($P_{FDR\text{-}corrected}$=0.0271) (**Figure 28**). As in **Figure 29**, the group difference between ON and OFF revealed similar differences

as in the control and OFF groups with significantly increased functional connectivity between the left dentate nucleus and the contralateral putamen ($P_{FDR\text{-}corrected}$=0.0351). The functional connectivity difference in the Early and Late subgroups of patients was also studied. The connectivity difference in OFF in both the Early and Late subgroups revealed a significant increase in the negative coupling between the STN and the cerebellar cortex (C7b) in the Late group compared to the Early group ($P_{FDR\text{-}corrected}$=0.0246) as shown in **Figure 30**.

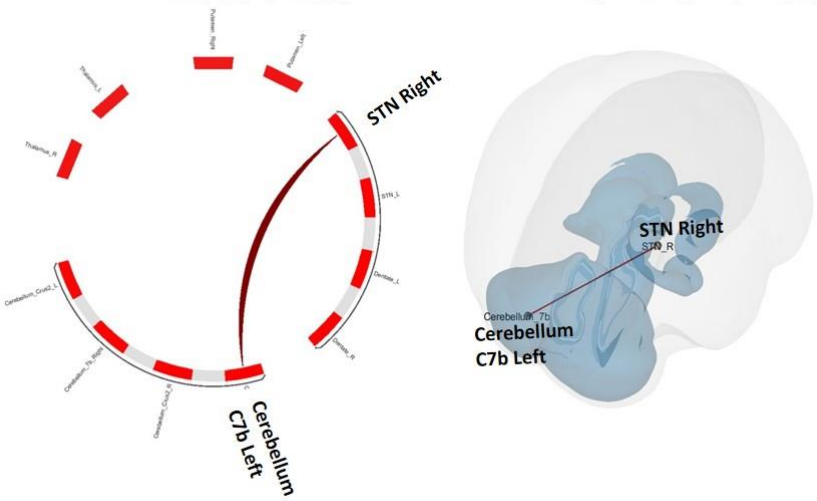

Figure 30: Functional connectivity changes in Early OFF vs. Late OFF. Figure showing the decreased connectivity in the Late group compared to the Early group in OFF between right STN and left cerebellar cortical area of C7b.

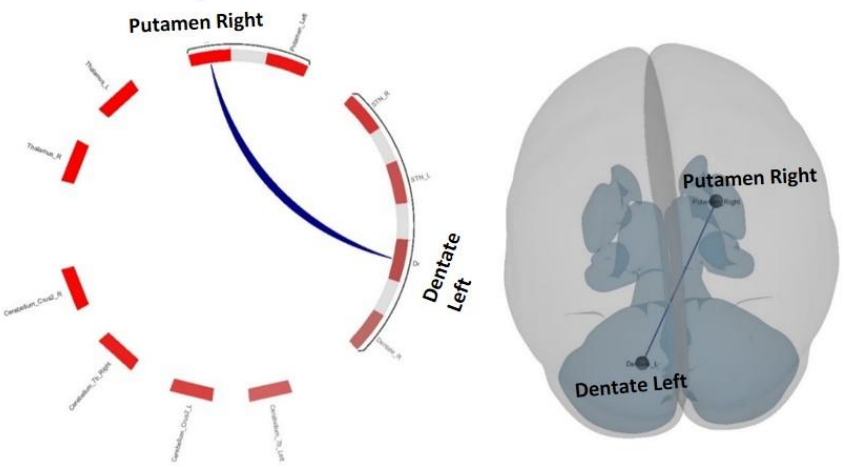

Figure 31: Functional connectivity changes in Early ON vs. Early OFF. Figure showing the decreased connectivity in ON compared to OFF during the Early stage between the left dentate nucleus and the right putamen.

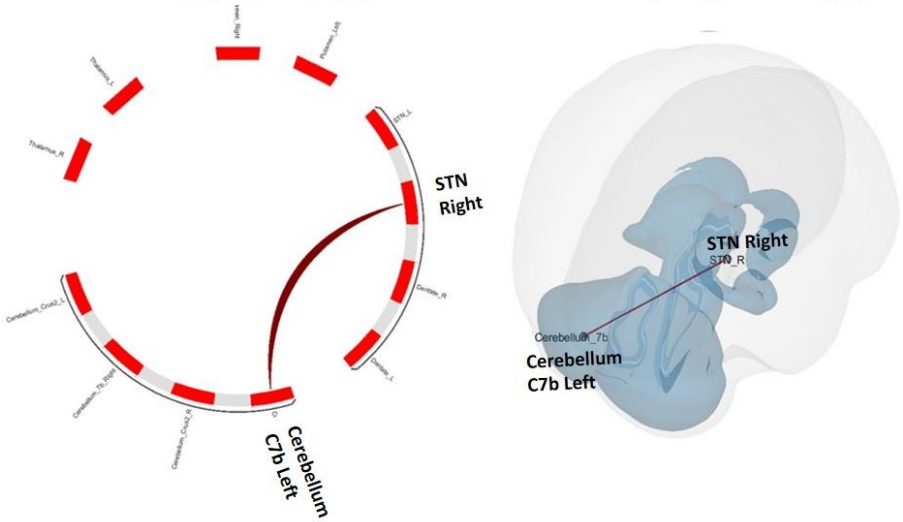

Figure 32: Functional connectivity changes in Late ON vs. Late OFF. Figure showing the increased connectivity in ON compared to OFF in the Late group between the right STN and left cerebellar cortical area of C7b

The effect of a single dose of levodopa was studied in the Early and the Late groups of patients. In the Early group, as shown in **Figure 31**, the functional connectivity between the left dentate nucleus and the right putamen was significantly reduced in ON compared to OFF (P_{FDR}-

$_{corrected}$=0.0052). However, in the Late group, patients in ON had significantly reduced negative coupling compared to OFF ($P_{FDR-corrected}$=0.0157) as shown in **Figure 32**.

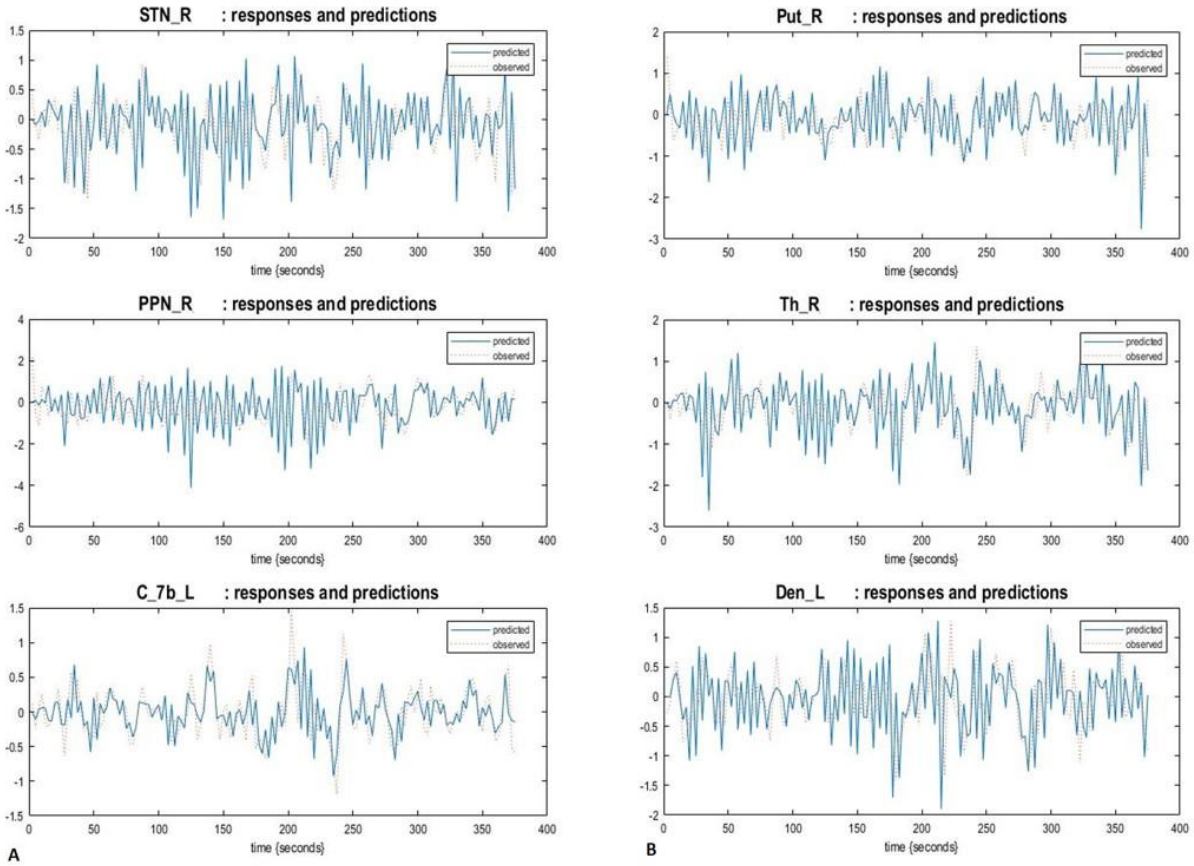

Figure 33: Time series data for ROIs in DCM. Figure showing the time series data observed from the Volume of Interest and the predicted time series data after parameter estimation.

The results from functional connectivity analysis established changes between the left cerebellum to the right basal ganglia nuclei between the different groups in OFF and ON based on the disease duration (Early vs. Late). Effective connectivity results provide the directionality component to the architecture of the C-BG network. The time series data for the regions were

extracted and the parameters were estimated for different network architectures shown in **Figure 9** and **Figure 10**. **Figure 33** shows the observed time series data for the regions in the CTS and the SPC pathways and their predicted time series data following the estimation of the model's neural as well as hemodynamic parameters(A DCM for resting state fMRI - PubMed, n.d.).

The model evidence for each model is calculated using Bayesian inference as in **Figure 34**. The log model evidence, which is the log of the probability of having observed the data given each of the models, is compared. In the CTS pathway, it was observed that, for all the groups, the winning model (model 5) had connections that were directed from the dentate nucleus to the putamen via the thalamus. In the case of the SPC pathway, model 2 which has the connections from STN to C7b via the pontine nucleus was found to be the winning model. **Error! Reference source not found.**, shows the significant difference during the t-test in the effective connectivity for connections from the winning model for the patients and control group under each condition.

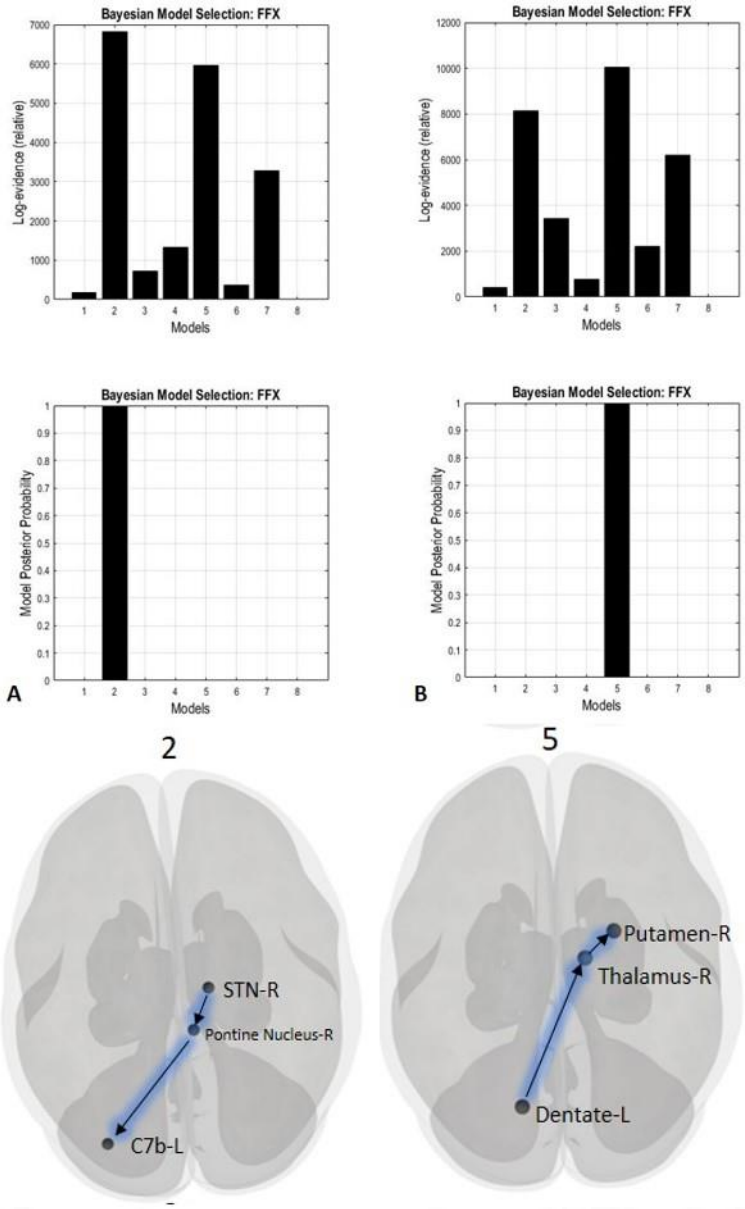

Figure 34: Winning models in Bayesian Model Comparison. Figure showing the results of Bayesian model comparison performed on the model space for the A) SPC pathway (winning model 2 with directed connections from right STN to left C7b via right pontine nuclei) and B) the CTS pathway (winning model 5 with directed connections from the left dentate nucleus to right putamen via the right thalamus).

Table 7: Table shows the p-value for the difference in effective connectivity strengths between different groups and conditions for the SPC and CTS pathways.

Condition	Subthalamo-ponto-cerebellar pathway		Cerebello-thalamo-striatal pathway	
	STN_R_to_PPN_R	PPN_R_to_C7b_L	Th_R_to_Put_R	Den_L_to_Th_R
Controls > Patients_OFF	0.088	0.494	0.188	0.021*
Patients_ON > Patients_OFF	0.039*	0.463	0.463	0.002*
Early_OFF>Late_OFF	0.030*	0.158	0.243	0.383
Early_ON>Early_OFF	0.215	0.199	0.329	0.017*
Late_ON>Late_OFF	0.010*	0.216	0.276	0.007*

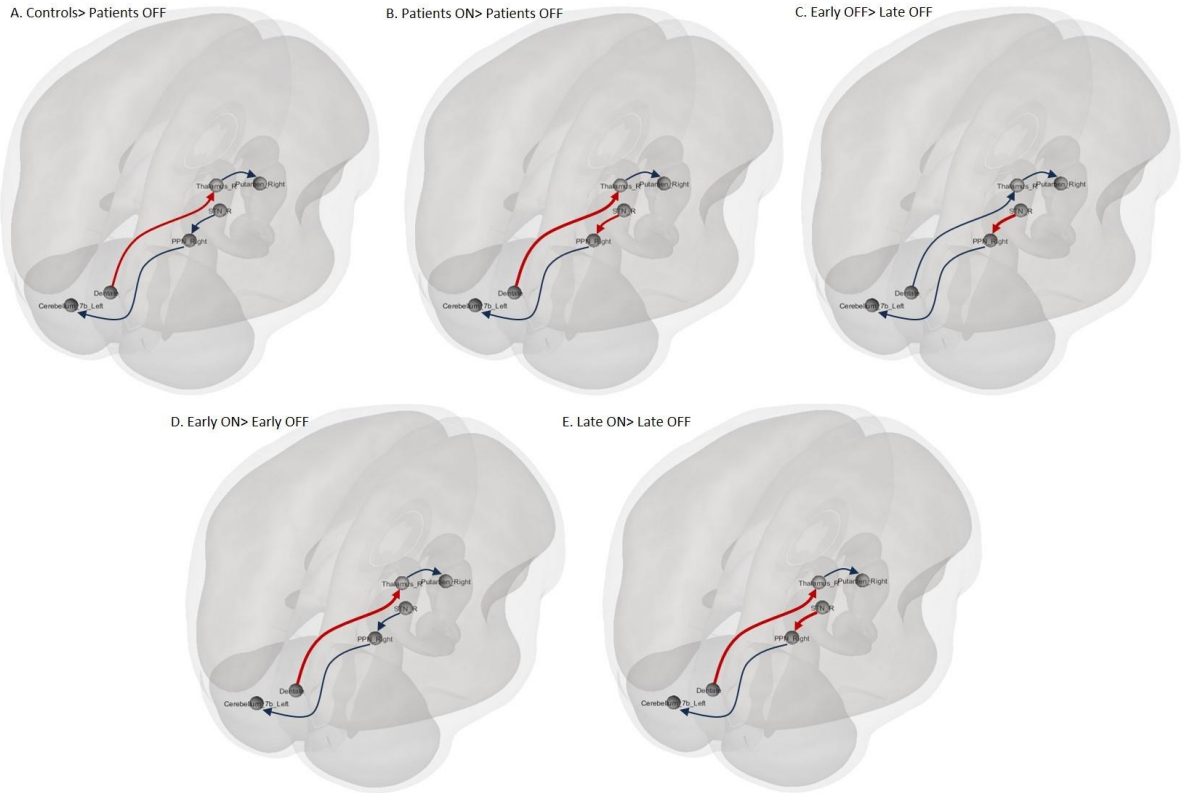

Figure 35: Changes in effective connectivity of CB-BG direct subcortical network. Figure showing the changes in effective connectivity during different conditions for the CB-BG network. Connections shown in red depict the significant changes during each condition.

The connections with significant changes in the endogenous connectivity under different conditions for the patient and control group are depicted in **Figure 35**. There was increased connectivity from the left dentate to the right thalamus in OFF compared to healthy controls as in **Figure 35**A. Similar increased effective connectivity was observed in the connections from the left dentate to the right thalamus in the OFF compared to the ON patient group as in **Figure 35**B. Also, it was observed that there was an increase in the connectivity from the right STN to the right pontine nuclei in the OFF compared to the ON state. During OFF, an increase in the strength of endogenous connections from the right STN to the right pontine nuclei in the Late group compared to the Early subjects as in **Figure 35**C. There were differences in the patterns of endogenous connectivity in the Early and Late stages during the administration of a single dose of Levodopa. In the Early stage, the reduction in endogenous connectivity was observed in the connections from the left dentate to the right thalamus as in **Figure 35**D whereas in the Late stage, the reduction in connectivity due to the administration of a single dose of Levodopa was observed in both the output connections form the right STN to the right pontine nuclei as well as the output connections from the left dentate nucleus to the contralateral thalamic nuclei as in **Figure 35**E.

CHAPTER 5 DISCUSSION

The results of the three experiments established unequivocally the presence of CB-BG direct subcortical network in human subjects and that it can be demonstrated using DWI. Also, for the first time, this study established the effect of age on the white matter bundle connecting the CB-BG network. Also, it was established for the first time that, the CB-BG tract plays a crucial role in memory and learning. The role of the CB-BG network in PD pathophysiology was also explored. The cerebello-thalamo-striatal ascending pathway is involved in the early stages of PD, most likely, in the propagation of the compensatory effect of the cerebellum secondary to basal ganglia dysfunction in PD. In the later stages, there is an altered connectivity between STN and cerebellum which is likely to be secondary to the pathological hyperactivity of the neurons in STN. Also, it was established for the first time that in PD, the action of a single dose of levodopa is facilitated by these networks in the early as well as late stages.

5.1 Comparison of DWI acquisition schemes for Tractography

Tractography using CSD was able to delineate the lateral projections of the CST successfully. However, the tractography results depict that the white matter bundle of CST is altered with different settings of b-value, NDED, and voxel size. Also, the noise levels leading to false positives in the tracts were observed in the results in certain settings. The desired combination of parameters for the application was selected based on the trade-offs between

tract quality, acquisition time, and computation complexity to process the resulting image data. The effect of different parameters on the tractography results is discussed below.

5.1.1 b-value

Higher b-values provide more sensitivity to restricted diffusion. Higher b-values can lead to increased average streamline length, reflecting better sensitivity to longer fiber tracts. In the tractography results, as the b-value increased from 1000s/mm^2 to 3000s/mm^2, the density of the WM bundle was also increased. But as the b-value was increased from 3000s/mm^2 to 10000s/mm^2, the additional information gained was found to be limited. But a downside of higher b-values is a decrease in SNR. The signal measured weakens as the b-value increases. This can introduce noise into the data, potentially leading to false positive reconstructions of streamlines, especially with deterministic tractography methods. The results from the study show that, at the brainstem region, the number of false positives increases with higher b-values. Thus even with a smaller b-value of 1000s/mm^2, the CSD tractography was able to establish the lateral projections resolving the dense crossing fibers present in this area.

5.1.2 Number of Diffusion Encoding Directions (NDED)

By increasing the NDED, the diffusion signal is sampled more comprehensively, which leads to a more accurate representation of the underlying complex diffusion patterns within white matter tracts. This can help

resolve ambiguities in fiber orientations, particularly in areas with crossing fibers. This allows for the visualization of finer details in the white matter architecture. To resolve the crossing fibers in the lateral projections of CST, increasing the diffusion encoding directions from 32 to 64, increased the quality of the tracts.

However, increasing the number of tracts from 64 to 128 to 256 did not add further details to the lateral projections observed. This is because the benefit of increasing encoding directions plateaus at some point. Beyond a certain number, the additional information gained might not be significant enough to justify the cost of scan time and computational resources. Acquiring data with more encoding directions takes longer scan time, which can be a drawback considering patient comfort and clinical feasibility. Also, processing the increased amount of data requires more powerful computers and longer processing times for tractography algorithms.

5.1.3 Voxel size

Smaller voxel size (e.g., 1mm) captures finer anatomical details of white matter tracts. This can improve the accuracy of tractography, especially in areas with complex fiber configurations. With larger voxels (e.g., 2mm), the signal from multiple tissues might be averaged within a single voxel. This can lead to underestimation of diffusion anisotropy and blurring of fiber tracts, reducing tractography accuracy due to the partial volume effect. Also, smaller voxels generally require longer scan times to maintain sufficient SNR. This can be a

trade-off between spatial resolution and data quality. This can also increase computational complexity and longer processing time for tractography.

5.1.4 Impact of scan time on PD patients

Longer scan time is challenging for PD patients who might experience tremors, fatigue, or difficulty staying still for extended periods. This can lead to motion artifacts and require additional techniques like advanced motion correction methods, which might not be suitable for all patients. Since the study requires scanning the patient both during their medication ON and OFF states an increased scan time due to higher parameter settings such as diffusion encoding direction, b-value or voxel size can cause increased patient discomfort and anxiety, motion artifacts due to tremors or involuntary movements leading to inability for some patients to complete the scan. As a result, a b-value of 1000s/mm^2 which was demonstrated to have enough power to resolve crossing fibers, NDED=64, above which the additional information practically plateaued and voxel size of 1.5mm which was a good spatial resolution at a manageable computational complexity was chosen for the study.

5.2 Establishing structural connectivity of the CB-BG network

The study confirmed the existence of the subcortical CB-BG connection using a larger dataset of 64 healthy individuals, extending previous observations made in primates and small samples of healthy subjects. For the first time, this study demonstrated that aging impacts the microstructure of the reciprocal CB-BG subcortical connections in humans. Furthermore, this investigation explored the cognitive functions associated with these tracts, revealing that the

variability in the microstructure of ascending and descending reciprocal CB-BG tracts correlates with cognitive performance. These results have significant implications for understanding neurodevelopmental and neurodegenerative conditions.

5.2.1 The white matter pathways that make up the cerebellum-basal ganglia (CB-BG) direct subcortical network.

Utilizing constrained spherical deconvolution tractography, which addresses the challenge of crossing fibers within white matter voxels, as outlined by Raffelt et al.(Da et al., 2015), confirmed the existence of ascending tracts originating from the output nuclei of the cerebellum (CB), specifically the dentate nucleus, to the contralateral putamen via the thalamus. These tracts predominantly passed through the centromedian nucleus of the thalamus before reaching the putamen, as depicted in **Figure 24**A. This validation holds significance as studies in mice have shown that connections from the dentate to the striatum involve passage through the anatomically equivalent thalamic nucleus.(Coutant et al., 2022) Consistent with this, a comparable trajectory of the cerebello-thalamo-striatal pathway through the thalamus was observed in a transneuronal viral transport study conducted in macaques.(Hoshi et al., 2005) This investigation revealed that the descending tracts from the subthalamic nucleus (STN) project to the contralateral cerebellar cortex through the middle cerebellar peduncles, with decussations near areas associated with the pontine nuclei, as illustrated in **Figure 18** and **Figure 19**. This study demonstrated that the subcortical cerebellum-basal ganglia (CB-BG) tracts in healthy human

participants follow similar pathways observed in non-human primate research, aligning with the findings by Milardi et al., who characterized the dentato-thalamic pathways.(Milardi et al., 2016)

Tractography was conducted on the cerebello-thalamo-cortical tract, a well-documented pathway by Yamada et al.,(Yamada et al., 2010) running from the dentate nucleus to the primary motor and sensory cortical regions. The analysis confirmed that this tract transits through the Ventral Intermediary Nucleus (Vim) of the thalamus, validating the anatomical accuracy of the tractography algorithms employed in this study. Furthermore, the research revealed that cerebellar (CB) tracts extend to the Anterior Cingulate Cortex (ACC) and medial Prefrontal Cortex (mPFC), traversing through the Ventral Tegmental Area (VTA) and the medial-dorsal nucleus of the thalamus. The connections from the VTA to the prefrontal cortex, known to modulate higher-order cognitive functions,(Björklund and Dunnett, 2007) have been linked to social behavior and reward circuitry by recent studies such as that of Carta et al.(Carta et al., 2019) The study investigated a direct pathway from the cerebellar output nuclei to the prefrontal cortex via the VTA. The tractography results depicted in **Figure 23** illustrate the anatomical pathways from the dentate nucleus to the prefrontal cortex through the VTA.

5.2.2 Age-related alterations in the morphological characteristics of the cerebellum-basal ganglia (CB-BG) connections.

Beyond the anatomical characteristics of the tracts, the study revealed a novel finding that there exists a negative linear correlation between age and Fiber

Density (FD) in the ascending and descending tracts within the cerebellum-basal ganglia (CB-BG) network. Fiber morphometric measures provide an indicator of the ability of the axonal bundle to relay information, depending on the number of axons and the volume of the axonal cross-section. The FD metric, calculated as an integral of the fiber orientation distribution in a fixel, is proportional to the intra-axonal volume of the fiber bundles in that fixel and is a measure of the number of axons in a fiber bundle.(Raffelt et al., 2012) The observed correlation between FD and age in the CB-BG reciprocal tracts may arise from a decline in free water volume within the fixel associated with aging, potentially indicating axonal degeneration.

Age-related alterations in the overall white matter morphology of the brain have been extensively documented in both human and animal studies, utilizing diffusion scalar metrics like Radial Diffusivity, Fractional Anisotropy, and Axial Diffusivity, as well as postmortem investigations.(Bennett and Madden, 2014; Bowley et al., 2010; Cox et al., 2016; Sala et al., 2012; Salat et al., 2005; Tang et al., 1997) However, limited research has focused on specific cerebellar tracts. The decline in Fiber Density (FD) with age suggests a reduction in the number of fibers within the white matter bundle connecting the CB-BG network as the person ages. Postmortem studies on age-related white matter (WM) atrophy in the corpus callosum have highlighted a decrease in fiber number and density as a key contributor to WM atrophy.(Hou and Pakkenberg, 2012) FD and FC serve as macrostructural and microstructural measures of fiber tract changes, respectively, with their combined measure, Fiber Density and Count (FDC), offering an overall assessment of the fiber bundle's

information relay capacity.(Raffelt et al., 2017) The preservation of FC in CB-BG connections with age may be attributed to the presence of varying caliber axons within the bundle, with larger axons being more resilient to aging, thereby maintaining FC.(Choy et al., 2020) This preservation of FC in CB-BG connections suggests their involvement in rapid information exchange crucial for updating cognitive and motor system requirements efficiently, which is a function integral to the cerebellum. Further studies involving a larger cohort of older individuals are necessary to establish the relationship between age-related motor function decline and FC within the CB-BG network.

To gain a comprehensive understanding of the functional changes associated with age-related degeneration in CB-BG tracts, it is essential to consider alterations in the basal ganglia (BG) and thalamic regions. The striatal regions of the putamen and caudate exhibit bilateral shrinkage with age, showing a negative correlation between volume and age.(Gunning-Dixon et al., 1998; Koikkalainen et al., 2007; Raz et al., 2003) Similarly, volumes and cell counts of the STN also decrease in an age-dependent manner.(Zwirner et al., 2016) Regarding the thalamus, which acts as a relay between CB and BG regions, its volume also demonstrates a declining trend with aging.(Pfefferbaum et al., 2013) The specific brain regions that age first and contribute to changes in FD within CB-BG tracts remain to be identified.

5.2.3 Correlations between psychometric measures, behavioral assessments, and the microstructural properties of cerebellum-basal ganglia (CB-BG) tracts.

We identified a positive correlation between Fiber Density (FD) in the subthalamo-cerebellar and cerebello-frontal tracts and the learning/retention domain of ACE-M scoring. The descending tracts connecting the STN to CrusII are predominantly linked to non-motor processes.(Guell and Schmahmann, 2020) Studies utilizing viral tracing in non-human primates have revealed the existence of second-order neurons projecting from CrusIIp to the STN.(Bostan et al., 2010) Furthermore, the foundational structure of a resting-state executive control network includes regions from the Basal Ganglia (BG) like the associative territory of the striatum, the caudate, and regions of the Cerebellum (CB) such as Crus I and II, in conjunction with the prefrontal cortical region, associated with non-motor functions like verbal fluency, working memory, and episodic memory.(Habas et al., 2009) The study demonstrates a correlation between FBA metrics of the tracts and cognitive scores involving the cerebello-frontal network and the reciprocal CB-BG network. The subthalamo-cerebellar tract from the STN to the pontine nuclei to Crus II exhibited a positive linear relationship with the FD metric, while the FBA metrics of the subthalamo-cerebellar tract to C7b did not show a significant linear relationship with any of the neuropsychological scores. This finding aligns with the understanding that the C7b region of the cerebellar cortex is primarily associated with motor tasks, while CrusII is predominantly

involved in non-motor functions.(Van Overwalle, Ma, et al., 2020; Van Overwalle, Manto, et al., 2020)

The investigation revealed a correlation between neuropsychological scores and Fiber Density (FD) values in tracts originating from the Cerebellum (CB) to the Anterior Cingulate Cortex (ACC) and medial Prefrontal Cortex (mPFC), passing through (a) the Ventral Tegmental Area (VTA) and (b) the mediodorsal nuclei of the thalamus. The FD values for these tracts exhibited a positive linear relationship with the 10-point score for the 10-minute recall of 3 words and the address in the ACE-M (Recall-10) assessment. Lower FD values may indicate a decrease in the information-carrying capacity of the white matter bundle, potentially leading to a decline in the ability to recall the word list and address from memory, and vice versa. Regarding the cerebello-thalamo-striatal tract, FD displayed a positive linear relationship with the ACE-M (Reg-24) scores, suggesting that this tract could play a key role in the initial learning process of words and addresses. Neuroimaging studies focusing on instrumental learning have highlighted the putamen's involvement in acquiring cue-response associations during the exploration phase.(Brovelli et al., 2011) This suggests that the properties of the cerebello-thalamo-putamen tract could influence learning and memory encoding processes.

5.2.4 Implications for movement disorders characterized by dysfunction in both the basal ganglia (BG) and cerebellum (CB)

The interconnections between the Cerebellum (CB) and Basal Ganglia (BG) play a crucial role in BG-related disorders like PD and dystonia.(Bologna and

Berardelli, 2017; Wu and Hallett, 2013) Evidence supporting the existence of the cerebello-thalamo-striatal pathway in humans stems from deep brain stimulation (DBS) studies conducted on patients with dystonia and tremors.(Paraguay et al., 2021) Despite being traditionally categorized as a BG disorder, in PD patients exhibiting tremor symptoms, DBS targeting the thalamic nuclei, specifically the Vim that receives input from the CB, has shown more significant therapeutic benefits compared to nuclei receiving inputs from the BG.(Narabayashi et al., 1987) Initial results from DBS of the dentate nucleus have demonstrated favorable outcomes for patients with dystonia and tremors.(Diniz et al., 2021) The STN serves as an excitatory nucleus influencing BG output. Therefore, age-related structural alterations in CB-BG tracts could impact the effectiveness of STN-DBS.

The heightened activity in the basal ganglia observed in PD patients is believed to be transmitted to the cerebellum through subthalamo-cerebellar connections.(Asanuma et al., 2005) Deep Brain Stimulation of the STN has been shown to alleviate this hyperactivity in the cerebellum, consequently enhancing motor function in PD patients.(Asanuma et al., 2006; Payoux et al., 2004) The gradual decline in nigrostriatal dopamine neurons associated with aging has been linked to age-related functional impairments,(Gibb and Lees, 1991) with a significant acceleration of this process leading to the development of PD. It is plausible that an expedited loss of subcortical tracts within the CB-BG system, as observed in aging, could substantially diminish cerebellar regulation over the BG, potentially contributing to the pathophysiology of PD in later stages of the disease. In the context of spinocerebellar ataxias (SCA),

characterized by clinical and genetic heterogeneity, the onset age of symptoms varies among different subtypes such as SCA1, SCA2, SCA3, SCA6, SCA7, ranging from the third to sixth decade of life(van de Warrenburg et al., 2005). Understanding the age-related effects on CB-BG circuits could provide insights into the diverse clinical presentations of the disease, including the emergence of parkinsonism and dystonia in certain SCA subtypes.(Meira et al., 2019)

5.3 Functional and effectivity connectivity changes in the CB-BG network in patients compared to controls

PD-related functional connectivity changes between the left cerebellum and right basal ganglia were observed. The administration of a single dose of levodopa was shown to ameliorate the increased functional connectivity between the regions. However, the changes in functional connectivity as well as the action of levodopa were shown to have different patterns in the early and later stages of the disease. In the later stages of PD, the functional connectivity change was primarily evident on the connection between the output nuclei of the right basal ganglia, the STN, and the cerebellar cortical region of C7b. One of the courses of action of levodopa in the early stage was through its action on the CTS tract while in the later stage of the disease, the action primarily involved the SPC tract. We utilized spectral DCM for resting state fMRI data to infer the causal influence of the regions involved on one another during the different stages of the disease and the action of levodopa. To our knowledge, this is the first study to examine the effective connectivity changes in the CTS

and SPC pathways in PD patients the effect of disease duration and levodopa on it.

5.3.1 Functional connectivity changes in PD in OFF compared to healthy controls

The increased functional connectivity between the left dentate nucleus and right putamen in OFF compared to the healthy controls could either be the compensatory effect of the cerebellum to dopamine depletion in the striatum in PD or primary pathophysiology. Akin to this finding in functional connectivity, hyperactivation of the cerebellum in PD patients has been previously reported in fMRI studies, though the exact implications of this change remain unclear.(Catalan et al., 1999) In fMRI studies, an increased BOLD signal has been demonstrated in the cerebellum of PD patients during task-based fMRI in OFF (Cerasa et al., 2006; Jahanshahi et al., 2010; Yu et al., 2007) and increased regional homegenity(Wu, Long, et al., 2009) and within cerebellar connectivity has been established in the cerebellum in the resting state.(Wu, Wang, et al., 2009) There are studies that suggest the cerebellar compensatory hypothesis in PD(Wu and Hallett, 2005; Yu et al., 2007) as well as provide arguments for a primary pathophysiological change in the cerebellum in PD.(Wu and Hallett, 2013) To date, the effect of PD on the resting state C-BG direct subcortical network remains unclear. Cerebellum lobule V was shown to have increased resting state connectivity with putamen(Simioni et al., 2015) but the causal influence of the regions involved was not explored.

In this study, using DCM, the directional connectivity from the left dentate to the right thalamus in the CTS pathway was demonstrated to have increased connectivity in patients with PD compared to healthy subjects. This highlights the potential role of the cerebello-thalamo-striatal pathway in facilitating a compensatory action of the cerebellum in response to dopaminergic depletion in the striatum in Early PD. Even though effective connectivity changes in brain networks in PD have been studied, the specific role of the two pathways in PD hasn't been explored. Changes in left cerebellar effective connectivity during automatic movements in PD compared to healthy subjects have been studied using psychophysiological interactions (PPI)(Wu et al., 2011) which measures the changes in network interaction due to the experimental stage alone.

5.3.2 Functional connectivity changes in PD during OFF based on disease duration

Functional connectivity analysis in this study revealed that the connectivity between the STN nucleus and the cerebellar motor cortical region C7b was reduced in the Late PD group compared to the Early PD group (**Figure 30**) during OFF. Functional connectivity changes during the disease involve a complex interplay of hypo and hyper-connectivity alterations in specific brain networks.(Xu et al., 2022) STN primarily sends glutamatergic projections to other brain regions including the cerebellum.(Bhuvanasundaram et al., 2022; Hamani et al., 2004) STN projects to the cerebellar cortex via the pontine nucleus (PN). However, it has been shown that, in mice models, there are

inhibitory responses in PN during the stimulation of STN which could be mediated via the GABAergic interneurons present in the PN.(Bhuvanasundaram et al., 2022) The over-activation of this component of the STN to C7b projection via PN in the later stages of PD could contribute to the reduction of functional connectivity in the late PD group. This theory is supported by the finding that, during the effective connectivity analysis the causal influence of STN directed towards the PN was significantly higher in the Late group compared to the Early group in OFF. Increased firing rate and enhanced neural activity in STN is established in PD patients.(Hutchison et al., 1998; Levy et al., 2002; Moran et al., 2008; Steigerwald et al., 2008) The excessive dopamine loss in the later stages of the disease could further diminish the inhibitory control of the GPe over STN leading to its hyperactive state which can in turn, override the compensatory effects of the cerebellar output as the disease progresses.

5.3.3 Functional connectivity change after a single dose of levodopa/Carbidopa (100/25mg (ON Vs OFF)

In this study, the functional connectivity analysis revealed a decrease in the FC values between the left dentate and right putamen after the administration of levodopa. Further exploring the causal influence between the regions in the medicated state, the directed connectivity from the left dentate to the contralateral thalamic nuclei was found to be decreased through the action of levodopa in PD patients. Also, in the effective connectivity analysis, the action of levodopa was found to significantly reduce the directed connectivity from

the STN to the PN in the SPC pathway. This supports the theory that the direct subcortical connections in the CB-BG network may participate in the reduction of motor symptoms of PD by levodopa. Even though several whole brain and BG-targeted connectivity studies have been conducted in patients after taking levodopa, the results have varied depending on factors such as brain region of interest, patient population (based on disease duration), dose of levodopa administered, and study design.

Disease duration remains one of the primary factors determining the course of FC changes in PD across the regions. Robert RL et.al demonstrated that a single dose of levodopa in drug-naïve PD patients has little change on the functional brain networks.(White et al., 2020) A significant increase in cerebellar functional connectivity was observed after a single dose of levodopa in patients with a mean disease duration of 12.4±2.6 years compared to the healthy subject group.(Mueller et al., 2019) Increased connectivity between the dentate nucleus and putamen was earlier reported in PD patients experiencing levodopa-induced involuntary movements or dyskinesias, with a disease duration of 7.48±3.36. Zhang et al, found that the connectivity between the left dentate to the right putamen was higher in dyskinetic PD patients compared to the non-dyskinetic group.(Zhang et al., 2022) Also, the amelioratory effect of levodopa on the otherwise increased functional connectivity in OFF patients was observed by Ballarini. et.al, while studying the effect of dopaminergic therapy in chronically treated patients.(Ballarini et al., 2018) Thus FC changes do capture the effect of levodopa on motor circuits in PD similar to the findings in our study and disease duration can alter the dynamics of the functional

changes in the circuit. As warranted, the improvement due to levodopa administration mediated by the C-BG direct subcortical network was studied during the Early and Late.

5.3.3.1 Effect of levodopa in the Early PD

In the current study, the Early PD group revealed that the increased connectivity between left dentate and right putamen in the OFF state was significantly reduced through the administration of a single dose of levodopa. The causal hyperactivation, estimated using DCM, from the left dentate to the right thalamus in the CTS pathway in OFF, was also found to be reduced by the action of levodopa in the PD group with a disease duration of less than 5 years. In mild-to-moderate-stage PD patients, it has been shown that cerebellar-whole brain connectivity is increased in the OFF state and the connectivity values are reduced in the ON state whereas the healthy subject group has the connectivity values at an intermediate level.(Mirdamadi, 2016; Sb et al., 2015) These results are coherent with ours as the single dose of L-Dopa was capable of bringing the increased left dentate to right putamen connectivity values to lower levels. Such an effect of levodopa on the hyper-connectivity state during OFF during the early stages when extended over a longer period could be a contributory factor to the long-term side effects of levodopa such as dyskinesia.

5.3.3.2 Effect of levodopa in the Late PD

In the FC analysis of this study, even though no significant difference was observed between the left dentate and right putamen connectivity after

administering a single dose of levodopa in the Late PD group, a restoration of the reduced connectivity between the STN and the cerebellar motor cortical region of C7b was observed. This could be mediated by the disynaptic projections from the STN to the cerebellar cortical regions via the pontine nucleus. This is further supported by the finding that, the effective connectivity from STN to PN was reduced by a single dose of levodopa in the later stages. STN-DBS has been shown to improve motor functions in advanced PD patients at a magnitude similar to levodopa treatment.(Vizcarra et al., 2019) The complete mechanism of levodopa in the late stages of PD is not exactly understood but the action of STN-DBS in advanced PD is primarily through the disruption of abnormal signal transmission from STN.(Chiken and Nambu, 2014) These findings are in coherence with our conclusion that the action of levodopa during the later stages of PD primarily involves the connection from STN to other brain areas including the cerebellar cortices.

CHAPTER 6 CONCLUSION

6.1 Summary

This study validated the presence of subcortical pathways connecting the cerebellum and basal ganglia in a large cohort of human subjects, similar to findings in non-human primates discovered a decade ago. The findings revealed a negative association between Fiber Density (FD) in the reciprocal CB-BG tracts and age and a positive association with specific cognitive performance metrics. Notably, the recall memory domain of the ACE-M assessment exhibited associations with FD in both the subthalamic-cerebello (Crus II) tract and the cerebello-frontal tracts extending to the prefrontal cortex. Moreover, the FD measure in the cerebello-thalamo-striatal tracts displayed a positive correlation with the learning and registration domain of the ACE-M score. Further exploration into the functional significance of these tracts in movement disorders such as PD was performed with the help of resting state fMRI.

The study provided the first evidence of the changes in the cerebellum-basal ganglia, direct, subcortical network and its potential role in the pathophysiology of PD. It was established that the connectivity between the cerebellar output, the dentate nucleus, and basal ganglia input nuclei, the putamen increases in the unmedicated (OFF) state in PD compared to the healthy subjects. The increased connectivity from the left dentate nucleus to the contralateral thalamus in the CTS pathway suggests a potential

compensatory role of the cerebellum in response to the dopaminergic loss and the changes in the neuronal activity in the basal ganglia output nuclei, including the STN. During the later stages of the disease, the connectivity of the STN with the cerebellar motor cortical region of C7b decreases, suggesting a primary pathophysiological role of the SPC pathway through the transmission of abnormal signals to the cerebellum. The action of levodopa on the subcortical connections varied in the early compared to the later stages of the disease. During the early stages of the disease, the levodopa reduced the increased connectivity from the dentate nucleus to the putamen. However, in the later stages of the disease the lost connectivity between STN and the cerebellar cortical area, C7b was restored. This was further supported by the increased effective connectivity values from the STN to the PN during OFF in the later stages of the disease.

Understanding the role of CB-BG network in PD and the associated changes during different stages of the disease is crucial in identifying new targets for therapeutics. For example, cerebellum can be a target for Deep Brain Stimulation to treat other movement disorders as well such as dystonia, ataxia and tremors. Dentate nucleus and superior cerebellar peduncle could be key targets for DBS to treat certain movement disorders(Tai and Tseng, 2022). Even better understading the physiology and pathophysiological communication in the network could help in identifying targets for non-invasive treatment option for patients with PD to treat symptoms such as LID. Further investigations are required to fully understand the network dynamics and optimum targets for therapeutics.

6.2 Limitations

One constraint of this study pertains to the utilization of a single shell and a relatively low b-value (b = 1000S/mm2) during the diffusion data acquisition. Enhancing the robustness of Fiber Orientation Distribution (FOD) and Apparent Fiber Density (AFD) estimation could be achieved through the incorporation of higher and multiple b-value acquisitions with the help of a scanner with more powerful magnetic field strength than 3T. Additionally, the study faces a limitation in the moderate effect size range (Cohen's f2: 0.15–0.35) observed in the multiple linear regression analysis concerning age versus FD. Despite the statistical significance of the negative linear relationship, the change in FD per unit alteration in age is minimal. Another constraint is the limited sample size of cognitive data. While the findings offer fresh insights into the functional significance of these tracts in memory encoding and retrieval, a longitudinal study with a larger sample size is imperative to validate the association between CB-BG tract parameters and cognitive assessments. Although the correlation values between neuropsychological scores and FD measurements shed light on the involvement of these tracts in the task, further exploration using tasks-based fMRI with the patient having to perform cognitive tasks is warranted to elucidate the precise role these tracts play in the memory and learning network. Overall, the study only looks into the resting state functional changes in the network. Further studies are required to understand the dynamics of the CB-BG interconnecting network during motor and cognitive tasks.

6.3 Future work

The current study focused on resting-state connectivity within the CB-BG interconnecting network. In the future, task-based fMRI can be used to investigate the changes in the CB-BG interconnecting network during specific tasks. This will help in understanding the functional role of the network in different cognitive and motor processes. The role of the CB-BG network in cerebellar control on motor cortex plasticity can be further investigated using combined fMRI and transcranial magnetic stimulation (TMS). It helps to understand the role of the specific pathway, that mediate the effect of cerebellar excitatory and inhibitory magnetic stimulations to the cerebral cortex. This can provide valuable insights into the mechanisms underlying cerebellar control of motor cortex plasticity and its role in the development of abnormal movements like bradykinesia, dystonia etc. Longitudinal studies are necessary to investigate the changes in the CB-BG network which can help in understanding the progression of neurological disorders involving these structures and the impact of therapeutic interventions on the network. The findings of this study can be applied to clinical settings, for example, to develop novel therapeutic sites for the application of TMS in PD patients in the early stages to enhance compensatory mechanisms and in the late stages of the disease to ameliorate the pathophysiology of complications such as Levodopa-induced dyskinesia. By understanding the changes in the CB-BG network, personalized interventions can be developed to target specific symptoms and improve clinical outcomes.

CHAPTER 7 BIBLIOGRAPHY

A DCM for resting state fMRI - PubMed (n.d.). Available at: https://pubmed.ncbi.nlm.nih.gov/24345387/ (accessed 25 January 2024).

Acosta-Cabronero J, Cardenas-Blanco A, Betts MJ, et al. (2017) The whole-brain pattern of magnetic susceptibility perturbations in Parkinson's disease. *Brain: A Journal of Neurology* 140(1): 118–131.

Analysis of partial volume effects in diffusion-tensor MRI - Alexander - 2001 - Magnetic Resonance in Medicine - Wiley Online Library (n.d.). Available at: https://onlinelibrary.wiley.com/doi/full/10.1002/mrm.1105?sid=nlm%3Apubmed (accessed 23 April 2021).

Andersson JLR and Sotiropoulos SN (2016) An integrated approach to correction for off-resonance effects and subject movement in diffusion MR imaging. *NeuroImage* 125: 1063–1078.

Andersson JLR, Hutton C, Ashburner J, et al. (2001) Modeling Geometric Deformations in EPI Time Series. *NeuroImage* 13(5): 903–919.

Asanuma K, Ma Y, Huang C, et al. (2005) The metabolic pathology of dopa-responsive dystonia. *Annals of Neurology* 57(4): 596–600.

Asanuma K, Tang C, Ma Y, et al. (2006) Network modulation in the treatment of Parkinson's disease. *Brain: A Journal of Neurology* 129(Pt 10): 2667–2678.

B K, Jn B, S B, et al. (2013) A 64-channel 3T array coil for accelerated brain MRI. *Magnetic resonance in medicine* 70(1). Magn Reson Med.

Baggio HC, Abos A, Segura B, et al. (2019) Cerebellar resting-state functional connectivity in Parkinson's disease and multiple system atrophy: Characterization of abnormalities and potential for differential diagnosis at the single-patient level. *NeuroImage: Clinical* 22: 101720.

Ballard IC, Murty VP, Carter RM, et al. (2011) Dorsolateral Prefrontal Cortex Drives Mesolimbic Dopaminergic Regions to Initiate Motivated Behavior. *The Journal of Neuroscience* 31(28): 10340–10346.

Ballarini T, Růžička F, Bezdicek O, et al. (2018) Unraveling connectivity changes due to dopaminergic therapy in chronically treated Parkinson's disease patients. *Scientific Reports* 8(1). 1. Nature Publishing Group: 14328.

Behzadi Y, Restom K, Liau J, et al. (2007) A component based noise correction method (CompCor) for BOLD and perfusion based fMRI. *NeuroImage* 37(1): 90–101.

Bennett IJ and Madden DJ (2014) Disconnected aging: cerebral white matter integrity and age-related differences in cognition. *Neuroscience* 276: 187–205.

Benninger DH, Thees S, Kollias SS, et al. (2009) Morphological differences in Parkinson's disease with and without rest tremor. *Journal of Neurology* 256(2): 256–263.

Bhuvanasundaram R, Krzyspiak J and Khodakhah K (2022) Subthalamic Nucleus Modulation of the Pontine Nuclei and Its Targeting of the Cerebellar Cortex. *Journal of Neuroscience* 42(28). Society for Neuroscience: 5538–5551.

Björklund A and Dunnett SB (2007) Dopamine neuron systems in the brain: an update. *Trends in Neurosciences* 30(5): 194–202.

Bologna M and Berardelli A (2017) Cerebellum: An explanation for dystonia? *Cerebellum & Ataxias* 4: 6.

Bostan AC and Strick PL (2018) The basal ganglia and the cerebellum: nodes in an integrated network. *Nature Reviews Neuroscience* 19(6): 338–350.

Bostan AC, Dum RP and Strick PL (2010) The basal ganglia communicate with the cerebellum. *Proceedings of the National Academy of Sciences* 107(18): 8452–8456.

Bowley MP, Cabral H, Rosene DL, et al. (2010) Age changes in myelinated nerve fibers of the cingulate bundle and corpus callosum in the rhesus monkey. *The Journal of Comparative Neurology* 518(15): 3046–3064.

Brittain J-S, Sharott A and Brown P (2014) The highs and lows of beta activity in cortico-basal ganglia loops. *The European Journal of Neuroscience* 39(11): 1951–1959.

Brovelli A, Nazarian B, Meunier M, et al. (2011) Differential roles of caudate nucleus and putamen during instrumental learning. *NeuroImage* 57(4): 1580–1590.

Caligiore D, Pezzulo G, Baldassarre G, et al. (2017) Consensus Paper: Towards a Systems-Level View of Cerebellar Function: the Interplay Between Cerebellum, Basal Ganglia, and Cortex. *Cerebellum (London, England)* 16(1): 203–229.

Caligiore D, Mannella F, Arbib MA, et al. (2017) Dysfunctions of the basal ganglia-cerebellar-thalamo-cortical system produce motor tics in Tourette syndrome. *PLOS Computational Biology* 13(3). Public Library of Science: e1005395.

Carta I, Chen CH, Schott A, et al. (2019) Cerebellar Modulation of the Reward Circuitry and social behavior. *Science (New York, N.Y.)* 363(6424).

Catalan MJ, Ishii K, Honda M, et al. (1999) A PET study of sequential finger movements of varying length in patients with Parkinson's disease. *Brain: A Journal of Neurology* 122 (Pt 3): 483–495.

Cerasa A, Hagberg GE, Peppe A, et al. (2006) Functional changes in the activity of cerebellum and frontostriatal regions during externally and internally timed movement in Parkinson's disease. *Brain Research Bulletin* 71(1): 259–269.

Chiken S and Nambu A (2014) Disrupting neuronal transmission: mechanism of DBS? *Frontiers in Systems Neuroscience* 8.

Choy SW, Bagarinao E, Watanabe H, et al. (2020) Changes in white matter fiber density and morphology across the adult lifespan: A cross-sectional fixel-based analysis. *Human Brain Mapping* 41(12): 3198–3211.

Concurrent decoding of distinct neurophysiological fingerprints of tremor and bradykinesia in Parkinson's disease - PubMed (n.d.). Available at: https://pubmed.ncbi.nlm.nih.gov/37249217/ (accessed 22 March 2024).

Coutant B, Frontera JL, Perrin E, et al. (2022) Cerebellar stimulation prevents Levodopa-induced dyskinesia in mice and normalizes activity in a motor network. *Nature Communications* 13(1). 1. Nature Publishing Group: 3211.

Cox SR, Ritchie SJ, Tucker-Drob EM, et al. (2016) Ageing and brain white matter structure in 3,513 UK Biobank participants. *Nature Communications* 7: 13629.

Da R, Re S, Gr R, et al. (2015) Connectivity-based fixel enhancement: Whole-brain statistical analysis of diffusion MRI measures in the presence of crossing fibres. *NeuroImage* 117. Neuroimage.

Diniz JM, Cury RG, Iglesio RF, et al. (2021) Dentate nucleus deep brain stimulation: Technical note of a novel methodology assisted by tractography. *Surgical Neurology International* 12: 400.

Etkin A and Wager TD (2007) Functional Neuroimaging of Anxiety: A Meta-Analysis of Emotional Processing in PTSD, Social Anxiety Disorder, and Specific Phobia. *The American Journal of Psychiatry* 164(10): 1476–1488.

Fahn S (2011) Classification of movement disorders. *Movement Disorders: Official Journal of the Movement Disorder Society* 26(6): 947–957.

Fermin ASR, Yoshida T, Yoshimoto J, et al. (2016) Model-based action planning involves cortico-cerebellar and basal ganglia networks. *Scientific Reports* 6: 31378.

Filippi M, Sarasso E and Agosta F (2019) Resting-state Functional MRI in Parkinsonian Syndromes. *Movement Disorders Clinical Practice* 6(2): 104–117.

French IT and Muthusamy KA (2018) A Review of the Pedunculopontine Nucleus in Parkinson's Disease. *Frontiers in Aging Neuroscience* 10: 99.

Functional organization of human occipital-callosal fiber tracts | PNAS (n.d.). Available at: https://www.pnas.org/content/102/20/7350 (accessed 23 April 2021).

Gibb WR and Lees AJ (1991) Anatomy, pigmentation, ventral and dorsal subpopulations of the substantia nigra, and differential cell death in Parkinson's disease. *Journal of Neurology, Neurosurgery, and Psychiatry* 54(5): 388–396.

Globas C, Bösch S, Zühlke C, et al. (2003) The cerebellum and cognition. Intellectual function in spinocerebellar ataxia type 6 (SCA6). *Journal of Neurology* 250(12): 1482–1487.

Guan X, Xuan M, Gu Q, et al. (2017) Influence of regional iron on the motor impairments of Parkinson's disease: A quantitative susceptibility mapping study. *Journal of magnetic resonance imaging: JMRI* 45(5): 1335–1342.

Guell X and Schmahmann J (2020) Cerebellar Functional Anatomy: a Didactic Summary Based on Human fMRI Evidence. *The Cerebellum* 19(1): 1–5.

Gunning-Dixon FM, Head D, McQuain J, et al. (1998) Differential aging of the human striatum: a prospective MR imaging study. *American Journal of Neuroradiology* 19(8). American Journal of Neuroradiology: 1501–1507.

Habas C, Kamdar N, Nguyen D, et al. (2009) Distinct Cerebellar Contributions to Intrinsic Connectivity Networks. *The Journal of Neuroscience* 29(26): 8586–8594.

Hacker CD, Perlmutter JS, Criswell SR, et al. (2012) Resting state functional connectivity of the striatum in Parkinson's disease. *Brain* 135(12): 3699–3711.

Hamani C, Saint-Cyr JA, Fraser J, et al. (2004) The subthalamic nucleus in the context of movement disorders. *Brain* 127(1): 4–20.

He N, Huang P, Ling H, et al. (2017) Dentate nucleus iron deposition is a potential biomarker for tremor-dominant Parkinson's disease. *NMR in Biomedicine* 30(4): e3554.

Helmich RC, Van den Berg KRE, Panyakaew P, et al. (2021) Cerebello-Cortical Control of Tremor Rhythm and Amplitude in Parkinson's Disease. *Movement Disorders* 36(7): 1727–1729.

Henrich MT, Geibl FF, Lakshminarasimhan H, et al. (2020) Determinants of seeding and spreading of α-synuclein pathology in the brain. *Science Advances* 6(46). American Association for the Advancement of Science: eabc2487.

Hilker R, Voges J, Weisenbach S, et al. (2004) Subthalamic nucleus stimulation restores glucose metabolism in associative and limbic cortices and in cerebellum: evidence from a FDG-PET study in advanced Parkinson's disease. *Journal of Cerebral Blood Flow and Metabolism: Official Journal of the International Society of Cerebral Blood Flow and Metabolism* 24(1): 7–16.

Holtbernd F and Eidelberg D (2012) Functional brain networks in movement disorders: recent advances. *Current opinion in neurology* 25(4): 392–401.

Hoover JE and Strick PL (1999) The Organization of Cerebellar and Basal Ganglia Outputs to Primary Motor Cortex as Revealed by Retrograde Transneuronal Transport of Herpes Simplex Virus Type 1. *The Journal of Neuroscience* 19(4): 1446–1463.

Hoshi E, Tremblay L, Féger J, et al. (2005) The cerebellum communicates with the basal ganglia. *Nature Neuroscience* 8(11). 11. Nature Publishing Group: 1491–1493.

Hou J and Pakkenberg B (2012) Age-related degeneration of corpus callosum in the 90+ years measured with stereology. *Neurobiology of Aging* 33(5): 1009.e1-1009.e9.

Huot P (2015) The pons and human affective processing — Implications for Parkinson's disease. *eBioMedicine* 2(11). Elsevier: 1592–1593.

Hutchison WD, Allan RJ, Opitz H, et al. (1998) Neurophysiological identification of the subthalamic nucleus in surgery for Parkinson's disease. *Annals of Neurology* 44(4): 622–628.

Ichinohe N, Mori F and Shoumura K (2000) A di-synaptic projection from the lateral cerebellar nucleus to the laterodorsal part of the striatum via the central lateral nucleus of the thalamus in the rat. *Brain Research* 880(1–2): 191–197.

Jahanshahi M, Jones CRG, Zijlmans J, et al. (2010) Dopaminergic modulation of striato-frontal connectivity during motor timing in Parkinson's disease. *Brain* 133(3): 727–745.

Jeurissen B, Leemans A, Tournier J-D, et al. (2013) Investigating the prevalence of complex fiber configurations in white matter tissue with diffusion magnetic resonance imaging. *Human Brain Mapping* 34(11): 2747–2766.

Jf S (2009) Akinesia, motor oscillations and the pedunculopontine nucleus in rats and men. *Exp Neurol* 215: 1–4.

Jovicich J, Czanner S, Greve D, et al. (2006) Reliability in multi-site structural MRI studies: effects of gradient non-linearity correction on phantom and human data. *NeuroImage* 30(2): 436–443.

Kim M, Ronen I, Ugurbil K, et al. (2006) Spatial resolution dependence of DTI tractography in human occipito-callosal region. *NeuroImage* 32(3): 1243–1249.

Koikkalainen J, Hirvonen J, Nyman M, et al. (2007) Shape variability of the human striatum--Effects of age and gender. *NeuroImage* 34(1): 85–93.

Kropotov JD and Etlinger SC (1999) Selection of actions in the basal ganglia–thalamocortical circuits: review and model. *International Journal of Psychophysiology* 31(3): 197–217.

Kumar K, Kelly M and Toth C (1999) Deep brain stimulation of the ventral intermediate nucleus of the thalamus for control of tremors in Parkinson's disease and essential tremor. *Stereotactic and Functional Neurosurgery* 72(1): 47–61.

Lee D-H, Park JW, Park S-H, et al. (2015) Have You Ever Seen the Impact of Crossing Fiber in DTI?: Demonstration of the Corticospinal Tract Pathway. *PLOS ONE* 10(7). Public Library of Science: e0112045.

Lehéricy S, Benali H, Van de Moortele P-F, et al. (2005) Distinct basal ganglia territories are engaged in early and advanced motor sequence learning. *Proceedings of the National Academy of Sciences of the United States of America* 102(35): 12566–12571.

Levy R, Ashby P, Hutchison WD, et al. (2002) Dependence of subthalamic nucleus oscillations on movement and dopamine in Parkinson's disease. *Brain: A Journal of Neurology* 125(Pt 6): 1196–1209.

Ma H, Chen H, Fang J, et al. (2015) Resting-state functional connectivity of dentate nucleus is associated with tremor in Parkinson's disease. *Journal of Neurology* 262(10): 2247–2256.

Ma Y, Tang C, Spetsieris PG, et al. (2007) Abnormal metabolic network activity in Parkinson's disease: test-retest reproducibility. *Journal of Cerebral Blood Flow and Metabolism: Official Journal of the International Society of Cerebral Blood Flow and Metabolism* 27(3): 597–605.

Manto M, Bower JM, Conforto AB, et al. (2012) Consensus Paper: Roles of the Cerebellum in Motor Control—The Diversity of Ideas on Cerebellar Involvement in Movement. *Cerebellum (London, England)* 11(2): 457–487.

McCarthy P (2019) FSLeyes. Zenodo. Available at: https://zenodo.org/record/3530921 (accessed 23 February 2022).

McMackin R, Muthuraman M, Groppa S, et al. (2019) Measuring network disruption in neurodegenerative diseases: New approaches using signal analysis. *Journal*

of Neurology, Neurosurgery & Psychiatry 90(9). BMJ Publishing Group Ltd: 1011–1020.

Meira AT, Arruda WO, Ono SE, et al. (2019) Neuroradiological Findings in the Spinocerebellar Ataxias. *Tremor and Other Hyperkinetic Movements* 9: 10.7916/tohm.v0.682.

Mf G, Sn S, Ja W, et al. (2013) The minimal preprocessing pipelines for the Human Connectome Project. *NeuroImage* 80. Neuroimage.

Milardi D, Arrigo A, Anastasi G, et al. (2016) Extensive Direct Subcortical Cerebellum-Basal Ganglia Connections in Human Brain as Revealed by Constrained Spherical Deconvolution Tractography. *Frontiers in Neuroanatomy* 10.

Mink JW (2018) Basal Ganglia Mechanisms in Action Selection, Plasticity, and Dystonia. *European journal of paediatric neurology : EJPN : official journal of the European Paediatric Neurology Society* 22(2): 225–229.

Mirdamadi JL (2016) Cerebellar role in Parkinson's disease. *Journal of Neurophysiology* 116(3). American Physiological Society: 917–919.

Moran A, Bergman H, Israel Z, et al. (2008) Subthalamic nucleus functional organization revealed by parkinsonian neuronal oscillations and synchrony. *Brain: A Journal of Neurology* 131(Pt 12): 3395–3409.

Mueller K, Jech R, Ballarini T, et al. (2019) Modulatory Effects of Levodopa on Cerebellar Connectivity in Parkinson's Disease. *Cerebellum (London, England)* 18(2): 212–224.

Narabayashi H, Maeda T and Yokochi F (1987) Long-term follow-up study of nucleus ventralis intermedius and ventrolateralis thalamotomy using a microelectrode technique in parkinsonism. *Applied Neurophysiology* 50(1–6): 330–337.

Network biomarkers for the diagnosis and treatment of movement disorders - ClinicalKey (n.d.). Available at: https://www.clinicalkey.com/#!/content/playContent/1-s2.0-S0969996108002489?returnurl=https:%2F%2Flinkinghub.elsevier.com%2Fretrieve%2Fpii%2FS0969996108002489%3Fshowall%3Dtrue&referrer=https:%2F%2Fpubmed.ncbi.nlm.nih.gov%2F (accessed 22 March 2024).

O'Callaghan C, Hornberger M, Balsters JH, et al. (2016) Cerebellar atrophy in Parkinson's disease and its implication for network connectivity. *Brain* 139(3): 845–855.

O'Doherty JP, Dayan P, Friston K, et al. (2003) Temporal difference models and reward-related learning in the human brain. *Neuron* 38(2): 329–337.

Paraguay IB, França C, Duarte KP, et al. (2021) Dentate nucleus stimulation for essential tremor. *Parkinsonism & Related Disorders* 82. Elsevier: 121–122.

Parihar R, Alterman R, Papavassiliou E, et al. (2015) Comparison of VIM and STN DBS for Parkinsonian Resting and Postural/Action Tremor. *Tremor and Other Hyperkinetic Movements* 5: 321.

Patriat R, Niederer J, Kaplan J, et al. (2020) Morphological changes in the subthalamic nucleus of people with mild-to-moderate Parkinson's disease: a 7T MRI study. *Scientific Reports* 10: 8785.

Payoux P, Remy P, Damier P, et al. (2004) Subthalamic Nucleus Stimulation Reduces Abnormal Motor Cortical Overactivity in Parkinson Disease. *Archives of Neurology* 61(8).

Pelzer EA, Hintzen A, Goldau M, et al. (2013) Cerebellar networks with basal ganglia: feasibility for tracking cerebello-pallidal and subthalamo-cerebellar projections in the human brain. *The European Journal of Neuroscience* 38(8): 3106–3114.

Peters SK, Dunlop K and Downar J (2016) Cortico-Striatal-Thalamic Loop Circuits of the Salience Network: A Central Pathway in Psychiatric Disease and Treatment. *Frontiers in Systems Neuroscience* 10: 104.

Pfefferbaum A, Rohlfing T, Rosenbloom MJ, et al. (2013) Variation in longitudinal trajectories of regional brain volumes of healthy men and women (ages 10 to 85 years) measured with atlas-based parcellation of MRI. *NeuroImage* 65: 176–193.

Pieperhoff P, Südmeyer M, Dinkelbach L, et al. (2022) Regional changes of brain structure during progression of idiopathic Parkinson's disease – A longitudinal study using deformation based morphometry. *Cortex* 151: 188–210.

Poewe W, Seppi K, Tanner CM, et al. (2017) Parkinson disease. *Nature Reviews Disease Primers* 3(1). Nature Publishing Group: 1–21.

Rădulescu A, Herron J, Kennedy C, et al. (2017) Global and local excitation and inhibition shape the dynamics of the cortico-striatal-thalamo-cortical pathway. *Scientific Reports* 7(1). Nature Publishing Group: 7608.

Raffelt D, Tournier J-D, Rose S, et al. (2012) Apparent Fibre Density: a novel measure for the analysis of diffusion-weighted magnetic resonance images. *NeuroImage* 59(4): 3976–3994.

Raffelt DA, Tournier J-D, Smith RE, et al. (2017) Investigating white matter fibre density and morphology using fixel-based analysis. *NeuroImage* 144: 58–73.

Raichle ME (1998) Behind the scenes of functional brain imaging: A historical and physiological perspective. *Proceedings of the National Academy of Sciences of the United States of America* 95(3): 765–772.

Raz N, Rodrigue KM, Kennedy KM, et al. (2003) Differential Aging of the Human Striatum: Longitudinal Evidence. *American Journal of Neuroradiology* 24(9). American Journal of Neuroradiology: 1849–1856.

Rolls ET, Huang C-C, Lin C-P, et al. (2020) Automated anatomical labelling atlas 3. *NeuroImage* 206: 116189.

Sala A and Perani D (2019) Brain Molecular Connectivity in Neurodegenerative Diseases: Recent Advances and New Perspectives Using Positron Emission Tomography. *Frontiers in Neuroscience* 13. Frontiers.

Sala S, Agosta F, Pagani E, et al. (2012) Microstructural changes and atrophy in brain white matter tracts with aging. *Neurobiology of Aging* 33(3): 488-498.e2.

Salat DH, Tuch DS, Greve DN, et al. (2005) Age-related alterations in white matter microstructure measured by diffusion tensor imaging. *Neurobiology of Aging* 26(8): 1215–1227.

Sb F, Ja B, Y K, et al. (2015) Altered cerebellar connectivity in Parkinson's patients ON and OFF L-DOPA medication. *Frontiers in human neuroscience* 9. Front Hum Neurosci.

Schroll H and Hamker FH (2013) Computational models of basal-ganglia pathway functions: focus on functional neuroanatomy. *Frontiers in Systems Neuroscience* 7: 122.

Schröter N, Rijntjes M, Urbach H, et al. (2022) Disentangling nigral and putaminal contribution to motor impairment and levodopa response in Parkinson's disease. *npj Parkinson's Disease* 8(1). Nature Publishing Group: 1–8.

Seidler RD, Noll DC and Chintalapati P (2006) Bilateral basal ganglia activation associated with sensorimotor adaptation. *Experimental Brain Research* 175(3): 544–555.

Setsompop K, Kimmlingen R, Eberlein E, et al. (2013) Pushing the limits of in vivo diffusion MRI for the Human Connectome Project. *NeuroImage* 80: 220–233.

Seymour B, O'Doherty JP, Dayan P, et al. (2004) Temporal difference models describe higher-order learning in humans. *Nature* 429(6992): 664–667.

Sha Z, Edmiston EK, Versace A, et al. (2020) Functional disruption of cerebello-thalamo-cortical networks in obsessive compulsive disorder. *Biological psychiatry. Cognitive neuroscience and neuroimaging* 5(4): 438–447.

Simioni AC, Dagher A and Fellows LK (2015) Compensatory striatal–cerebellar connectivity in mild–moderate Parkinson's disease. *NeuroImage : Clinical* 10: 54–62.

Singh SP (2014) Magnetoencephalography: Basic principles. *Annals of Indian Academy of Neurology* 17(Suppl 1): S107–S112.

Smith SM (2002) Fast robust automated brain extraction. *Human Brain Mapping* 17(3): 143–155.

Smith SM, Jenkinson M, Woolrich MW, et al. (2004) Advances in functional and structural MR image analysis and implementation as FSL. *NeuroImage* 23 Suppl 1: S208-219.

Steigerwald F, Pötter M, Herzog J, et al. (2008) Neuronal activity of the human subthalamic nucleus in the parkinsonian and nonparkinsonian state. *Journal of Neurophysiology* 100(5): 2515–2524.

Tai C-H and Tseng S-H (2022) Cerebellar deep brain stimulation for movement disorders. *Neurobiology of Disease* 175: 105899.

Tang Y, Nyengaard JR, Pakkenberg B, et al. (1997) Age-induced white matter changes in the human brain: a stereological investigation. *Neurobiology of Aging* 18(6): 609–615.

Tournier J-D, Calamante F, Gadian DG, et al. (2004) Direct estimation of the fiber orientation density function from diffusion-weighted MRI data using spherical deconvolution. *NeuroImage* 23(3): 1176–1185.

Tournier J-D, Smith R, Raffelt D, et al. (2019) MRtrix3: A fast, flexible and open software framework for medical image processing and visualisation. *NeuroImage* 202: 116137.

Tournier J-D, Calamante F and Connelly A (n.d.) Improved probabilistic streamlines tractography by 2nd order integration over fibre orientation distributions.: 1.

Turner RS, Desmurget M, Grethe J, et al. (2003) Motor subcircuits mediating the control of movement extent and speed. *Journal of Neurophysiology* 90(6): 3958–3966.

van de Warrenburg BPC, Hendriks H, Dürr A, et al. (2005) Age at onset variance analysis in spinocerebellar ataxias: a study in a Dutch-French cohort. *Annals of Neurology* 57(4): 505–512.

Van Overwalle F, Manto M, Cattaneo Z, et al. (2020) Consensus Paper: Cerebellum and Social Cognition. *The Cerebellum* 19(6): 833–868.

Van Overwalle F, Ma Q and Heleven E (2020) The posterior crus II cerebellum is specialized for social mentalizing and emotional self-experiences: a meta-analysis. *Social Cognitive and Affective Neuroscience* 15(9): 905–928.

Vizcarra JA, Situ-Kcomt M, Artusi CA, et al. (2019) Subthalamic deep brain stimulation and levodopa in Parkinson's disease: a meta-analysis of combined effects. *Journal of Neurology* 266(2): 289–297.

Weissenbacher A, Kasess C, Gerstl F, et al. (2009) Correlations and anticorrelations in resting-state functional connectivity MRI: A quantitative comparison of preprocessing strategies. *NeuroImage* 47(4): 1408–1416.

White RL, Campbell MC, Yang D, et al. (2020) Little Change in Functional Brain Networks Following Acute Levodopa in Drug-Naïve Parkinson Disease. *Movement disorders : official journal of the Movement Disorder Society* 35(3): 499–503.

Whitfield-Gabrieli S and Nieto-Castanon A (2012) Conn: A Functional Connectivity Toolbox for Correlated and Anticorrelated Brain Networks. *Brain Connectivity* 2(3). Mary Ann Liebert, Inc., publishers: 125–141.

Wichmann T (2018) Pathophysiologic Basis of Movement Disorders. In: Niranjan A, Lunsford LD, and Richardson RM (eds) *Progress in Neurological Surgery*. S. Karger AG, pp. 13–24. Available at: https://www.karger.com/Article/FullText/480718 (accessed 30 March 2020).

Wichmann T and DeLong MR (2003) Pathophysiology of Parkinson's disease: the MPTP primate model of the human disorder. *Annals of the New York Academy of Sciences* 991: 199–213.

Wichmann T and Soares J (2006) Neuronal firing before and after burst discharges in the monkey basal ganglia is predictably patterned in the normal state and altered in parkinsonism. *Journal of Neurophysiology* 95(4): 2120–2133.

Wu T and Hallett M (2005) A functional MRI study of automatic movements in patients with Parkinson's disease. *Brain: A Journal of Neurology* 128(Pt 10): 2250–2259.

Wu T and Hallett M (2013) The cerebellum in Parkinson's disease. *Brain* 136(3): 696–709.

Wu T, Wang L, Chen Y, et al. (2009) Changes of functional connectivity of the motor network in the resting state in Parkinson's disease. *Neuroscience Letters* 460(1): 6–10.

Wu T, Long X, Zang Y, et al. (2009) Regional homogeneity changes in patients with Parkinson's disease. *Human Brain Mapping* 30(5): 1502–1510.

Wu T, Wang L, Hallett M, et al. (2011) Effective connectivity of brain networks during self-initiated movement in Parkinson's disease. *NeuroImage* 55(1): 204–215.

Xu J, Yu M, Wang H, et al. (2022) Altered Dynamic Functional Connectivity in de novo Parkinson's Disease Patients With Depression. *Frontiers in Aging Neuroscience* 13.

Yamada K, Akazawa K, Yuen S, et al. (2010) MR Imaging of Ventral Thalamic Nuclei. *American Journal of Neuroradiology* 31(4): 732–735.

Yu H, Sternad D, Corcos DM, et al. (2007) Role of hyperactive cerebellum and motor cortex in Parkinson's disease. *NeuroImage* 35(1): 222–233.

Zhang H, Wang L, Gan C, et al. (2022) Altered functional connectivity of cerebellar dentate nucleus in peak-dose dyskinesia in Parkinson's disease. *Frontiers in Aging Neuroscience* 14: 943179.

Zwirner J, Möbius D, Bechmann I, et al. (2016) Subthalamic nucleus volumes are highly consistent but decrease age-dependently-a combined magnetic resonance imaging and stereology approach in humans. *Human brain mapping* 38.

ANNEXURES

List of publications from Thesis

1. **Radhakrishnan, V**., Gallea, C., Valabregue, R., Krishnan, S., Kesavadas, C., Thomas, B., James, P., Menon, R., Kishore, A., 2023. Cerebellar and basal ganglia structural connections in humans: Effect of aging and relation with memory and learning. Frontiers in Aging Neuroscience 15. https://doi.org/10.3389/fnagi.2023.1019239.

Curriculum Vitae

Personal details

Name: Vineeth Radhakrishnan

Email: vineethradhakrishnan09@gmail.com

Education

1. Bachelor of Electronics and Communication Engineering.
   Amrita University, India, GPA: 8.3/10,
   Graduated: June 2012
2. Masters in Biomedical Engineering
   Grand Valley State University (GVSU), MI, USA, GPA: 3.76/4
   Graduated: April 2016

Journal Publications

1. Radhakrishnan, V., Gallea, C., Valabregue, R., Krishnan, S., Kesavadas, C., Thomas, B., James, P., Menon, R., Kishore, A., 2023. Cerebellar and basal ganglia structural connections in humans: Effect of aging and relation with memory and learning. Frontiers in Aging Neuroscience 15.(Impact Factor: 4.5).
2. Vysakha KV, Radhakrishnan V, James P, et al. Quantifying abnormal writing kinematics in writer's cramp using a novel software platform. Acta Neurol Belg. Published online April 4, 2024. (Impact Factor: 2.7).
3. Chandrababu, K., Radhakrishnan, V., Anjana, A.S. et al. Unravelling the Parkinson's puzzle, from medications and surgery to stem cells and genes: a comprehensive review of current and future management strategies. Exp Brain Res 242, 1–23 (2024). (Impact Factor: 2.1).
4. Vijayaraghavan, Asish, Scaria, Sam, Radhakrishnan, Vineeth, Puthenveedu, Divya K, Krishnan, Syam, Kesavapisharady, Krishnakumar. Subthalamic Deep Brain Stimulation for Parkinson's Disease—An Unexpected Encounter in the Lead Trajectory. Annals of Indian Academy of Neurology 26(4):p 597-599, Jul–Aug 2023. (Impact Factor: 1.7).
5. Krishnan S, George SS, Radhakrishnan V, Raghavan S, Thomas B, Thulaseedharan JV, Puthenveedu DK. Quantitative susceptibility mapping from basal ganglia and

related structures: correlation with disease severity in progressive supranuclear palsy. Acta Neurol Belg. 2023 Aug 14. (Impact Factor: 2.7).

6. Rajan, R., Anandapadmanabhan, R., Nageswaran, S., Radhakrishnan, V., Saini, A., Krishnan, S., Gupta, A., Vishnu, V.Y., Pandit, A.K., Singh, R.K., Radhakrishnan, D.M., Singh, M.B., Bhatia, R., Srivastava, A., Kishore, A., Srivastava, M.P., 2023. Automated analysis of pen-on-paper spirals for tremor detection, quantification, and differentiation. Annals of Movement Disorders 6, 17. (Impact Factor: 0.33).

Conference Publications

1. Megalingam, R.K., Unnikrishnan, D.K.M., Radhakrishnan, V., Jacob, D.C., 2012. HOPE: An electronic gadget for home-bound patients and elders, in 2012 Annual IEEE India Conference (INDICON). Presented at the 2012 Annual IEEE India Conference (INDICON), pp. 1272–1277. https://doi.org/10.1109/INDCON.2012.6420814
2. Megalingam, R.K., Radhakrishnan, V., Jacob, D.C., Unnikrishnan, D.K.M., Sudhakaran, A.K., 2011b. Assistive Technology for Elders: Wireless Intelligent Healthcare Gadget, in 2011 IEEE Global Humanitarian Technology Conference. Presented at the 2011 IEEE Global Humanitarian Technology Conference, pp. 296–300. https://doi.org/10.1109/GHTC.2011.94
3. Megalingam, R.K., Nair, R.N., Radhakrishnan, V., 2011a. Automated Wireless Carpooling System for an eco-friendly travel, in 2011 3rd International Conference on Electronics Computer Technology. Presented at the 2011 3rd International Conference on Electronics Computer Technology, pp. 325–329. https://doi.org/10.1109/ICECTECH.2011.5941913
4. Megalingam, R.K., Radhakrishnan, V., Sudhakaran, A.K., Unnikrishnan, D.K.M., Jacob, D.C., 2011c. Real-Time, Remote, Home Based, Non-invasive, Elder Monitoring System, in Lin, J.C., Nikita, K.S. (Eds.), Wireless Mobile Communication and Healthcare, Lecture Notes of the Institute for Computer Sciences, Social Informatics and Telecommunications Engineering. Springer Berlin Heidelberg, Berlin, Heidelberg, pp. 263–270. https://doi.org/10.1007/978-3-642-20865-2_33
5. Kannan Megalingam, R., Radhakrishnan, V., Krishnan Melepurath Unnikrishnan, D., Chakko Jacob, D., Kakkanattu Sudhakaran, A., 2010. Autonomous Smart Server Guard for advanced safety measure using wireless mobile technology, in 2010

International Conference on Mechanical and Electrical Technology. Presented at the 2010 International Conference on Mechanical and Electrical Technology, pp. 654–658. https://doi.org/10.1109/ICMET.2010.5598441

Conference abstract presentations

1. Radhakrishnan, V., Krishnan, S., Gallea, C., Kesavadas, C., Thomas, B., Kishore, A., 2023. Role of cerebellum basal ganglia direct subcortical network in the pathophysiology of Parkinson's disease.[abstract] IBRO Neuroscience Reports 15, S480.
2. V. Radhakrishnan, C. Gallea, S. Krishnan, B. Thomas, C. Kesavadas, A. Kishore. Role of the direct subthalamo-cerebellar tract in memory and learning: Implications for the pathophysiology of late-stage Parkinson's Disease [abstract]. Mov Disord. 2023; 38 (suppl 1)
3. V. Radhakrishnan, C. Gallea, C. Kesavadas, B. Thomas, S. Krishnan, A. Kishore. Study of age-related neurodegeneration of Cerebellum Basal Ganglia direct subcortical white matter tracts using fixel-based analysis. [abstract]. Mov Disord. 2022; 37 (suppl 1).
4. V. Radhakrishnan, S. Krishnan, B. Thomas, C. Gallea, C. Kesavadas, A. Kishore. Resting State Functional and Structural Connectivity Changes of Cerebellum Basal Ganglia Interconnecting Network in Parkinson's Disease [abstract]. Mov Disord. 2020; 35 (suppl 1).

Awards/Honors

1. Travel Grant to attend Movement Disorders Congress, Denmark 2023.
2. Travel Grant to attend the 11th IBRO World Congress of Neuroscience, Spain 2023.
3. Travel Grant to attend Movement Disorders Congress, Spain 2022.
4. Travel Grant for presenting award paper for MDSICON 2020.
5. Third prize for award paper presentation in MDSICON 2020.
6. IEEE Student Enterprise Award during the year 2011-2012.
7. IEEE Standards Education Committee Award.
8. Award of Appreciation from Amrita University for outstanding performance during the year 2010−2011.

Experience

1. **Senior Research Fellow,** Non-Invasive Brain Stimulation (NIBS) Lab, Sree Chitra Tirunal Institute for Medical Science and Technology (SCTIMST), Kerala, India 2016 July – Present.
2. **Controls Engineer,** Viastore Systems Inc, MI, USA 2015-2016 March
3. **Guest Student,** Van Andel Institute, MI, USA 2013-2014
4. **Graduate Assistant,** Grand Valley State University, MI, USA 2012
5. **Research Associate,** Humanitarian Technology Labs, Amrita University 2010-2012

Invited Talks and Workshops

1. Conducted a one-day workshop as part of PANCHADASHA 2019, an IEEE Student Branch event of Amrita Vishwa Vidyapeetham, Amritapuri campus, Kerala, on Jan 13, 2019, on the topic of Neuroplasticity modulation via Transcranial Magnetic Stimulation (TMS) and its imaging using functional Magnetic Resonance Imaging (fMRI).
2. Invited talk on Brain Connectivity in Motor Network on 9th October 2021, as part of UDBODH 2021, webinar series during the COVID pandemic year 2020-21, organized by Humanitarian Technology (HuT) Labs, Dept. of ECE, and Amrita IEEE Student Branch of Amrita Vishwa Vidyapeetham University, Kerala, India in association with Megara Robotics Pvt. Ltd., Chennai, India.

Areas of interest

Neuroimaging, Movement Disorders, Neuroscience

APPENDICES

APPENDIX A – ETHICS COMMITTEE APPROVAL

श्री चित्रा तिरुनाल आयुर्विज्ञान और प्रौद्योगिकी संस्थान
तिरुवनन्तपुरम - 695 011, केरल, भारत
SREE CHITRA TIRUNAL INSTITUTE FOR MEDICAL SCIENCES AND TECHNOLOGY
THIRUVANANTHAPURAM - 695 011, INDIA
(An Institute of National importance under Govt. of India)

Institutional Ethics Committee
(IEC Regn No. ECR/189/Inst/KL/2013)

SCT/IEC/816/OCTOBER-2015 26.11.2015

Dr. Asha Kishore
Professor
Department of Neurology
SCTIMST, Thiruvananthapuram

Dear. Dr. Asha Kishore,

The Institutional Ethics Committee reviewed and discussed your application to conduct the study entitled "RESTING STATE CONNECTIVITY BETWEEN THE BASAL GANGLIA AND CEREBELLUM IN HEALTH AND PARKINSON'S DISEASE: A COMBINED FUNCTIONAL MAGNETIC RESONANCE AND DIFFUSION TENSOR IMAGING STUDY (IEC/816)" on 17th October, 2015.

The following documents were reviewed:

Original submission

1. *Covering letter addressed to the Chairperson, IEC, SCTIMST, dated 21.09.2015*
2. *TAC Approval Letter*
3. *IEC Application Form*
4. *TAC Application Form*
5. *Declaration signed by all investigators*
6. *Project Proposal*
7. *Informed Consent Forms in English and Malayalam*
8. *CVs of PI and Co-PI*

Revised submission

1. *Covering letter addressed to the Chairman, IEC, SCTIMST dated 19.11.2015*
2. *Copy of the IEC Recommendation letter dated 03.11.2015*
3. *TAC Approval Letter*
4. *Copy of the response to the TAC comments, dated 8.09.2015*
5. *IEC Application Form*
6. *TAC Application Form*
7. *Project Proposal*
8. *Modified Patient Information Sheet and Consent Form in English and Malayalam*
9. *CV of the Investigators*

Page 1 of 2

तार : चित्रमेट Grams : Chitramet
फोन Phone : 2443152
फाक्स Fax : (91)471-2446433 2550728
ई-मेइल E-mail : sct. @sctimst.ac.in
वेबसाईट Website : www.sctimst.ac.in

The following members of the Ethics Committee were present at the meeting held on 17th October, 2015 at G. Parthasarathi Board Room, AMCHSS, SCTIMST.

SL. No.	Member Name	Highest Degree	Gender	Scientific /Non Scientific	Affiliation with Institution(s)
1.	Justice Gopinathan. P.S	BSc. LLB	Male	Legal Expert (Chairperson)	No
2.	Dr. Asha Kishore	MD	Female	Clinician (Neurologist)	Yes
3.	Shri. O.S. Neelakandan Nair	BE	Male	Engineer	Yes
4.	Dr. R V G Menon	PhD	Male	Lay Person	No
5.	Dr. Meenu Hariharan	DM	Female	Clinician (Gastro-Enterologist)	No
6.	Smt. Sathi Nair	MA	Female	Lay Person	No
7.	Dr. Kala Kesavan. P	MD	Female	Pharmacologist	No
8.	Dr. K R S Krishnan	ME, PhD	Male	Biomedical Scientist/Engineer	No
9.	Dr. V. Raman Kutty	MPH(Harvard) MPhil, MD	Male	Public Health	Yes
10.	Dr. Mala Ramanathan	MSc, PhD, MA	Female	Ethicist/Social Scientist (Member Secretary)	Yes

IEC Decision

The IEC approved the conduct of the study in the present form.

Remarks:

The Institutional Ethics Committee expects to be informed about the progress of the study, any SAE occurring in the course of the study, any changes in the protocol and patient information/informed consent and asks to be provided a copy of the final report.

There was no member of the study team who participated in voting / decision making process. The ethics committee is organized and operated according to the requirements of Good Clinical Practice and the requirements of the Indian Council of Medical Research (ICMR).

Sincerely,

Mala Ramanathan
Member Secretary, IEC

APPENDIX B - PUBLICATIONS

1. **Radhakrishnan, V**., Gallea, C., Valabregue, R., Krishnan, S., Kesavadas, C., Thomas, B., James, P., Menon, R., Kishore, A., 2023. ***Cerebellar and basal ganglia structural connections in humans: Effect of aging and relation with memory and learning***. Frontiers in Aging Neuroscience 15.**(*Impact Factor: 4.5*)**. https://doi.org/10.3389/fnagi.2023.1019239.
2. Vysakha KV, **Radhakrishnan V**, James P, et al. ***Quantifying abnormal writing kinematics in writer's cramp using a novel software platform.*** Acta Neurol Belg. Published online April 4, 2024. **(*Impact Factor: 2.7*)** https://doi.org/10.1007/s13760-024-02532-x
3. Chandrababu, K., **Radhakrishnan, V**., Anjana, A.S. et al. ***Unravelling the Parkinson's puzzle, from medications and surgery to stem cells and genes: a comprehensive review of current and future management strategies***. Exp Brain Res 242, 1–23 (2024). **(*Impact Factor: 2.1*)** https://doi.org/10.1007/s00221-023-06735-1
4. Vijayaraghavan, Asish, Scaria, Sam, **Radhakrishnan, Vineeth**, Puthenveedu, Divya K, Krishnan, Syam, Kesavapisharady, Krishnakumar. ***Subthalamic Deep Brain Stimulation for Parkinson's Disease—An Unexpected Encounter in the Lead Trajectory***. Annals of Indian Academy of Neurology 26(4):p 597-599, Jul–Aug 2023. **(*Impact Factor: 1.7*)** https://doi.org/10.4103/aian.aian_360_23
5. Krishnan S, George SS, **Radhakrishnan V**, Raghavan S, Thomas B, Thulaseedharan JV, Puthenveedu DK. ***Quantitative susceptibility mapping from basal ganglia and related structures: correlation with disease severity in progressive supranuclear palsy***. Acta Neurol Belg. 2023 Aug 14. **(*Impact Factor: 2.7*)** https://doi.org/10.1007/s13760-023-02352-5.
6. Rajan, R., Anandapadmanabhan, R., Nageswaran, S., **Radhakrishnan, V**., Saini, A., Krishnan, S., Gupta, A., Vishnu, V.Y., Pandit, A.K., Singh, R.K., Radhakrishnan, D.M., Singh, M.B., Bhatia, R., Srivastava, A., Kishore, A., Srivastava, M.P., 2023. ***Automated analysis of pen-on-paper spirals for tremor detection, quantification, and differentiation.*** Annals of Movement Disorders 6, 17. **(*Impact Factor: 0.33*).** https://doi.org/10.4103/aomd.aomd_50_22.

APPENDIX C – PLAGIARISM CHECK REPORT

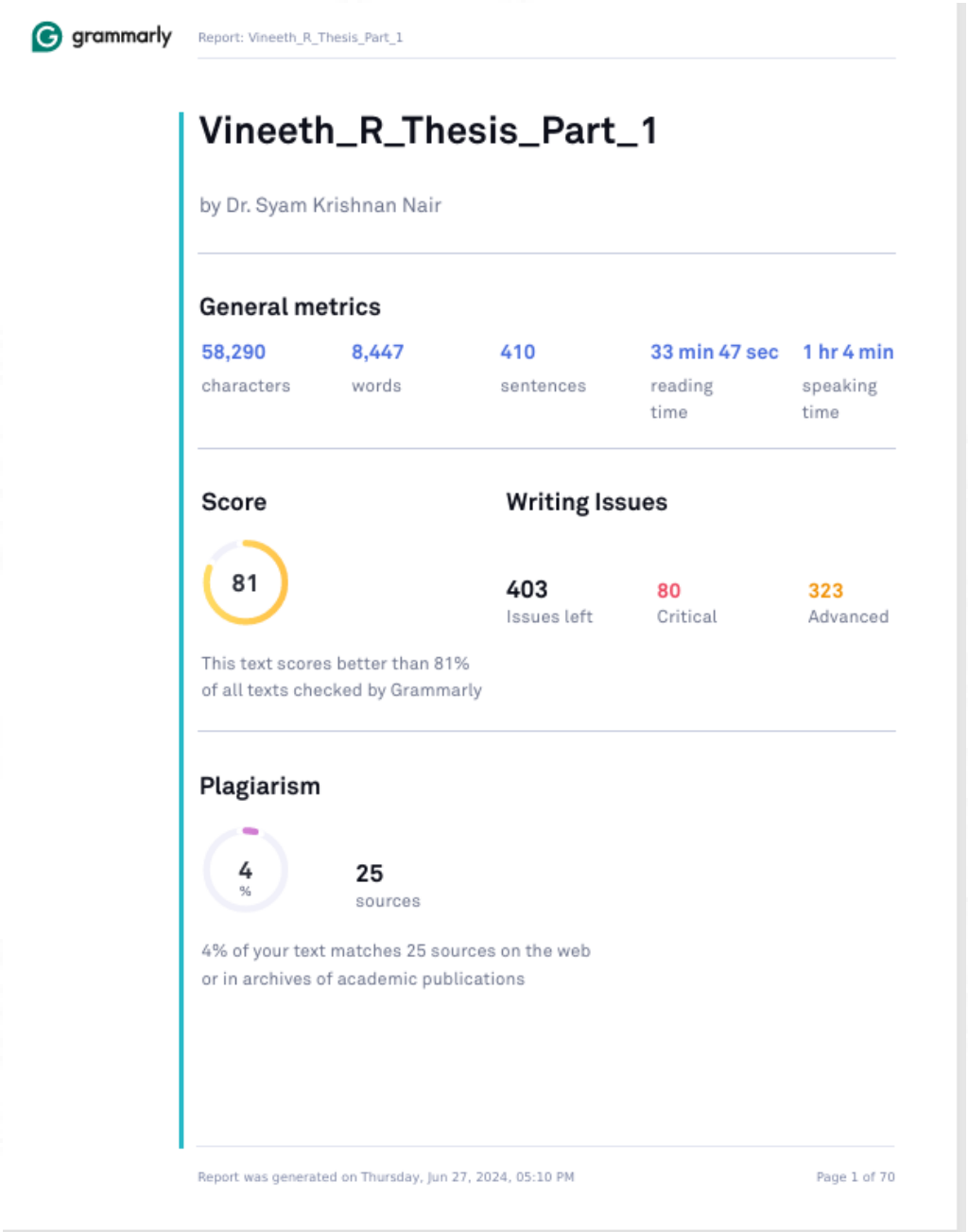

grammarly Report: Vineeth_R_Thesis_Part_1

Vineeth_R_Thesis_Part_1

by Dr. Syam Krishnan Nair

General metrics

58,290	8,447	410	33 min 47 sec	1 hr 4 min
characters	words	sentences	reading time	speaking time

Score

81

This text scores better than 81% of all texts checked by Grammarly

Writing Issues

403	80	323
Issues left	Critical	Advanced

Plagiarism

4 %

25 sources

4% of your text matches 25 sources on the web or in archives of academic publications

Report was generated on Thursday, Jun 27, 2024, 05:10 PM

Page 1 of 70

grammarly Report: Vineeth_R_Thesis_Part_2

Vineeth_R_Thesis_Part_2

by Dr. Syam Krishnan Nair

General metrics

44,657	6,658	276	26 min 37 sec	51 min 12 sec
characters	words	sentences	reading time	speaking time

Score

This text scores better than 82% of all texts checked by Grammarly

Writing Issues

292	57	235
Issues left	Critical	Advanced

Plagiarism

20 sources

4% of your text matches 20 sources on the web or in archives of academic publications

Report was generated on Thursday, Jun 27, 2024, 05:44 PM

Page 1 of 55